BAYERISCHE JULIUS-MAXIMILIANS –UNIVERSITÄT WÜRZBURG
FAKULTÄT FÜR MEDIZIN
INSTITUT FÜR MEDIZINISCHE STRAHLENKUNDE UND ZELLFORSCHUNG

Caspase-1 as a target of bacterial tumor therapy

Caspase-1 als Angriffsziel bakterieller Tumortherapie

Dissertation
zur Erlangung des naturwissenschaftlichen Doktorgrades
der Bayerischen Julius-Maximilians-Universität Würzburg

vorgelegt von
Katharina Monika Galmbacher
aus Erlenbach

Würzburg, 2008

Eingereicht am : ……

Miglieder der Promotionskommission:

Vorsitzender:

1. Gutachter:

2. Gutachter:

3. Gutachter:

Tag des Promotionskolloquiums: ……

Doktorurkunde ausgehändigt am: ……

Ich versichere, dass die vorliegende Arbeit nur unter Verwendung der angegebenen Hilfsmittel angefertigt und von mir selbständig durchgeführt und verfasst wurde.

Diese Dissertation hat weder in gleicher noch in ähnlicher Form in einem anderen Prüfungsverfahren vorgelegen.

Neben dem akademischen Grad „Diplom-Biologin Univ.“ habe ich keine weiteren akademischen Grade erworben oder zu erwerben versucht.

Würzburg, ……

Index

List of figures

I. Abstracts

I.1. Abstact

In neoplastic diseases the tumor stroma and especially tumor-associated macrophages (TAMs) play an important role in tumor growth and progression. TAMs exhibit an intensive cross-talk with tumor cells resulting in the promotion of angiogenesis and the inhibition of local protective immune responses in certain tumor entities. Therefore, TAMs are a potential target for tumor therapy.

Here it was shown that intravenously applied intracellular bacteria like *Salmonella* and *Shigella* primarily target TAMs. To exploit this feature a growth attenuated *Shigella* strain with the capacity to induce apoptosis in macrophages was designed. *Shigella* are invasive bacteria that penetrate the colonic tissue and initiate an acute inflammation. In macrophages, *Shigella* rapidly induces caspase-1 processing and apoptosis via the virulence factor IpaB. By genomic deletion of the *aroA*-locus a metabolically attenuated strain defective in intracellular growth but with retained capacity of infection, cell-to-cell spread, caspase-1 processing and apoptosis induction in macrophages was designed. It was shown that this strain primarily targets TAMs in 4T1 cell induced and transgenic MMTV-HER2/new breast cancer models. *Shigella* were almost exclusively found intracellularly, whereas growth attenuated *Salmonella* were also found extracellularly at late time points. The metabollically attenuated *Shigella* strain with retained virulence, but not avirulent *Shigella* strains, was able to activate caspase-1 and induce apoptosis in TAMs at all time points (4 h, 6 h and 7 d *p.i.*) in both breast cancer models. This unrestricted apoptosis induction translated into a substantial, long-lasting and highly significant reduction of TAMs number (up to 70 %) in both models. In contrast, *Salmonella* could only induce apoptosis in TAMs at early time points (6 h *p.i.*) and failed to reduce TAMs in both models.

In the 4T1 model, the effect on tumor size was monitored and treatment of the mice with the attenuated *Shigella* strain resulted in a complete block of tumor growth. Finally, *Shigella* primarily infected the macrophage fraction, activated caspase-1 and induced apoptosis in cells derived from a human ovarian carcinoma *ex vivo*.

Taken together, this data suggests that growth attenuated intracellular bacteria capable of inducing apoptosis in TAMs are a promising therapeutic option for certain cancer diseases where TAMs have a proven role for tumor growth or progression.

I.2. Zusammenfassung

Tumorstroma und Tumor-assoziierte Makrophagen (TAMs) spielen in neoplastischen Erkrankungen eine wichtige Rolle im Bezug auf Tumorwachstum und Progression. In einigen Krebsarten besteht zwischen den Tumor-assoziierten Makrophagen und den Krebszellen eine intensive Interaktion, welche zu vermehrter Angiogenese und zur Unterdrückung lokaler Immunantworten führt. Aus diesem Grund stellen TAMs einen vielversprechenden Angriffspunkt für eine Krebstherapie da.

In dieser Arbeit wird gezeigt, dass intrazelluläre Bakterien wie *Salmonella* und *Shigella* hauptsächlich TAMs im Tumorgewebe infizierten. Um dieses Verhalten näher zu untersuchen, konstruierten wir einen im Wachstum abgeschwächten *Shigella* Stamm, welcher jedoch noch die Fähigkeit hat, Apoptose in Makrophagen zu induzieren. *Shigellen* sind invasive Bakterien, die in das Darmgewebe einwandern und dort eine massive Inflammation induzieren. Intrazelluläre *Shigellen* aktivieren Caspase-1 und induzieren dadurch Apoptose in Makrophagen durch den sekretierten Virulenzfaktor IpaB. Durch eine Deletion des genomischen *aroA*-Gens, wurde ein *Shigella* Stamm konstruiert, der Defekte im intrazellulären Wachstum aufweist. Dennoch war dieser Stamm noch fähig eukaryotische Zellen zu infizieren, sich interzellulär fortzubewegen, Caspase-1 zu aktivieren und Apoptose in Makrophagen zu induzieren. Es wurde gezeigt, dass dieser *Shigellen* Stamm nach i.v. Injektion hauptsächlich die TAMs im 4T1-induzierten und transgenen MMTV-HER2/neu Brustkrebsmodel infizieren. Diese attenuierten *Shigellen* wurden im Tumorgewebe hauptsächlich intrazellulär detektiert, im Gegensatz dazu wurden attenuierte *Salmonellen* zu späten Zeitpunkten (7 d *p.i.*) auch extrazellulär im Tumorgewebe aufgefunden. Der metabolisch aber nicht in der Virulenz attenuierte *Shigella* Stamm konnte in beiden Brustkrebsmodellen zu allen Zeitpunkten (4 h, 6h and 7 d *p.i.*) Caspase-1 in TAMs aktivieren und Apoptose induzieren. Diese Apoptose führte in beiden Brustkrebsmodellen zu einer langandauernden und hoch signifikanten Reduktion der TAMs-Anzahl (bis zu 70 %). Im Gegensatz dazu konnten *Salmonellen* nur zu frühen Zeitpunkten (6 h *p.i.*) Apoptose in TAMs induzieren und dies führte in beiden Modellen zu keiner Reduzierung der TAMs-Anzahl.

In dem 4T1-induzierten Tumormodel wurden die Mäuse mit dem attenuierten *Shigella* Stamm behandelt, was zu einer kompletten Blockierung des Tumorwachstums führte, dies traf aber nicht für den avirulenten Stamm zu. Darüberhinaus infizierte *Shigella* hauptsächlich die Makrophagen Fraktion eines Ovarkarzinoms *ex vivo* und induzierte in diesen Zellen Caspase-1 Aktivierung und Apoptose.

Zusammenfassend zeigen diese Daten, dass im Wachstum attenuierte intrazelluläre Bakterien dazu fähig sind Apoptose in TAMs zu induzieren. Dadurch werden sie zu einem vielversprechenden Therapeutikum zur Behandlung von betimmten Krebserkrankungen, bei denen TAMs eine erwiesene Rolle im Tumorwachstum und der Tumorprogression spielen.

II. Introduction

II.1. Bacterial tumor therapy

In 1868, the German physician W. Busch intentionally infected a cancer patient with erysipelas hoping for tumor regression. Although rapid tumour shrinkage occurred, the patient died nine days after infection. In 1883, after identifying *Streptococcus pyogenes* as the causative agent of erysipelas, F. Fehleisen reported tumor regression in cancer patients upon treatment with live streptococci[1]. In 1891, the American surgeon W.B. Coley also noted the cure of cancer by a severe *Streptococal* infection[2]. Since then, other bacteria have been shown to infiltrate, replicate and then preferentially accumulate in tumors[1,3].

As tumors or metastases develop, they stimulate angiogenesis to promote the formation of new blood vessels. This abnormal vascular supply found in tumors is an important factor for bacterial colonisation of the tumor. However, the newly formed vessels are highly disorganised with incomplete endothelial linings and blind ends, resulting in sluggish blood flow, leakiness for particles and inefficient delivery of nutrients and oxygen to the tumor or metastases. This leads to multiple regions of hypoxia (<1% oxygen or 0–20 mmHg) and anoxia within the tumor[4,5]. The combination of poor nutrient delivery and oxygen starvation results in non-proliferating hypoxic/anoxic cells within tumors and promotes growth of anaerobic and facultative anaerobic bacteria. Areas of necrosis provide nutrients such as purines to further promote the growth of the bacteria. It is also believed that these areas with low oxygen and high interstitial pressure are an immunological sanctuary, where bacterial clearance mechanisms are inhibited[4,5].

This leads to the use of bacteria as vectors to target therapeutic gene expression to tumors and its usefulness in cancer gene therapy. Any bacterium suitable for use as a tumor-targeting vector must possess several features. It must be genetically tractable, non-pathogenic or attenuated so it is well-tolerated by the host, exhibit accumulation within tumors, be motile and be susceptible to antibiotics so it can be cleared from the body following gene delivery. Thus, the ideal bacterial vector could be administered systemically, deliver its therapeutic payload specifically to the primary or secondary tumor and not to normal tissues thereby eliminating unwanted side effects[6]. Once in the tumor, the motile bacteria should then disperse throughout the tissue, overcoming the diffusion and distal pressure gradients and deliver the therapeutic agents to all regions of the lesion. Motility is a major advantage that bacteria have over viral vectors, as viruses exhibit a lack of specificity for tumors and, when they are present, they are poorly distributed throughout the tumor mass (often confined to

peri-vascular regions). In addition, the metabolically active bacteria should replicate and continue to produce active agents whilst the tumor remains infected, thus amplifying a low dose to an effective level only within the target tumor[6].

II.1.1. Extracellular and intracellular bacteria in tumor therapy

For some extracellular bacteria, such as genetically modified obligate anaerobe *Clostridia*, an anti-tumor effect was observed[7]. Other extracellular bacteria such as *E. coli* accumulated in tumor tissue, induced some inflammatory responses, but failed to confer protection[8]. Also facultative intracellular bacteria such as *Salmonella* have been used for tumor therapy and their intratumoral accumulation was studied using different technologies, albeit beyond cellular resolution[9,10]. In most syngenic experimental models a moderate therapeutic effect was shown, whereas more pronounced efficacy has been seen in xenograft models[10-13]. It was speculated that the induction of an inflammatory response is mediating the anti-tumor effect.

Intracellular bacteria have been shown to target tumors, albeit with modest therapeutic efficacy[14]. As an example, i.v. injected *Salmonella* and intratumorally injected *Shigella* induced necrosis in a colon cancer model (which is normally not associated with high numbers of macrophages), but protection was only reached after depletion of neutrophils[15].

Besides exerting a toxic effect, intracellular bacteria can deliver DNA into eukaryotic cells[16]. Therefore, intracellular bacteria could be employed to deliver toxins or prodrug converting enzymes directly into tumor cells. In contrast to the therapeutic approaches with extracellular bacteria, the efficacy of tumor therapy with intracellular bacteria is dictated by the fraction of tumor cells which are infected. However, no information on the distribution of intracellular bacteria in different tumor cell types is available. In this work the tumoral distribution of intracellular bacteria such as attenuated *Shigella* should be quantitatively determined after i.v. application. Importantly, phagocytic cells such as macrophages or dendritic cells are the primary target of intracellular pathogens. Within the macrophage, bacteria such as *Salmonella* and *Shigella* can survive using distinct virulence mechanisms and can induce apoptosis of the infected macrophages through activation of caspase-1 mediated by IpaB (*Shigella*) or SipB (*Salmonella*)[17,18]. In contrast to the physiological situation, the phagocytic defects of tumor-associated macrophages might block the uptake of intracellular bacteria and favor the direct infection of tumor cells.

To analyse the distribution of *Salmonella* and *Shigella* after i.v. application in tumors with high numbers of macrophages, we quantitatively determined the bacterial counts of bacteria in

the extracellular space or within tumor cells, distinguishing between the macrophage and non-macrophage fraction.

II.2. *Shigella flexneri*

Members of the genus *Shigella* are gram-negative facultative anaerobes that belong to the family *Enterobacteriaceae*. The genus is divided into four species: *Shigella flexneri, Shigella boydii, Shigella sonnei* and *Shigella dysenteriae.* These species are further divided into serotypes based on biochemical differences and variations in their O-antigen. Based on this classification scheme, *Shigella flexneri* is divided into 13 serotypes[19].

II.2.1. Pathogenesis of *Shigella flexneri*

S. flexneri is highly infectious, requiring as little as 100 cells to cause disease in adult volunteers[20]. This low infective dose is in part attributed to *S. flexneri*`s ability to survive the low acidity of the host`s stomach, via an up-regulation in acid resistance genes[21]. Once *S. flexneri* reach the colon, they begin to invade the mucosa, penetrating, replicating within and spreading between the mucosal epithelial cells. This behaviour and the subsequent inflammatory response of the host destroy the colonic epithelial layer generating the clinical symptoms of shigellosis (Fig. 1)[22].

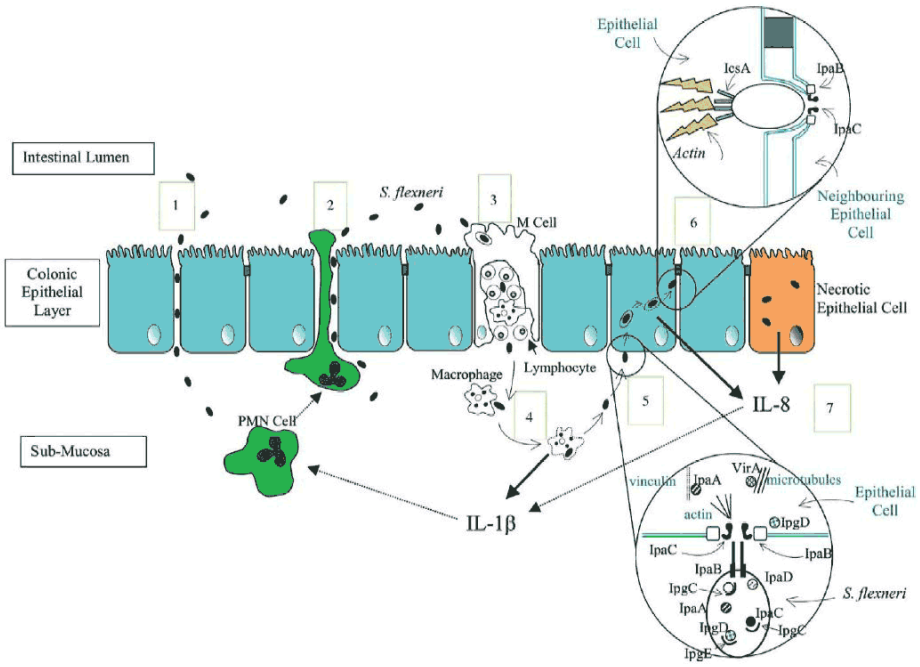

Figure 1: Pathogenesis of *Shigella flexneri*[19]

1. Lumenal bacteria invade the colonic epithelial layer by three known mechanisms. *S. flexneri* can

manipulate the tight junction proteins, allowing paracellular movement into the sub-mucosa.

2. PMN cells recruited by IL-8 and IL-1β produced in response to *S. flexneri* invasion create gaps between epithelial cells.
3. Endocytic M cells transcytose bacteria, releasing them into an intraepithelial pocket filled with B and T lymphocytes and macrophages
4. Macrophages phagocytose the bacteria. *S. flexneri* escapes the phagosome and induces apoptosis. The apoptotic macrophages release IL-1β.
5. Submucosal *S. flexneri* contact the basolateral membrane of epithelial cells, activating secretion of proteins through their type-III secretion system. Proteins chaperoned in the cytosol of *S. flexneri* are secreted into the epithelial cells´ cytoplasm through a pore formed by IpaB and IpaC. IpaC polymerises actin, IpgD dissociates the plasma membrane from the actin cytoskeleton, VirA destabilises microtubules and IpaA forms a complex with vinculin, depolymerising actin. This creates cell surface extensions which form around the bacterium, driving the epithelial cell to take up *S. flexneri* into a vacuole.
6. IpaB and IpaC lyse the vacuole, releasing *S. flexneri* into the epithelial cell´s cytoplasm. The *S. flexneri* protein, IcsA is displayed on only one pole of the bacterium, creating a polymerised actin tail behind the bacterium. This propels *S. flexneri* through the cytoplasm until it contacts the plasma membrane, the force of the contact creates a protrusion into the neighbouring epithelial cell. Both membranes are lysed by IpaB and IpaC, releasing *S . flexneri* into the neighbouring epithelial cell.
7. Intracellular *S. flexneri* induces the epithelial cell to release IL-8. IL-8 and the IL-1b released from apopotic macrophages are chemotactic to PMN cells (represented by dotted arrows), attracting and inducing them to migrate through the epithelial layer to the lumen. This epithelial disruption amplifies *S. flexneri* invasion of the epithelial layer.

S. flexneri invades epithelial cells through a macropinocytic process, where *S. flexneri*-induced rearrangements of the host cell cytoskeleton engulf the bacterium into a vacuole (Fig. 1). The virulence plasmid pWR100 of *S. flexneri* encodes two loci crucial to this invasive phenotype, the ipa locus and the mxi-spa locus (Fig. 2).

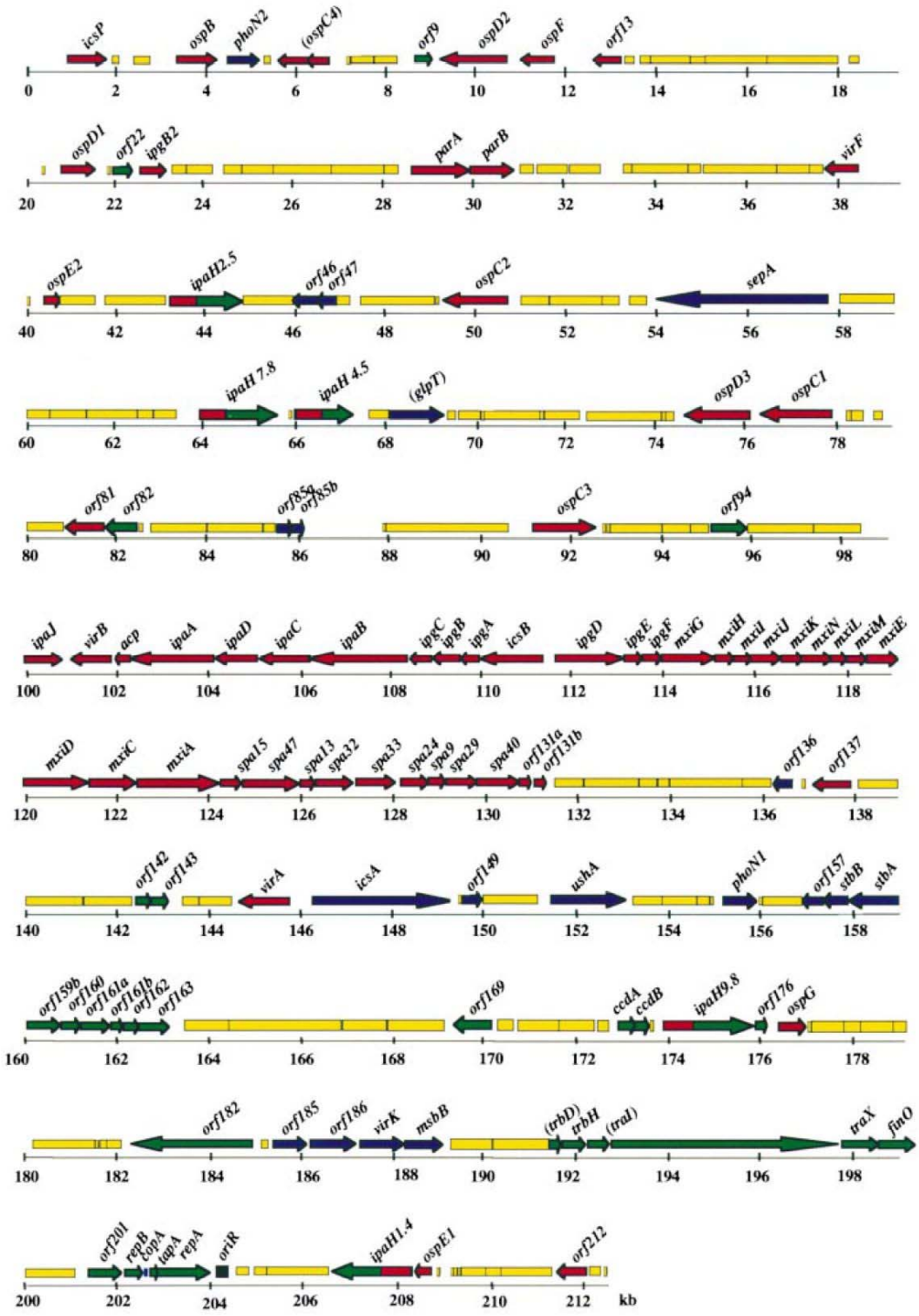

Figure 2: The virulence plasmid pWR100[23]

The virulence plasmid pWR100 is composed of 213 494 bp. Sequence analysis identified 93 DNA fragments that have over 90 % identity with known insertion sequence (IS) elements.

The ipa operon encodes the ‘‘invasion plasmid antigens’’, IpaA, IpaB, IpaC and IpaD, which are the effectors of bacterial entry into the host cell. The mxi-spa operon encodes the components of a type-III secretion system, which is a flagella-like structure used to deliver

proteins, such as the Ipa proteins, from the bacterial cytoplasm to the cytoplasmic membrane or even cytosol of the host cell[24]. The mxi-spa operon and IpaB, IpaC and IpaD are essential for *in vitro* epithelial cell invasion[25,26]. The Ipa proteins are synthesized and stored within the bacteria, where they are associated with chaperone proteins until secretion is activated by contact with a host cell[17,27]. A complex formed by IpaB and IpaD may play a role in the regulation of this secretion[28]. Both proteins are hydrophobic allowing this complex to insert into the membrane of the host cell to form a pore[29]. It is presumed that the other effector molecules, delivered by the type-III secreton, are able to access the host cytoplasm through this pore. The C-terminal domain of IpaC activates host cell Rho GTPases, triggering actin polymerisation and filopodial extensions in the vicinity of the bacteria[30]. IpaA is secreted into the cytosol of the host epithelial cell where it binds the cytoskeleton-associated protein vinculin. The IpaA–vinculin complex depolymerises actin filaments, organising an entry foci around the bacterium[30,31]. IpgD is injected into the epithelial cell by the *S. flexneri* type-III secretion system, where it acts as a phosphoinositide phosphatase, uncoupling the plasma membrane from the actin cytoskeleton, allowing membrane extensions to form[22].

The macropinocytic vacuole containing the *Shigella* bacterium is rapidly lysed by the IpaB invasin, which acts as membranolytic toxin in the phagosome membrane, releasing *Shigella* into the host cell cytoplasm[32]. *S. flexneri* can replicate inside the cytoplasm of epithelial cells *in vitro* with a doubling time of 40 minutes. Epithelial cells are observed undergoing necrotic-like death during shigellosis (Fig. 1)[33]. *Shigella* is able to exploit the host cells actin assembly machinery to move through the host cell cytoplasm and into adjacent epithelial cells. This intra- and intercellular spread is a crucial step in the virulence of *Shigella* and is driven by the outer membrane protein, IcsA (VirG)[34-36]. Actin polymerisation at the pole of the bacterium creates propulsive force, which drives the bacterium through the cytoplasm of the cell until it contacts the host cell membrane, forming a protrusion into the neighbouring epithelial cell[37]. The bacteria are then surrounded by two cellular membranes, which are lysed by secreted IpaB and IpaC[38]. Thus, *Shigella* is able to replicate and spread within the intestinal epithelial layer whilst avoiding exposure to the extracellular environment and its circulating immune cells[19].

II.3. Caspase-1 (ICE)

Importantly, phagocytic cells such as macrophages or dendritic cells are the primary target of intracellular pathogens such as *Shigella*. Within the macrophage, *Shigella* can survive using distinct virulence mechanisms and can induce apoptosis of the infected macrophages through

activation of caspase-1 mediated by IpaB[17,18]. Caspases form a family of aspartate-specific cysteine endopeptidases. Further investigations identified a family of molecules that were named caspases, because they all had a cystein residue at their catalytic sites and exhibited protease activity targeting the aspartate residue of the substrate protein[39]. To date, 14 mammalian caspases have been identified, of which 11 have human homologs[40]. Many of the caspase family members are activated during programmed cell death and their proteolytic activity is a central biochemical feature of the apoptotic process[41]. Extensive studies of caspases in inflammation and apoptosis validated the enzymes as attractive drug targets[42].
Caspase-1 (also known as interleukin 1β-converting enzyme or ICE) was originally identified as a monocyte-specific endopeptidase responsible for the post-translational processing of the proinflammatory cytokine interleukin 1β (IL-1β)[43-45], a major mediator of inflammatory diseases such as rheumatoid arthritis. Soon thereafter, caspase-1 was shown to process interleukin-18 (IL-18), a cytokine structurally similar to IL-1 that is involved in T-cell activation[46]. Caspase-1 is expressed as a procaspase-1 zymogen that is processed into a catalytically competent form through autoproteolysis induced by protein oligomerization *in vitro*[47], but may require caspase-5 for efficient activation *in vivo* (Fig. 3)[48-50].

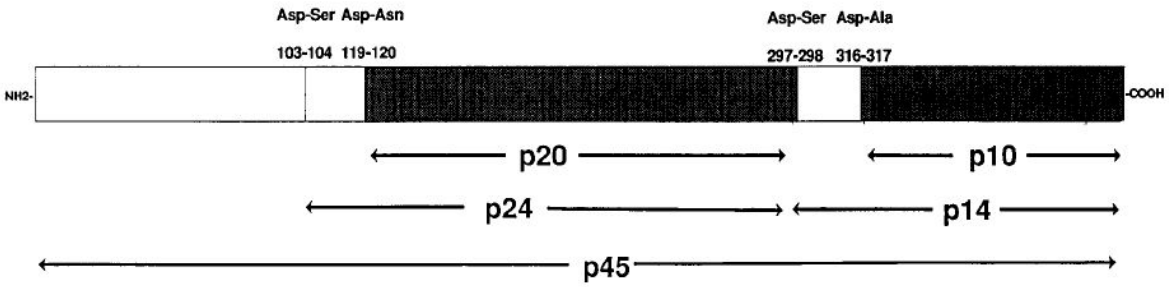

Figure 3: Primary structure of human IL-1β-converting enzyme precursor[51]

Full-length p45 ICE may be cleaved at four Asp-X cleavage sites indicated to produce mature heterodimeric p10/p20 ICE.

The cleavage reaction removes the 119-residue propeptide and an 18-residue sequence that separates the large (p20; residues 120–298) and small (p10; residues 317–404) subunits of the mature enzyme (Fig. 3). The functional form of caspase-1 is thought to be a tetramer composed of two p20–p10 heterodimers[52,53]. Caspase-1 is expressed in cells of the monocytic/macrophage cell line and in pancreatic cancer cells[54].

II.3.1. Activation of caspase-1

Activation of inflammatory caspases, such as caspase-1 and caspase-5, occurs upon assembly of an intracellular complex, designated the inflammasome (Fig. 4).

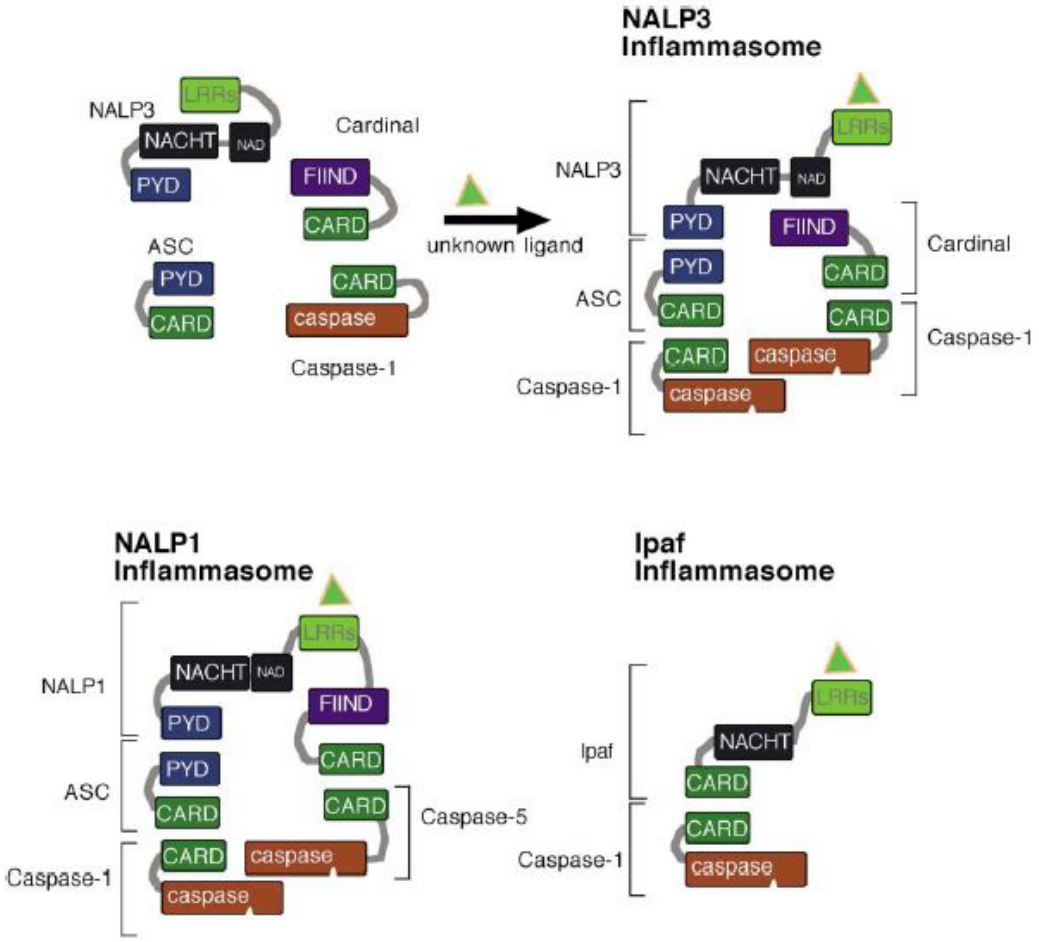

Figure 4: The Inflammasomes[55]

Unknown exogenous (from bacteria) or endogenous (bacteria, viruses: "danger signals") ligands bind to the LRRs of NALPs and induce assembly of the complex. FIIND, F-interacting domain.

Inflammasome is a name given to a large, signal-induced multiprotein complex, a so-called caspase-activating platform, that mediates the activation of pro-inflammatory caspases. Platform proteins generally consist of a ligand sensing domain (frequently repeats of domains, the structure of leucine-rich repeats, LLR), a nucleotide binding oligomerization domain (NACHT), and a recruitment domain (CARD, PYD).

In the Ipaf inflammasome Ipaf associates with caspase-1 and activates caspase-1 upon overexpression (Fig. 3)[56-58]. In the NALP1 inflammasome NALP1 recruits the adaptor protein ASC. The CARD region of ASC then interacts with and activates caspase-1. In addition, NALP1 binds and activates caspase-5. In the NALP1 inflammasome complex, caspase-5 and

caspase-1 are therefore brought into close proximity thereby facilitating crossactivation. Thus, in contrast to the NALP1 inflammasome, the NALP3 inflammasome activates only caspase-1[55].

II.4. Caspase-1 and *S. flexneri*

II.4.1. Apoptosis of macrophages

Once released into the intraepithelial pocket of the M cell, *Shigella* is engulfed by resident macrophages, possibly through a bacterial driven macropinocytic event similar to *Shigella* entry of epithelial cells[59]. *S. flexneri* is able to evade the killing mechanisms of the macrophage by IpaB mediated lysis of the phagocytic vacuole (Fig. 1). The membrane lysing properties of the virulence plasmid IpaB invasin allows the bacteria to gain free access to the cytoplasm[32]. Once in the macrophage cytosol, secreted IpaB binds and activates caspase-1[60]. Procaspase-1 undergoes autocatalytic cleavage into p10 and p20 fragments, which form the active caspase-1 tetramer. Activation of p45 ICE occurs through a sequential series of proteolytic steps to generate p35, p22/p12, and p20/p10 fragments of progressively increasing catalytic activity[61].

IpaB, a 62-kDa protein, is necessary and sufficient to induce programmed cell death in macrophages[60]. The binding of IpaB to caspase-1 is crucial in the induction of apoptosis in macrophages infected with virulent *S. flexneri*[60].

Caspase-1 dependent apoptosis is not an immunologically silent cell death, as activated caspase-1 cleaves and activates the pro-inflammatory cytokines IL-1b and IL-18[46]. Macrophage apoptosis occurs within 4 h of *in vivo Shigella* infection, releasing bacteria into the sub-mucosa[62].

II.5. Tumor-associated macrophages (TAMs)

Solid tumors comprise not only malignant cells, but also many other non-malignant cell types. The tumor microenvironment contains many resident cell types, such as adipocytes and fibroblasts, but it is also populated by migratory haematopoietic cells, most notably macrophages, neutrophils and mast cells. These haematopoietic cells have pivotal roles in the progression and metastasis of tumors[63-67], and this work will focus on one such class - the tumor-associated macrophages (TAMs). Pollard argues (2004) that tumor microenvironment, in a similar way to that seen in normal development, educates macrophages to perform supportive roles that promote tumor progression and metastasis (Fig. 5)[68].

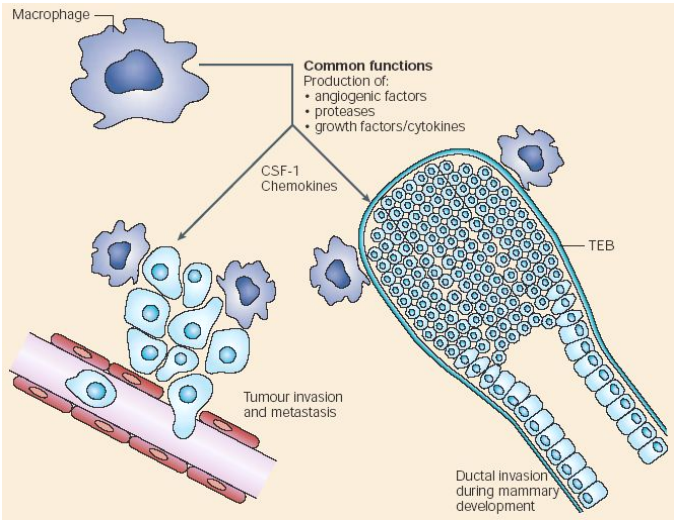

Figure 5: Macrophages have important developmental roles[68]

The immunological and repair functions of macrophages are well documented. It is known that they are among the first cells to arrive at sites of wounding and/or infection, where they perform several functions. They produce cytokines and chemokines to orchestrate the recruitment and actions of other immune cells, and produce growth factors, angiogenic factors and proteases to promote tissue repair. They also kill pathogens through the production of reactive oxygen and nitrogen radicals and present foreign antigens to cytotoxic T cells. Less well appreciated is their important role in tissue morphogenesis during development. Developmental defects include osteopetrosis, dermal hypoplasia, aberrant development of the sex-steroidhormone feedback response in the brain, delayed and aberrant pancreatic morphogenesis and impaired branching morphogenesis of the mammary gland. In the case of mammary gland[69], as shown in the figure, the ends of the developing ducts form a unique multi-laminate structure called the terminal end bud (TEB). As these TEBs form, they recruit macrophages; the absence of these in the *Csf-1*-null mutant mouse results in delayed ductal development and a poorly branched, atrophic ductal tree. This shows that cells of the mononuclear phagocytic lineage have important developmental roles through their remodelling and trophic functions. It seems likely that tumors co-opt the normal developmental roles of macrophages to promote their own development and invasion through the surrounding stroma[65]. In contrast to normal epithelia, however, tumor cells - owing to intrinsic transforming mutations - have lost positional identity, and so they continue to send out 'help me' signals that result in invasion into the vasculature.

TAMs are recruited to tumors by a range of growth factors and chemokines, which are often produced by the tumor cells themselves (Fig. 6)[66,67,70]. Clinical studies have shown a correlation between an abundance of TAMs and poor prognosis[70]. These data are particularly strong for breast, prostate, ovarian and cervical cancers. In contrast to colorectal cancer, where high TAMs numbers tended to be found in patients with a good prognosis or those with less recurrence, increased TAM density is usually associated with advanced tumor progression and metastasis[71].

II.5.1. TAMs and Cytokines

The local cytokine milieu in the tumor tends to block the immunological functions of these newly recruited mononuclear phagocytes - such as antigen presentation and cytotoxicity - towards tumors, and diverts them towards specialized TAMs that are immunosuppressed (Fig. 6)[72]. A principal component of this cytokine mixture is CSF-1, which locally blocks the maturation of dendritic cells so that they are unable to present antigens and promotes the development of immunosuppressed trophic TAMs. The cytokine profile of the tumor microenvironment is therefore important to the phenotype of the local mononuclear phagocytes. In determining this balance, another macrophage colony-stimulating factor GM-CSF together with interferon-γ (IFN- γ), are likely to be important, as these direct macrophages towards more cytotoxic and antigen-presenting phenotypes[73].

II.5.2. TAMs and tumor progression

The clinical evidence described above indicates that an abundance of TAMs has a negative impact on patient survival in many tumor types (Fig. 6)[68].

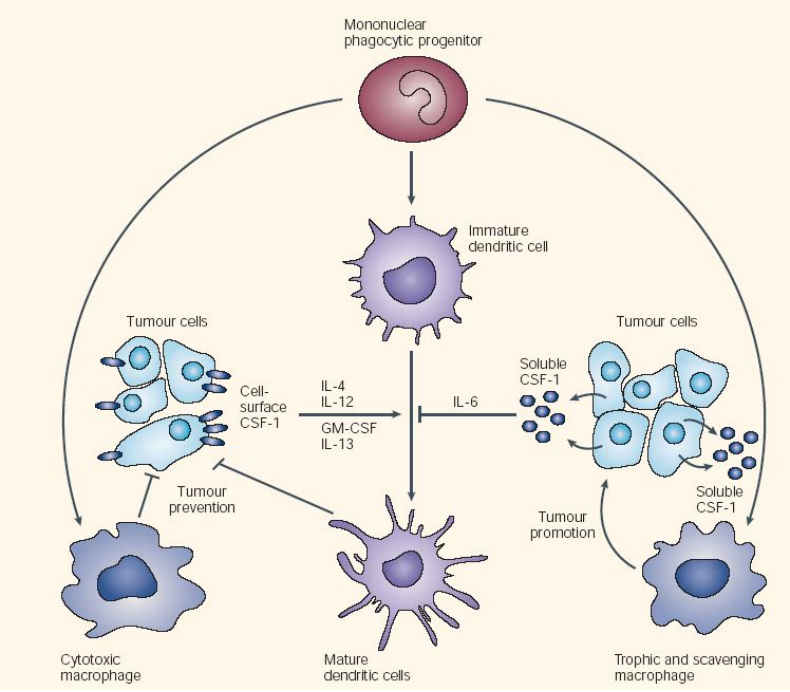

Figure 6: Pro- and anti-tumorigenic properties of macrophages depend on the cytokine microenvironment in the tumor[68]

Tumors are populated by macrophages and dendritic cells that are derived from mononuclear phagocytic progenitor cells. In many tumors, a high concentration of soluble colony-stimulating factor-1 (CSF-1) educates

macrophages to be trophic to tumors and, together with interleukin-6 (IL-6), inhibits the maturation of dendritic cells. This creates a microenvironment that potentiates progression to metastatic tumors. By contrast, CSF-1 presented in a transmembrane form on the tumor surface activates macrophages to kill tumor cells. This - together with high concentrations of IL-4, IL-12, IL-13 and GM-CSF - causes dendritic cells to mature, allowing the presentation of tumor antigens to cytotoxic T cells, with the consequent rejection of the tumor.

Lin et al. used mice carrying a null mutation in the gene that encodes *Csf-1* (colony stimulating factor-1) to prevent macrophages accumulating in mammary tumors of transgenic mice[74]. In this macrophage-deficient mice, the incidence and initial rates of growth of primary tumors were not different from those seen in normal mice, but the rate of tumor progression was slowed and their metastatic ability was almost completely abrogated when compared with mice that contained normal numbers of macrophages. Interestingly, overexpression of *Csf-1* in wild-type mice also accelerated tumor progression and increased their metastatic rate. Taken together, these experiments support a role for TAMs in tumor progression and metastasis and provide experimental support for the clinical observations that increased TAM density promotes tumor malignancy.

II.5.3. Functions of TAMs

Macrophages are therefore multifunctional cells, the phenotypes of which are modified by the local environment, and have important roles in the morphogenesis of tissues. The diverse functions of TAMs are summarized in figure 7.

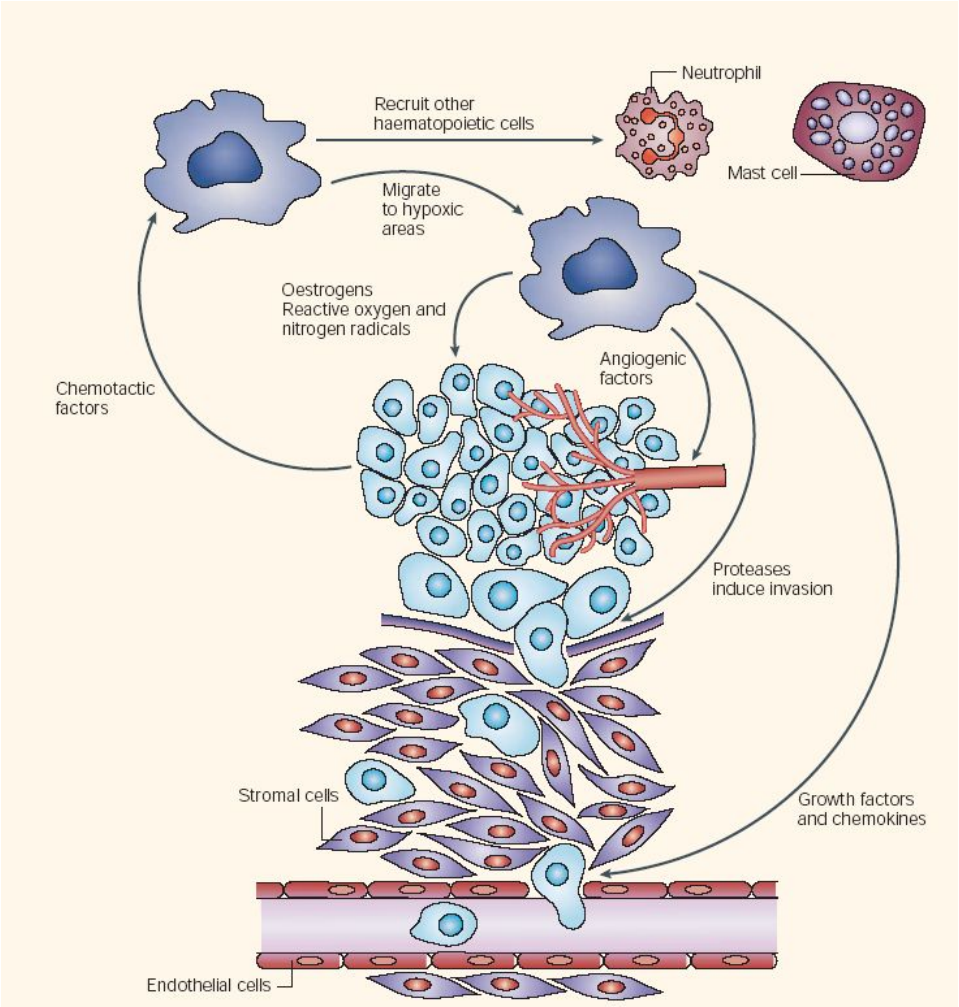

Figure 7: Pro-tumorigenic functions of tumor-associated macrophages[68]

Macrophages are recruited to tumors by chemotactic factors and provide many trophic functions that promote tumor progression and metastasis. These tumor-associated macrophages (TAMs) migrate to hypoxic areas within the tumor, where they stimulate angiogenesis by expressing factors such as vascular endothelial growth factor (VEGF), angiopoietins (ANG1 and ANG2), and recruit other haematopoietic cells such as mast cells and neutrophils. TAMs also promote tumor invasion by producing proteases - such as urokinase-type plasminogen activator (uPA), matrix metalloproteinase 9 (MMP-9) and cathepsins - that break down the basement membrane and remodel the stromal matrix. MMP-9 also contributes to angiogenesis. Various growth factors and chemokines such as epidermal growth factor (EGF), transforming growth factor-β (TGF-β), interleukin-8 (IL-8) and tumor necrosis factor-α (TNF-α) contribute to the migration of tumor cells towards vessels and provide proliferative and anti-apoptotic signals to these cells. Macrophages that are attracted to sites of inflammation or tissue breakdown can also initiate or promote tumorigenesis through their synthesis of oestrogens and the generation of mutagens as a by-product of their production of reactive oxygen and nitrogen-oxide radicals.

It is widely recognized that tumors require angiogenesis to grow beyond a certain size. This process involves a wide range of soluble mediators that are both stimulatory and inhibitory, including basic fibroblast growth factor (bFGF), VEGF, the angiopoietins (ANG1 and

ANG2), IL-1, IL-8, tumor necrosis factor-α (TNF-α), thymidine phosphorylase (TP; also known as vascular-derived endothelial growth factor), the matrix metalloproteinases MMP-9 and MMP-2, and nitric oxide (NO)[11,75]. These molecules, which are expressed in a coordinated spatial and temporal fashion, result in the proliferation and migration of endothelial cells, matrix remodelling and the eventual formation of stabilized vessels[76]. Macrophages are perfectly designed to promote these processes, as their monocytic precursors can migrate into sites where they differentiate into macrophages, and these wandering cells can synthesize the required angiogenic molecules on demand in specific locations[77]. Macrophages are important, although not the only producers of VEGF, which is a key component of the process of angiogenesis in tumors[78,79]. It was suggested that hypoxia - or the cytokines that are produced in response to this condition - is one of the local attractants for macrophages, and that hypoxia itself upregulates the transcription factor hypoxia-inducible factor-2α (HIF-2α) in macrophages. HIF-2α, in turn, induces VEGF expression (Fig. 7)[66,79]. TAMs also produce many other proangiogenic cytokines for example. they are key producers of TNF-α[80].

In conclusion, migratory TAMs are equipped to enter areas of the tumor where vascularization is needed. Here, these cells synthesize angiogenic regulators, which results in the formation of new vessels that allows further tumor growth and access of tumor cells to the vasculature for escape into the circulation. At these sites, a complex mixture of factors - ranging from hypoxia to cytokines - controls the expression of these regulators. This is consistent with the hypothesis that macrophages are educated to perform specialized tasks at specific sites.

II.5.4. TAMs and therapeutic opportunities

The presence of TAMs in a tumor provides an environment that enhances the survival, proliferation and migration of epithelial cells that have accumulated primary oncogenic mutations. However, macrophages might have an even more sinister role by playing a significant part in establishing the primary oncogenic events in epithelial cells (Fig. 7). There is a growing body of evidence to indicate that inflammation - as a result of chronic infection, continuous exposure to irritants or genetic makeup - is a causative event in many cancers.

Pollard argued (2004) that microenvironment educates macrophages to take on specific phenotypes that can increase the risk of cancer and, once cancers are formed, promote their progression[68]. The intracellular regulators of these different tumor promoting pathways might

therefore be potential therapeutic targets. The experiments in mouse models that are described above - in which tumor progression and metastasis are reduced by the ablation of *CSF-1*- support this idea. Another antitumor strategy is for example the immunization against molecules overexpressed by TAMs and thereby remodel the tumor microenvironment that attracts these macrophages and mediates their function[81]. So TAMs represent a promising target to therapeutic intervention and for this reason our experimental approach is to target and to deplet this tumor promoting TAMs with attenuated bacteria like *Shigella* and *Salmonella*.

II.6. Attenuated bacteria

In our project the wildtype *Shigella flexneri M90T* can not be used, because it is highly virulent and disease causing. Therefore we wanted to engineer an attenuated *Shigella* strain which is negatively affected on its growth ability in comparison to the wildtype strain *Shigella flexneri M90T.* In this context "attenuated" means weakened or thinned. Attenuated strains of disease-causing bacteria and viruses are often used as vaccines. The weakened strains are used as vaccines because they stimulate a protective immune response while causing no disease or only mild disease in the person receiving the vaccine.

To establish a metabolic block we planed to knockout a gene of an important amino acid pathway such as the gene *aroA*. In this way the engineered metabolic mutant is expected to show a reduction in growth rate. On the other hand this constructed mutant should not be affected in its virulence in comparison to the *Shigella* wildtype strain because the mutant should still be able to invade eukaryotic cells, to induce apoptosis in macrophages by activating caspase-1 and to spread to neighbouring cells. In contrast to the strain described in this work dedicated for bacterial tumor therapy, attenuated vaccine strains against shigellosis usually bear attenuations in both growth and virulence. An example is the live attenuated SC602 vaccine using *S. flexneri 2a* which was developed at the Pasteur Institute. In this vaccine, deletions were made in *iucA* (gene of an iron transport island) as well as *virG/icsA* genes[82].

And also other studies have shown that an *aroA*-knockout in other bacteria such as *Salmonella* leads to an attenuation in bacteria[83].

II.6.1. The enzyme 5-Enolpyruvylshikimate-3-phosphate synthetase (AroA)

5-Enolpyruvylshikimate-3-phosphate (EPSP) synthase (AroA) is a key enzyme in the aromatic amino acid biosynthetic pathway in microorganisms and plants (Fig. 8).

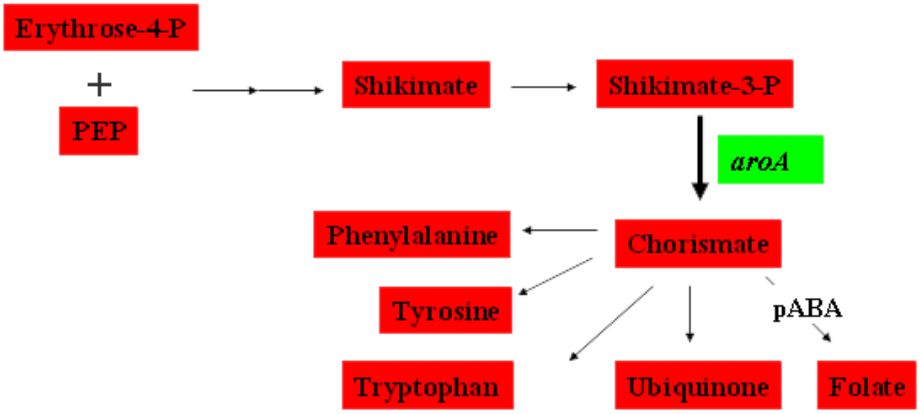

Figure 8: The aromatic amino acid biosynthetic pathway

Higher animals, with the exception of some protozoa, lack the aromatic biosynthesis path and must take up all needed aromatic metabolites from the nutrition.

Blocking the path for aromatic biosynthesis in bacteria such as *Shigella* therefore causes requirement for at least the three major aromatic amino acids and for *p*-aminobenzoate (pABA), needed for making folic acid, which *Shigella* cannot assimilate from their environment[84]. Folats are cofactors needed for several enzymatic reactions involving the transfer of 1-carbon fragments, used in the biosynthesis of purines, thymine, serine and panthothenate and also of formyl-Met-t-RNA needed for the initiation of new polypeptide chains.

The necessity for tyrosine, phenylalanine or tryptophan would not be expected to prevent the growth of *Shigella* strain in the tissues of an animal host since these amino acids (acquired from the diet or by recycling cellular protein) are available in plasma. By contrast, there is no mechanism ensuring the presence of pABA in cytosol or plasma despite its rapid conjugation and excretion, which explains the reduced virulence of for example pABA-requiring *Salmonella typhi* mutant[85]. Sansonetti and colleagues showed that a complete block in aromatic biosynthesis by an *aroA*-knockout led to an attenuated *Shigella* strain, and so this strain is worth to trail as a vector for live attenuated bacterial tumor therapy[34,86].

II.7. Transgenic mouse models

To investigate the complex tumor/stroma relationships and the role of TAMs in tumor growth we decided to use transgenic mice besides the 4T1-induced breast cancer model. Syngenic murine tumor models like the 4T1-cell induced breast cancer model involve rapidly growing tumors which are sometimes highly immunogenic[87]. These tumors are often anaplastic and therefore not a good model for the slow-growing well-differentiated human tumors. In addition, rapidly growing models may not develop the complex tumor/stroma relationships which are targeted by many novel therapies[87]. Transplantable tumors have often been derived from cell lines selected for high viability *in vitro,* and thus may be more resistant to apoptosis than their *in vivo* counterparts[87]. Consequently there is a need for a spontaneous and metastatic tumor model in immunocompetent mice. The major advantage of this model is a closer resemblance to the biological mechanisms of the human disease[87]. Non- or weakly-immunogenic tumors arise in this immunocompetent mice spontaneously and stochastically. This provides a better parallel for the development of human malignancies and makes it more likely that metastases will arise via the same mechanisms as in human cancer. This is of potential value in preclinical studies of therapy, adjuvant or maintenance, and chemoprophylaxis. Recent data suggested that these tumors are biologically diverse like human tumors, in between one individual mouse as in between littermates or different mouse strains[87].

For this reasons we also used transgenic mouse models like the spontaneous breast cancer MMTV-HER2/neu VFB model and the transgenic lung cancer *S-PC*-c-Raf-BxB-11 model to investigate the role of TAMs in tumor growth[87].

II.7.1. MMTV-HER2/neu FVB mice

To investigate the role of TAMs in breast tumor growth and progression we also used the transgenic breast cancer model MMTV-HER2/new FVB besides the artificial 4T1-induced breast tumor model.

The HER2 (ErbB-2 and c-neu) receptor

The HER2/new gene is a proto-oncogene, which is overexpressed in approximately 25-35 % of breast cancers. It is a member of the ErbB protein family, more commonly known as the epidermal growth factor receptor (EGF-R) family. HER2/new has also been designated as CD340 (cluster of differentiation 340). It is a cell membrane surface-bound receptor tyrosine kinase and is normally involved in the signal transduction pathways leading to cell growth and differentiation. HER2/new plays a crucial role in the pathogenesis of breast cancer which

is exploited by approved breast cancer treatments (Herceptin®). The oncogene *her2* is so-named because it has similar structure to human epidermal growth factor receptor, or HER1.
In our studies we used transgenic mice that express the *HER2/new* gene under the control of the mouse mammary tumor virus (MMTV) promoter (Fig. 9)[88].

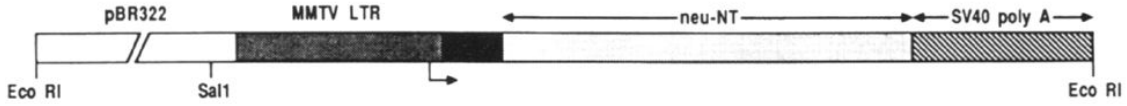

Figure 9: Structure of the *MMTVIc-neu* transgene[88]

The unshaded region represents sequences within the pBR322 vector backbone. The transcriptional start site within the MMTV LTR is illustrated by the lower arrow and the 5' noncoding sequences derived from the *MMTVIv-Ha-ras* vector pA9 are illustrated by the shaded box. The boundaries of the *her2* (*c-neu*) cDNA and SV40 processing signals are shown by the appropriate arrows. Relevant restriction endonuclease sites are also identified in the figure[88].

Transgenic mice generated to evaluate the relevance of a cellular proto-oncogene like *her2* (*c-neu*) to mammary development and tumorigenesis utilized the mouse mammary tumor virus long terminal repeat (MMTVLTR) sequence to target the expression of HER2/*new* to the mammary epithelium of virgin, pregnant and lactating mice[88-90]. These mice express the *HER2/new* transgene in the mammary gland at very high levels and develop HER2-positive mammary tumors within 6–8 months[88].

II.7.2. *SP-C*-c-Raf-BxB-11 mice

In order to investigate the role of TAMs in lung adenomas and to find out whether TAMs isolated from lung tumors can be infected and depleted by attenuated *Shigella*, we used transgenic *SP-C*-c-Raf-BxB-11 mice which express a oncogenic c-Raf.

II.7.2.1. C-Raf: keyplayer in Ras/Raf signaling

The Ras/Raf/MEK/ERK signaling pathway is an evolutionary conserved signaling cascade that links receptor activation at the cell membrane to the modification of cytoplasmic or nuclear targets that are required for the execution of developmental programs as well as for cell survival and proliferation[91]. As summarized in figure 10 a wide variety of growth factors and differentiation factors, as well as tumor-promoting substances, employ this pathway. Most of these stimuli activate Ras proteins by inducing the exchange of GDP with GTP, which converts Ras into its active conformation[92].

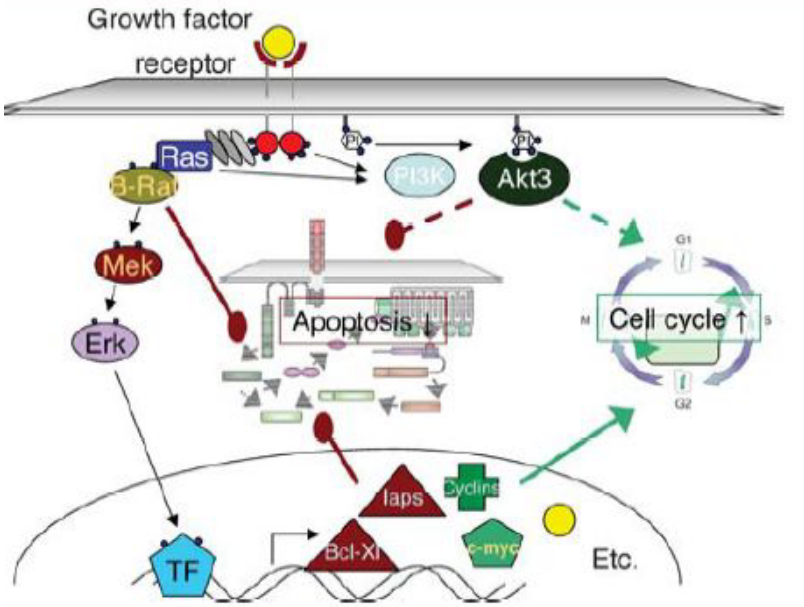

Figure 10: The mitogenic cascade[93]

The mitogenic cascade as well as the Akt signaling pathway is initiated by growth factors binding to the receptor. The signal is carried on by a cascade of protein kinases leading to transcriptional activation of proteins possessing anti-apoptitic and cell cycle stimulating properties. Ras: receptor activated substrate, Raf: Rous sarcoma associated factor, Mek: mitogen-activated protein kinase or Erk kinase, Erk: extra cellular signal regulated kinase, TF: transcription factor, PI: phosphatidylinositol, PI3K: phosphatidylinositol-3 kinase, Akt: protein kinase B/Akt, c-Myc: v-Myc myelocytomatosis viral oncogene homolog.

Activated Ras functions as an adapter that binds to Raf kinases with high affinity and causes their translocation to the cell membrane, where Raf activation takes place[94]. Once activated, Raf kinases transmit the signal to downsteam MEK1, 2 kinases, which in turn phosphorylate and activate ERK1, 2 kinases. Afterwards phosphorylated ERK activates a multitude of cytoplasmic and nuclear transcription factors that are important for cell fate decisions and cell-type-specific functions[91,93].

II.7.2.2. The serine / threonine kinase c-Raf-1

Mammals possess three Raf proteins: a-Raf, b-Raf and c-Raf-1. All three Raf isoforms share Ras as a common upstream activator and MEK as the only commonly accepted downstream substrate[95,96]. The ubiquitously expressed c-Raf is certainly the best studied. Knocking out the *c-raf-1* gene in an inbred background results in death during midgestation. In an outbred strain, c-Raf-1 knock-out mice die shortly after birth, showing general growth retardation and developmental defects that are most apparent in placenta, lung and skin. Overall, the phenotype of the knock-out mice are reasonably consistent with the expression data, and

indicate that c-Raf-1 serves a general role in tissue formation[92]. Overexpression of c-Raf-1 induces adenomas in murine lung[97].

Inactive c-Raf-1 is localized in a multi-protein complex of 300-500 kDa[98]. Ras can interact with two domains in the c-Raf-1 N-terminus: the Ras-binding domain (RBD; amino acids 55-131) and the cysteine-rich domain (CRD; amino acids 139-184)[99,100]. Cell culture experiments have shown that deletion of the NH_2-terminal regulatory domain leads to a constitutively active kinase that is highly oncogenic in animals as well as in cultured cells[101,102].

Kerkhoff and colleagues have generated transgenic mice [(C57BL/63DBA-2)F1] expressing the wild-type human c-Raf-1 protein or the oncogenically activated NH2-terminal deletion mutant c-Raf-1-BxB under the control of human *SP-C* promoter (Fig. 11). c-Raf-1-BxB is a constitutively active c-Raf-1 kinase and is highly transforming in cell culture experiments[103,104]. In mice, the *SP-C* gene is expressed in type II epithelial cells lining the lung alveoli[105-107]. The promoter region of the human *SP-C* gene has been shown to direct the expression of chimeric genes in transgenic animals in a lung epithelial cell-specific manner[106]

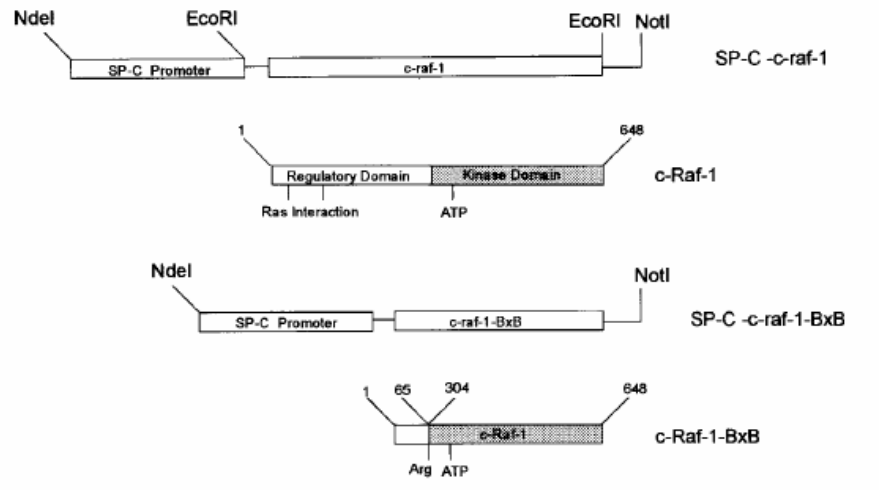

Figure 11: Structure of the c-Raf-1 and c-Raf-1-BxB proteins[108]

Structure of the c-Raf-1 and c-Raf-1-BxB proteins and recombinant DNA constructs directing the expression of the *raf* sequences under the control of the *SP-C* promoter. For the generation of transgenic mice, expression cassettes of the *SP-C*-c-*raf*-1 or *SP-C*-c-*raf*-1-BxB vectors were released by digestion with the *Nde*I and *Not*I restriction endonucleases. The purified DNA fragments were injected into fertilized eggs of C75BL/63DBA-2 F1 mice. The c-Raf-1-BxB protein lacks the regulatory NH_2-terminal sequences of the c-Raf-1 protein, including the Ras interaction domain. In contrast to the wild-type c-Raf-1 kinase, which requires activating upstream regulators, the c-Raf-1-BxB kinase is constitutively active. In mice, the *SP-C* gene is expressed in type II epithelial cells lining the lung alveoli[105-107].

The group around Kerkhoff showed that lung-targeted overexpression of c-Raf-1 protein in transgenic mice leads to the development of lung adenomas within 1 year of age[108].

In this work we were specifically interested in the role of TAMs in c-Raf-1 induced lung cancer biology and therefore examined whether a depletion of TAMs in this transgenic mouse model could ba achieved by an infection with *Shigella*.

II.8. Goal of the project

The goal of this project is to analyse the distribution of attenuated *Salmonella* and *Shigella* after i.v. application in tumors with high numbers of macrophages. For this reason we wanted quantitatively determine the bacterial counts of bacteria in the extracellular space or within tumor cells, distinguishing between the macrophage and non-macrophage fraction. We wanted to show that TAMs are the primary target of bacteria like *Salmonella* and *Shigella* in a 4T1-induced and a transgenic MMTV-HER2/new breast cancer model. We also wanted to investigate whether metabolically attenuated, virulent *Shigella* strains, but not avirulent *Shigella* strains or *Salmonella*, are able to activate caspase-1 and induce apoptosis in TAMs at all time points in both breast cancer models. In addition we wanted to find out whether this unrestricted apoptosis induction causes a substantial depletion of TAMs, which could be correlated with a therapeutic effect. Finally, we wanted to investigate if apoptosis induction by *Shigella* could be confirmed *ex vivo* in freshly isolated TAMs from mouse lung adenomas and a human ovarian carcinoma.

III. Material

III.1. Instruments

Instrument	Manufacturer
Bacterial incubator	Heraeus B 6200
Bacterial shaker	Scientific innova 4330 New Brunswick
Bacterial shredder	Fast Prep FP120 Thermo Electron Corporation
Cell culture incubator	Heraeus Instrument
Cell culture microscope	Leica
Cell counter chamber	Bürker
Clean bench	Heraeus
Developing cassette	Dr. Goos-suprema GmbH
Developing machine	Agfa
DNA Sequencer	ABI PRISM 373 ABI
Electrophoresis power supply	Bio-Rad
Electrophoresis unit	small Bio-Rad
Freezer (-20°C)	Liebherr
Freezer (-80°C)	Nunc Advantage
Fridge (4°C)	Liebherr
Gene pulser	Bio-Rad
Horizontal electrophoresis gel	PEQLAB
Heat block	Liebisch
Ice machine	Scotsman
Mega centrifuge	J-6B Beckman; Megafuge 1.0 R Heraeus
Microwave	Siemens
Mini centrifuge	5417R, Biofuge 15 Eppendorf; Heraeus
Mini-Protean II Fine scale	Bio-Rad
Pipettes	Eppendorf
Thermocycler	T-Gradient Thermoblock Biometra
Timer	Roth
Vortex genie	Scientific industries
FACS machine	Becton Dickinson
pH-meter	Microprocessor, WTW
MACS® permanent magnet	Miltenyi Biotec GmbH
MACS® mini columns	Miltenyi Biotec GmbH

III.2. Chemical reagents

Reagent	Manufacturer
1 kb DNA ladder	Invitrogen, MBI
Adenosin-5'Triphosphate (ATP)	Sigma
Agarose, ultra pure	Invitrogen
Ammonium Acetate	Sigma
Ammonium peroxydisulfate (APS)	Sigma
Avertin	Sigma
Bacto-Agar	Roth
Bovine serum albumin (BSA)	Sigma
Bromphenolblue	Sigma

Reagent	Manufacturer
β-Mercaptoethanol	Roth
Caspase-1 inhibitor YVAD-CHO (2,5 mM)	Bio Cat
Congo red dye (Cr)	Sigma
Diaminobenzidin (DAB)	Sigma
dNTPs	MBI
Entellan	Merck
Eosin	Sigma
Ethylenediaminetetraacetic acid-disodium salt (EDTA)	Fermentas
Ethanol	Roth
Ethidiumbromide	Invitrogen
Gentamicin	Sigma
Giemsa dye	Sigma
Glycerol	Sigma
Hematoxylin	Sigma
Hoechst 33342 dye	Sigma
Isopropanol	Merck
Kanamicin	Sigma
L-arabinose	Sigma
Mowiol	Calbiochem
Ponceau	Sigma
Protein ladder, BenchMark TM	Invitrogen, MBI
SeaPlaque Agarose	Biozym Scientific GmbH
SDS ultra pure	Roth
Staurosporine (4 µM)	Sigma
TEMED	Roth
Triton X-100	Sigma
Trypanblue	Sigma
Trypticase soy agar (1.2 % agar) (TSA)	Difco Laboratories
Xylol	Roth

III.3. Buffers and Solution

Name	Composition (Concentration)	Manufacturer
Acrylamide/Bis solution	40 % Acrylamide/N,N'-metylene-bis-acrylamide, 37.5:1 (2.6 % C), pre made solution	Bio-Rad
Ampicillin stock	100 mg/ml Ampicillin in water	Sigma
Carbonate buffer	7 g/l sodium hydrogen carbonate	Applichem
Carbonate buffer pH 9.6	4.2 g/l sodium hydrogen carbonate 5.3 g/l di-sodium hydrogen carbonate	Sigma
Chloramphenicol stock	20 mg/ml Chloramphenicol in ethanol	Sigma
Coomassie Protein	pre made solution	Thermo Scientific
Erythrocyte-Lysisbuffer	100 ml 50 mM Tris, pH 7.65 900 ml 155 mM ammonium chloride, pH 7.2	Applichem
G418 (geniticin)	50 mg/ml G418 sulphate in water	Sigma
Gentamicin	50 mg/ml Gentamycin in water, pre	Sigma

Name	Composition (Concentration)	Manufacturer
	made	
Kanamycin stock	25 mg/ml Kanamycin in water	Sigma
Laemmli buffer	50 mM Tris-HCl pH 6.8, 10 % glycerol, 5 % β-mercaptoethanole, 2 % sodium dodecyl sulphate (SDS), 0.05 % bromphenol blue	Sigma, , Applichem Roth
6 x DNA-loading buffer	1 mg/ml bromophenol blue, 2 mg/ml xylene cyanol FF, 400 mg/ml sucrose	Sigma Sigma
Phosphate buffered saline (PBS)	ready made, 9.55 g/l	Applichem
PBS milk	PBS, 5 % nonfat dried milk powder	Applichem
PBS TWEEN	PBS, 0.05 % TWEEN	Roth
SDS PAGE buffer	3 g/l Tris, 14.4 g/l, 1 g/l SDS	Applichem
Stripping Buffer	1 M glycine, 1 % SDS; Adjust pH to 2.5 with HCl	Applichem Applichem
TBE buffer	ready made, 20 ml/l	Applichem
Towbin buffer	3 g/l Tris, 14.4 g/l, 20 % methanol	Applichem

III.4. Enzymes

Items	Manufacturer
BioTherm Taq DNA polymerase	Genecraft
Pfu polymerase	Stratagene
DNAse	Fermentas
Dispase	Invitrogen

III.5. Consumable Material

Name	Manufacturer
96-well plates	Nunclon A/S, Greiner bio-one
Cell culture flasks; 75 cm^3 and 125 cm^3	Greiner bio-one
Cell culture plates; 24 wells	Greiner bio-one
Gene pulser cuvette, 0.1 cm electrode gap	Bio-Rad
Cryo.s tubes 1.5 ml	Greiner bio-one
Insulin syringe	Braun
Micro tube; 1.5 ml, 2 ml	Sarstedt
Nitrocellulose; Hybond ECL	Amersham
Parafilm	Hartenstein
Pasteurpipettes	Hartenstein
Petri dish, 12 cm	Greiner bio-one
Pipette ipps	Hartenstein
Sterile filter Millex-GS; 0.22 µm	Millipore
X-ray film	Amersham

III.6. Molecular weight standards

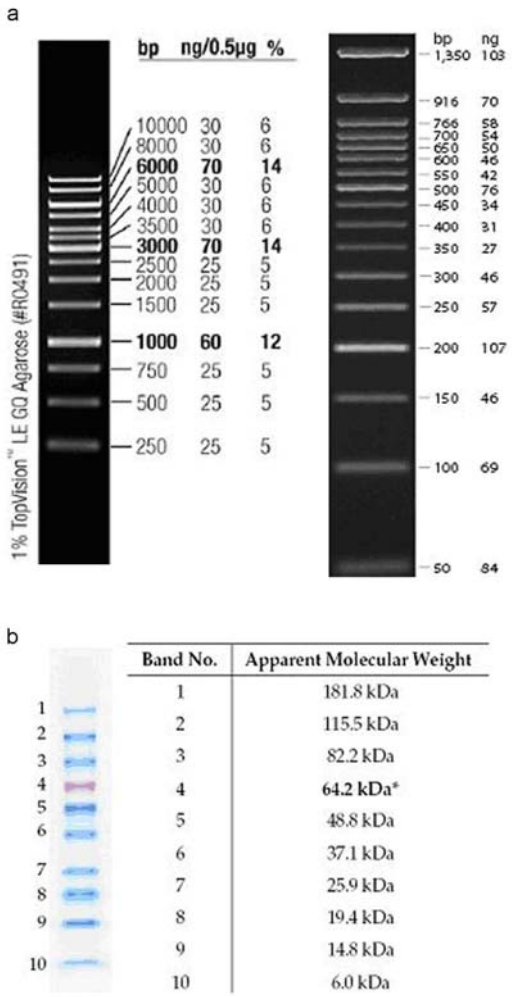

Figure 12: Molecular weight standards

a) Molecular weight standards for DNA: Gene Ruler TM 1 kb-DNA-Ladder (Fermentas) (left) and New England BioLabs 50 bp-DNA-Ladder (right). **b**) Molecular weight standards for proteine: BenchMark™ Pre-Stained Protein Ladder (Invitrogen)

III.7. Cell culture media

Items	Manufacturer
RPMI 1640 with L-Glutamin	Gibco
Minimal Essential Medium	Invitrogen
Trypsin/EDTA	Gibco
L-Glutamin, 200 mM (100x)	Gibco
MEM non-essential amino acids, 100x	Invitrogen
MEM Natriumpyruvat, 100 mM	Invitrogen
Natriumbicarbonat 7,5 %	Invitrogen
Dulbecco`s Mod Eagle Medium (DMEM) with high glucose	Gibco
Dulbecco`s PBS	Gibco
Fetal calf serum (FCS)	Pan Biotech GmbH

III.8. Chemicals

All Chemicals not mentioned elsewhere were obtained from Sigma, Difco, Roth or Applichem.

III.9. Antibodies used for Western Blot analysis, Cell separation (MACS®), FACS analysis and Histology

Antibodies for Western Blot analysis	Manufacturer
Anti-caspase-1 (ICE, rabbit polyclonal)	Sigma
Anti-cleaved PARP (cPARP, mouse polyclonal)	BD Pharmingen
Anti-GAPDH (mouse polyclonal)	Chemicon international
Anti-β-actin (rabbit polyclonal)	Sigma
Anti-rabbit IgG conjugated peroxidase	GE heltcare
Anti-mouse IgG conjugated peroxidase	GE heltcare

Antibodies for MACS® Technology	Manufacturer
Anti-mouse F4/80 (rat monoclonal, clone BM8)	Acris Antibodies GmbH
Anti-human F4/80 (rat monoclonal, clone BM8)	Santa Cruz
Anti-rat IgG antibody, labelled with magnetic beads	Miltenyi Biotec GmbH

Antibodies for FACS	Conjugated	Manufacturer
Anti-mouse CD11b	Fluorescein isothiocynate (FITC)	Miltenyi Biotec GmbH
Anti-mouse Gr-1	Phycoerythrin (PE)	Miltenyi Biotec GmbH
Anti-mouse F4/80	Phycoerythrin (PE)	Acris Antibodies

→ As isotype controls we used a mouse IgG_{2B} Isotype (R & D Systems) conjugated with either phycoerythrin (Clone 133303) or fluorescein (Clone 133303)

Antibodies for fluorescence microscopy	Conjugated	Manufacturer
Anti- mouse monoclonal Cytokeratin (clone AE1+AE3)		Abcam
Anti-mouse IgG	Tetramethyl Rhodamine Iso-Thiocyanate (TRITC)	Dianova

Antibodies for Histology	Conjugated	Manufacturer
Anti- mouse F4/80 (rat monoclonal, clone BM8)		Acris Antibodies GmbH
Anti- mouse CD45 (rat monoclonal, clone 30-F11)		BD Pharmingen
Anti- cow Cytokeratin (rabbit polyclonal)		DAKO
Anti-rat IgG	Peroxidase	Vector Laboratories
Anti-goat IgG	Biotin	DAKO

III.10. Kits

Items	Manufacturer
ECL™ Western blotting detection reagents	Amersham
QIAEX® II Gel Extraction Kit	Qiagen
QIAGEN® Plasmid Kit (Mini, Midi, Mega)	Qiagen
QIAquick® PCR purification Kit	Qiagen
RNeasy® Mini Kit	Qiagen
First Strand® cDNA Synthesis Kit	Fermentas
Peroxidase-based detection kit	Vector Laboratories

III.11. Software

Program	Manufacturer
CellQuest Pro 4	BD
GraphPad Prism 4	GraphPad Software, Inc
MS Excel 2003	Microsoft
MS Word 2003	Microsoft
Photoshop CS2	Adobe
Improvision Openlab 3.1.7.	Apple

III.12. Bacterial strains

Bacteria strain	Relevant characteristics	References
Salmonella enterica serovar. Typhimurium *aroA* SL7207 $pTolC_{Kan}$	*his*G46, DEL407 [*aroA*544::Tn10 (Tc. S.)][84]	Stocker, BAD, 2000[84]
Shigella flexneri M90T serotype 5a	[streptomycin (Sm) resistant][109,110]	Maurelli, AT, 1984[110]; Allaoui, A, 1992[109]
Shigella flexneri M90TΔaroA serotype 5a	[streptomycin (Sm) resistant][109,110], *AroA*-deletion	This work
Shigella flexneri BS176 serotype 5a	noninvasive variant of *M90T*, lacking the virulence plasmid pWR100[23,111]	Sansonetti, PJ, 1982[111]; Buchrieser, C, 2000[23];
Shigella flexneri BS176ΔaroA serotype 5a	noninvasive variant of *M90T*, lacking the virulence plasmid pWR100[23,111], *AroA*-deletion	This work
DSM 21058	*Shigella flexneri M90TΔaroA serotype 5a,* Patented strain (Patent 08-01Z) deposited at German Collection of Microorganisms and Cell Cultures, [streptomycin (Sm) resistant][109,110], *AroA*-deletion	This work

→Trypticase soy agar (1.2 % agar) (TSA) containing 100 mg of Congo red dye (Cr) per litre was used to select Cr+ clones of *Shigella* spp.[110]

III.13. Cell lines

Cell line (culture medium)	Source
B78-D14 (1640 RPMI +2 mM L-glutamin + 10 % (v/v) FCS + 10 µl/ml Hygromycin B + 8 µl/ml G418)	Rymsa, B[112]; Lode H N[113]
4T1 (1640 RPMI + 2 mM L-glutamin + 10 % (v/v) FCS)	ATCC: CRL-2539
P815-PSA (RPMI 1640, 10 % fetal bovine serum + 1x MEM non-essential amino acids + 1 mM sodium pyruvate + 2 mM L-glutamine + 50 mM β-mercaptoethanol + 10 µl/ml Hygromycin B + 8 µl/ml G418)	Fensterle, J[114]
HeLa	ATCC CCL-2
RAW 264.7 (RPMI 1640, 10 % fetal bovine serum + 1x MEM non-essential amino acids + 1 mM sodium pyruvate + 2 mM L-glutamine + 50 mM β-mercaptoethanol)	ATCC TIB-71
J774A.1 (1640 RPMI + 2 mM L-glutamin + 10 % (v/v) FCS)	ATCC TIB-67

III.14. Mouse lines

Mouse line	Source
BALB/cOIaHsd	**Harlan Winkelmann GmbH**
C57BL/6JOIaHsd	Harlan Winkelmann GmbH
DBA/2	Harlan Winkelmann GmbH
MMTV-HER2/new FVB	The Jackson Laboratory[88]
SP-C-c-RAF-BXB-11	MSZ (Würzburg)[108]

→ All procedures involving mice were conducted in accordance with the Regierung von Unterfranken (Würzburg, Germany). All animals were housed at the Institut für Medizinische Strahlenkunde und Zellforschung (MSZ) animal care facility.

III.15. Liquid medium and agar plates for *E. coli*, *S. typhimurium* and *S. flexneri* cultures

Items	compounds
LB medium	10 g bacto trypton 5 g yeast extract 10 g NaCl

⇨ The pH of the medium was adjusted to 7.0 with 10 M NaOH. The total volume was added up to 1000 ml with dH_2O and autoclaved at 121 °C, 15 psi for 20 min

BHI medium	37 g BHI

⇨ Powder was dissolved in 1000 ml dH_2O and autoclaved at 121 °C, 15 psi for 20 min

LB Agar Plates	10 g bacto trypton 5 g yeast extract

Items	compounds
	10 g NaCl 15 g agar

⇨ Components were dissolved in 1000 ml dH_2O and autoclaved at 121 °C, 15 psi for 20 min. After autoclaving, the medium was cooled down to 60 °C to add respective antibiotic, immediately distributed in bacteria dishes under the laminar hood and allowed to solidify at RT. The plates were stored at 4 °C.

BHI Agar Plates
37 g BHI
15 g agar

⇨ Components were dissolved in 1000 ml dH_2O and autoclaved at 121 °C, 15 psi for 20 min. After autoclaving, the medium was cooled down to 60 °C to add respective antibiotic, immediately distributed in bacteria dishes under the laminar hood and allowed to solidify at RT. The plates were stored at 4 °C.

III.16. Plasmids

Name	Relevant characteristics	References
$pTolC_{Kan}$	KanR, copie of *TolC*	Hotz, C, unpublished
pKD3	CmR, π dependent, chloramphenicol resistance gene, flanked by FLP recombinase recognition sites (FRT sites)[115]	Datsenko, KA, 2000[115] (Andersen, C; Würzburg)
pKD4	KanR, π dependent, kanamycin resistance gene, flanked by FLP recombinase recognition sites (FRT sites)[115]	Datsenko, KA, 2000[115] (Andersen, C; Würzburg)
pCP20	Ampicillin and CmR plasmid that shows temperature-sensitive replication and thermal induction of FLP synthesis[116]	Cherepanov, PP, 1995[116] (Andersen, C; Würzburg)

III.17. Primers

Name	Sequence (5`→ 3`) (Source: MWG)
AroA_up	GGGGTTTTTATTTCTGTTGTAGAGAGTTGAGTTCATGGAATCGTGTAGGCTGGAGCTGCTTC
AroA_down	GGCCGTGCATTTGGGATCAAGAATCGTCACTGGTGTATCTGCATATGAATATCCTCCTTA
AroAFr_up	GATTTCTACCGCAATGACG
AroAFr_down	GGAAACAAGTGAGCGTTTC
C1	TTATACGCAAGGCGACAAGG[115]
C2	GATCTTCCGTCACAGGTAGG[115]
K1	CAGTCATAGCCGAATAGCCT[115]
K2	CGGTGCCCTGAATGAACTGC[115]
Casp1RT_left	TGCCCTCATTATCTGCAAC
Casp1RT_right	GGTCCCACATATTCCCTCCT
actin s1	GTCGTACCACAGGCATTGTGATGG
actin as	GCAATGCCTGGGTACATGGTGG
pWR100_up	GATGCAGGCCAAGAGGTTAG
pWR100_down	GCGTTGATGACCGCATC

IV. Methods

IV.1. General cloning techniques

IV.1.1. Plasmid DNA isolation

Mini preparation of plasmid DNA: A single colony from the bacterial plate was inoculated in 5 ml LB or BHI medium supplemented with selective antibiotic and cultured overnight at 37 °C, 190 rpm/min in a shaking incubator. Mini preparation of plasmid DNA was done according to the instructions of Qiagen (Plasmid mini kit). Plasmid DNA was dissolved in dH_2O and stored at –20 °C.

Midi preparation of plasmid DNA: A single colony from the bacterial plate was inoculated into 50 ml of LB or BHI supplemented with antibiotic and cultured overnight at 37 °C, 190 rpm/min in a shaking incubator. Plasmid DNA was isolated using Qiagen kit (Plasmid midi kit). Plasmid DNA was dissolved in dH_2O and stored at –20 °C.

Mega preparation of plasmid DNA (endotoxin free): A single colony from the bacterial plate was inoculated into 500 ml of LB or BHI supplemented with antibiotic and cultured overnight at 37 °C, 190 rpm/min in a shaking incubator. Plasmid DNA was isolated using Qiagen kit (EndoFree Plasmid mega kit). Plasmid DNA was dissolved in PBS endotoxin free and stored at –20°C.

IV.1.2. DNA quantification

DNA samples were diluted 1:25 – 1:50 depending on estimated concentrations. DNA concentration was determined by measuring the absorbance at λ = 260 nm (A_{260}) in a spectrophotometer using a quartz cuvette. The concentration was calculated based on the DNA coefficient of 1 unit at 260 nm being equal to 50 µg/ml DNA. The purity of the DNA was determined by analysis of the A_{260}/A_{280} ratio.

IV.1.3. DNA agarose gel electrophoresis

Agarose gel electrophoresis was employed to check the progression of a restriction enzyme digestion, to quickly determine the yield and purity of a DNA isolation or PCR reaction and

to size fractionate DNA molecules, which then could be excised from the gel. An agarose gel was prepared according to the protocol described by Sambrook and Russel[117] and after cooling down to 50 °C ethidium bromide (Roth) was added to a final concentration of 1 µg/ml. DNA samples were electrophoreted in 1 x TBE buffer (180 V, 30-40 min).

IV.1.4. Gel extraction

The desired DNA fragment was quickly extracted from an agarose gel using a scalpel under low strength UV light (λ=300 nm) to limit DNA damage. The gel slice was then purified using the Qiagen Gel Extraction kit (Qiagen). The gel slice was accordingly solubilized for 10 min, or until completely dissolved, at 50 °C in a buffer containing chaotropic salts.

IV.1.5. General PCR method

PCR is an enzymatic method for *in vitro* synthesis of multiple copies of specific sequences of DNA. The reaction mixture for general PCR containing the following components:

template-DNA	1-5 µl
primer 1 (10 pmol/µl)	0,5 µl
primer 2 (10 pmol/µl)	0,5 µl
25 mM $MgCl_2$	2 µl
10 mM dNTPs	0,5 µl
10 x PCR buffer	5 µl
Taq polymerase	0.5µl
dH_2O	up to 50 µl

The PCR mixture was immediately incubated in thermocycler for amplification using cycling programm as follows:

1.	95°C	3 min	denaturation
2.	95°C	1 min	denaturation
3.	50°C	1 min	annealing
4.	72°C	90 sec	elongation
5.	72°C	3 min	
6.	4°C	break	

30 CYCLES

The annealing temperature is dependent on primers, normally 5-10 °C below the T_m of the primers. The time of elongation is determined taking into account of the characteristic of the polymerase and the length of desired DNA fragments. *Taq* polymerase can synthesize 1 kb of DNA in 1 min, and *Pfu* polymerase requires 2 min to synthesize 1 kb of DNA. In this work *Taq* polymerase was used for screening.

IV.1.6. Purification of PCR products

Purification of DNA fragments like PCR products or restriction digests was carried out using the Qiagen PCR purification kit. The purification principal is based on the adherence of the DNA to a silica-gel covered membrane in a spin-column format. The washing steps removed nucleotides, primers and short stranded DNA molecules ensuring that only longer stranded DNA molecules were retained in the eluate.

IV.1.7. Generation of *Shigella aroA*-mutant

Gene knockout by Datsenko and Wanner[115]

Linear DNA containing antibiotic resistance genes were prepared from pKD3 using the method described by Datsenko and Wanner[115]. At first a PCR-product was generated by using primers AroAFr_up and AroAFr_down with 36 nucleotid extensions that are homologous to the *AroA*-gene. As a template, the pKD3 plasmid, which carries a chloramphenicol resistance gene flanked with FRT sites, was used. The next step was the transformation of the PCR-product in electrocompetent *S. flexneri BS176* strain, which express the lambda red recombinase. Chloramphenicol resistant colonies were then screened with primers AroA_up and AroA_down. Finally, the resistance cassette was eliminated by using the helper plasmid pCP20 carrying the flipase gene. Subsequently, the plasmid with temperature sensitive replicon was eliminated by incubation at 43 °C. The resulting strain was termed *S. flexneri BS176ΔaroA*.

To create a strain which is attenuated in growth but not in its virulence we used the engeneered strain *S. flexneri BS176ΔaroA*. Subsequently the 200 kb virulence plasmid pWR100 of *S. flexneri M90T* was isolated by the large-construct kit (QIAGEN). After that this virulence plasmid and the helper plasmid pCP20[116], carrying an ampicilin-resistance, were transformed in the already constructed *S. flexneri BS176ΔaroA* strain. After this double transformation and incubation at 30 °C overnight the ampicilin-resistant colonies were screened for the virulence plasmid pWR100 (pWR100_up 5`-GATGCAGGCC

AAGAGGTTAG-3`; pWR100_down 5`-GCGTTGATGACCGCATC-3`) and for the *aroA*-knockout (AroAFr_up 5`-GATTTCTACCGCAATGACG-3`; AroAFr_down 5`-GGAAACAAGTGAGCGTTTC-3`). This strain was termed *S. flexneri M90TΔaroA*. The pCP20 plasmid containing a temperature sensitive replicon was cured by incubation overnight at 43 °C.

IV.2. Transformation of *S. typhimurium* and *S. flexneri*

IV.2.1. Preparation of competent cells

1 ml of overnight culture was inoculated in 49 ml LB medium (1:50) in side arm flasks and grown at 37 °C with vigorous agitation (about 3 h) till to OD_{600} 0.6 – 0.8. Bacterial cells were transferred to sterile 50 ml polyproylene tubes and centrifuged at 2,000 x g for 20 min at 4 °C. The pellet was first washed with 50 ml ice-cold 10 % glycerin and centrifuged at 2,000 x g for 20 min at 4 °C. Then the pellet was washed with 25 ml ice-cold 10 % glycerin and centrifuged at 2,000 x g for 20 min at 4 °C. After that the pellet was washed again with 10 ml ice-cold 10 % glycerin and centrifuged at 2,000 x g for 20 min at 4 °C. Finally the pellet was resuspended in 0.5 ml ice-cold 10 % glycerin. These competent cells were used directly for transformation or aliquoted and stored at –80 °C.

IV.2.2. Transformation of competent cells

Electroporation was used to transform *S. typhimurium* and *S. flexneri.* It was carried out with fresh or frozen competent cells prepared as described above. 1 – 5 µl of DNA (100 ng) was added to 50 – 70 µl of competent cells on ice. After a short incubation of 1 min on ice the mix was gently transferred to pre-chilled 0.1 cm electroporation cuvette and electroporated (Bio-Rad, Gene Pulser at 1.8 kV, 25 µF and 200 Ohm, program: bacteria). After electroporation the cells were immediately resuspended in BHI medium and then gently transferred into a sterile 1.5 ml tube. After 1 h of incubation at 37 °C, the cell suspension was plated on selective agar-plates and incubated at 37 °C overnight.

IV.3. Preparation of bacteria infection aliquots

For the production of bacteria aliquots for an *in vivo* infection of mice the *Salmonella* strains from the respective glycerolstocks were freshly plated out on LB agar-plates with appropriate

antibiotics. The next day an overnight culture was generated from a single colony. The strains have to be cultivated up to an optical density (OD_{600}) of 1.0-1.5. Subsequently, the work must be continued on ice, so that a further growth is prevented. The bacteria cells were pelleted with 2,000 x g and 4 °C for 20 min and washed twice with 20–40 ml of steril ice-cold PBS. After the second wash step the pellet was resuspended in 10 ml ice-cold PBS with 20 % final concentration glycerol, aliquoted to 1 ml portions and frozen at –80 °C. Two days before the infection two aliquots were thawed in each case in order to determine the bacteria's number per ml. The bacteria's number is calculated thereby as follows:

Bacteria's number / ml (CFU) = number of colonies × number of dilutions of 10 times × 10

For *in vitro* infections of eukaryotic cells *Salmonella* grown to stationary phase were used, if not indicated otherwise. Bacteria were washed three times in ice cold PBS (2,000 x g, 10 min, 4 °C) and then bacteria`s number / ml (CFU) were determined.

Shigella strains were freshly plated on LB agar plates with appropriate antibiotics from the respective glycerolstocks for infection. The next day an overnight culture was manufactured from a single colony. The strains were cultivated up to an optical density (OD_{600}) of 0.8-1.0. OD_{600} of 1 means approximately 1 x 10^8 bacteria. Bacteria were washed three times in ice cold PBS (2,000 x g, 10 min, 4 °C) and then bacteria`s number / ml (CFU) was determined as described previously.

IV.4. Gene expression analysis

IV.4.1. RT-PCR

Up to 1 x 10^7 cells of every cell line (B78-D14, 4T1 and J774A.1), were disrupted in RLT buffer and homogenized by the protocol of Rneasy® Mini Kit (Qiagen) for RNA isolation. The cDNA synthesis was performed by the protocol of First Strand® cDNA Synthesis Kit (Fermentas). DNA concetration was determined as described before. Subsequently PCR was peformed with *Taq* Polymerase. To determine caspase-1 expression the primers Casp1RT_left 5`-TGCCCTCATTATCTGCAAC-3` and Casp1RT_right 5`-GGTCCCACATATTCCCTC CT-3` were used. The *ß-actin*-gene was used as a control (Primer: actin s1: 5`-GTCGTACCACAGGCATTGTGATGG-3` and actin as 5`-GCAATGCCTGGGTACAT GGTGG-3`).

IV.4.2. SDS-PAGE separation and Western Blot analysis of proteins

Shigella-infected or uninfected cells from six-well cell culture dishes were washed twice with PBS and lysed in 120 µl of 2 x Laemmli buffer. Insoluble material was removed by centrifugation (20,000 *g* , 5 min, 4 °C). The supernatants were removed and the cell pellets were resuspended in Laemmli buffer with β-mercaptoethanol.

For immunoblotting, 10 – 30 µl of lysates were separated. SDS-PAGE of the extracted proteins was performed essentially as described by Laemmli[118], but using the apparatus and methods from Bio-Rad. Briefly, a 1.0 mm or 0.75 mm thick discontinuous gel was cast using a 10 % running gel overlayed with a 4 % stacking gel. The gel was loaded with appropriate protein suspensions and a weight marker for comparison and run for 1-2 h at 0.04 mA.

Whole proteins were separated by SDS-PAGE[118] and analysed by immunoblotting. The separated proteins were transferred to nitrocellulose filter according to the method of Towbin[119]. After the blotting the nitrocellulose membrane was treated for 2 h with 5 % mager-milk (Applichem) in order to block all the idrophobic sites. Subsequently, the proteins were probed with anti-caspase-1, anti-PARP, anti-β-actin or anti-GAPDH antibody and were incubated overnight at 4 °C. Then the membrane was washed with PBS-Tween (washing buffer) three times for 10 min. The bound antibodies were detected respectively by addition of anti-rabbit and anti-mouse horseradish peroxidase conjugated immunoglobulins. These were incubated 2 h at room temperature. After this time the membrane was washed with PBS-Tween three times for 30 min, then the bound antibodies were followed by ECL detection kit.

Components of a Laemmli gel:

	20 ml running gel						10 ml stacking gel
	5 %	6 %	7,5 %	10 %	12 %	12,5 %	
Acrylamid/ Bisacr. 40 %	2,7 ml	3,2 ml	3,8 ml	5 ml	6,2 ml	6,5 ml	1,1 ml
dH_20	14,4 ml	13,9 ml	13,3 ml	12,1 ml	10,9 ml	10,6 ml	7,55 ml
3M Tris pH 9,0	2,5 ml						1M Tris pH 6,8 1,25 ml
20 % SDS	100 µl						50 µl
TEMED	20 µl						10 µl
10 % APS	200 µl						100 µl

IV.4.3. Stripping of the nitrocellulose membrane

Stripping is the term used to describe the removal of primary and secondary antibodies from a nitrocellulose membrane membrane. Stripping is useful when one wants to investigate more than one protein on the same blot, for instance a protein of interest and a loading control like GAPDH or β-actin. Stripping of the nitrocellulose membrane was performed by incubating in stripping buffer for 15 min two times. Subsequently there is a short incubation time in tap water and 5 min in PBS/Tween. After that the nitrocellulose membrane is ready for blocking stage described previously.

IV.5. *In vitro* experiments

IV.5.1. Fluorescence microscopy of cells

4T1 cells and RAW 264.7 macrophages were grown on coverslips for 36 h in 10 % fetal calf serum plus RPMI medium 1640. After two washings with icecold PBS, cells were fixed for 15 min with 3.7 % paraformaldehyde at room temperature. After 5 min quenching with 10 mM NH_4Cl in PBS, the primary antibody (Mouse monoclonal to pan Cytokeratin, prediluted) was incubated for 30 min with cells. After three washes with PBS, Tetramethyl Rhodamine Iso-Thiocyanate (TRITC)-labeled secondary antibody (dilution 1:200) were diluted in PBS/BSA and incubated with cells for 30 min. After three washes with PBS, the cells were treated with 0.1 µg/ml Hoechst 33342 dye for 30 min. Excess dye was washed out with PBS and water. The cells were covered with Mowiol and subjected to fluorescence microscopy.

IV.5.2. HeLa cell invasion- and survival assay

Invasion and survival in HeLa cells was assessed using a modified gentamicin protection assay as previously described[120]. HeLa cells grown to semiconfluence were trypsinized and adjusted to 2 x 10^5 cells/ml. Six-well plates were seeded with 2 ml of HeLa cell suspension and incubated overnight to reach 90 % confluence. HeLa cells were washed, and medium was changed 2 h before the addition of bacteria. Log-phase (OD_{600}: 0.6 – 0.8) cultures of *Shigella* (grown in LB medium) were added at an estimated MOI of 100 and plates were incubated at 37 °C for 1 h. Subsequently plates were washed three times with PBS and then incubated with DMEM containing gentamicin (100 µg/ml) for 1 h at 37 °C in 5 % CO_2. HeLa cells were

lysed in a 0.1 % Triton X-100 solution for 10 min at different time points and CFU was determined by plating serial dilutions on agar plates and by counting the colonies.

IV.5.3. Intra- and intercellular growth assay

IV.5.3.1. Giemsa staining

To study bacterial intracellular multiplication and behavior of cell-to-cell spreading histologically, Giemsa staining of the cells was performed. Briefly, HeLa-cells (1 x 10^5) in 45 mm diameter tissue culture plates on coverslips (Ø 20 mm) infected at a multiplicity of infection of 100 for 1 h, were washed two times with PBS and fixed for 5-7 min with methanol at room temperature. Plates were air dried and stained for 20 min with Giemsa dye (1:20). Afterwards the plates were washed three times with distilled water, they were air dried and observed under oil immersion. Time points of 1 h and 4 h *p.i.* were examined.

IV.5.3.2. L-Top agar assay (Cell to cell spreading assay)

To determine cell to cell spread with a growth attenuated strain a new assay was employed. HeLa cells (7 x 10^5 per well) in grown in 6-well tissue culture plates were infected at a MOI of 500 for 1 h and then washed twice with PBS. Infected cells were irradiated at 20 Gy. Subsequently, a monolayer of uninfected HeLa cells grown in 6 well plates were incubated with the irradiated *Shigella*-infected HeLa cells in a ratio of 70 : 1 for 2 h, 8 h and 12 h. After 1 h incubation with 100 µg/ml gentamicin, the concentration of gentamicin was reduced to 10 µg/ml. At all time points the number of infected cells was determined by plating serial dilutions on agar plates and by counting the colonies.

IV.5.4. Assay for apoptosis induction

IV.5.4.1. *In vitro* activation of caspase-1

1 x 10^6 RAW 264.7 macrophages per well were seeded and incubated overnight at 37 °C and 5 % CO_2. The next day the macrophages were infected at a MOI of 10 with *S. flexneri M90T*, *S. flexneri M90TΔaroA* (both mid-logarithmic growth phase) and *S. typhimurium* ΔaroA (stationary growth phase) for different time points (1 h, 2 h and 3 h *p.i.*). Subsequently, a Western Blot analysis for caspase-1 activation of the cell lysate was performed.

IV.5.4.2. *In vitro* activation of caspase-1 and induction of apotosis by *aroA*-mutants

To determine the capacity of the *S. flexneri ΔaroA*-mutants to induce caspase-1 activation and apoptosis, 1 x 10^6 J774A.1 mouse macrophages per well were seeded and incubated overnight at 37 °C at 5 % CO_2. Next day macrophages were infected at a MOI of 100 of *S. flexneri M90T*, *S. flexneri M90TΔaroA* and *S. flexneri BS176ΔaroA* (all mid-logarithmic growth phase). After 1 h of infection, cells were incubated for 1 h with 300 µg/ml gentamicin. Then the concentration of gentamicin was reduced to 10 µg/ml for 1 h. After that the cellular lysates were analyzed by Western Blot analysis at different time points using an anti-caspase-1 antibody recognizing the active 20 kDa fragment of caspase-1 and an anti-PARP antibody recognizing the cleaved 85 kDa fragment described as cPARP. Cleaved PARP is an approved marker for apoptosis[121]. The caspase-1 specific inhibitor YVAD-CHO was used as control. β-actin was used as loading control.

IV.5.4.3. Hoechst 33342 staining

To investigate induction of apoptosis histologically we stained with Hochst dye. Hoechst 33342 is a cell-permeant nuclear counterstain that emits blue fluorescence when bound to dsDNA. This dye is often used to distinguish condensed pycnotic nuclei in apoptotic cells. Hoechst dyes preferentially bind to AT regions of the DNA. These probes are UV excited (346 nm maximum) and emit maximally at around 460 nm (violet/blue). Hoechst 33342 has the advantage of being cell membrane permeant and can, therefore, stain nuclei in living cells as well as fixed cells.

J774A.1 macrophages were infected with the different *Shigella* strains for 1 h at a MOI of 100. After that cells were washed three times with PBS and incubated for 1 h with 100 µg/ml gentamicin. Subsequently macrophages were incubated for 1 h with 50 µg/ml gentamicin. As positiv control for apoptosis induction we used macrophages incubated with 4 µmol/l staurosporine for 6 h. Not infected J774A.1 macrophages were used as negativ control. After that, cells were fixed for 10 min in 4 % para-formaldehyde at room temperature. Then we washed three times with PBS. Subsequently macrophages were stained with Hoechst 33342 dye and incubated for 10 – 15 min at room temperature or 37 °C. After that we rinsed three times with PBS. Subsequently stained cells were mounted in antifade mounting medium (Mowiol). Mounted cells were stored overnight in the dark at 4 °C.

IV.5.5. Gentamicin assays

The gentamicin (an aminoglycoside antibiotic) survival assay is the most frequently used method for measuring eukaryotic host cell penetration by bacteria. The specificity of the assay for the enumeration of intracellular bacteria depends on the antibiotic's limited penetration of the eukaryotic cell[122,123]. Thus, bacteria that have penetrated eukaryotic cells are protected from the bactericidal effects of gentamicin, whereas extracellular bacteria are immediately killed by the antibiotic. For this reason, gentamicin is routinely added to experimental media and events that occur subsequent to bacterial invasion, such as cell survival and replication, are measured.

In order to find the optimal gentamicin concentration to determine the bacterial counts in the extracellular space or within tumor cells *in vivo*, distinguishing between macrophage and non-macrophage fraction, we setup three gentamicin assays.

IV.5.5.1. Extracellular activity of gentamicin

In the first gentamicin assay 1 x 10^6 *S. typhimurium* ΔaroA were treated for ½ h, 1 h and 2 h with 50, 100, 200 and 300 µg/ml gentamicin at 37 °C. Subsequently CFU was determined by plating of serial dilutions on agar plates to determine the bactericidal effect of gentamicin on extracellular *S. typhimurium* ΔaroA.

IV.5.5.2. Intracellular activity of gentamicin

In the second gentamicin assay J774A.1 macrophages were infected with 1 x 10^6 *S. typhimurium* ΔaroA (from stationary growth phase). Bacteria were washed three times with DMEM medium for 10 min at 2,000 x g and 4 °C. After 1 h of infection, cells were incubated for 1 h with 50, 100, 200 and 300 µg/ml gentamicin at 37 °C followed by a 1 h incubation with 10 µg/ml gentamicin after washing with PBS. CFU was determined after cell lysis by plating of serial dilution on agar plates.

IV.5.5.3. Gentamicin activity assay at different temperatures

In this assay 1 x 10^6 *S. typhimurium* ΔaroA were incubated overnight at 4, 25 and 37 °C to investigate the gentamicin effect on *S. typhimurium* ΔaroA at different temperatures. Next day CFU was determined by plating serial dillutions on agar plates.

IV.6. *In vivo* experiments

IV.6.1. Tumor cell transplantation

Six- to eight-week-old female mice were injected subcutaneously with either 1 x 10^4 murine 4T1 mammary cancer cells (ATCC: CRL-2539), 1 x 10^6 B78-D14^{112} melanoma cells or 1 x 10^6 P815-PSA^{124} mastocytoma cells each resuspended in 100 µl PBS into each flank of shaven abdominal skin of BALB/c, C57Bl/6 or DBA/2 mice.

IV.6.2. Monitoring of 4T1 breast tumor growth

Balb/c mice were transplanted with 1 x 10^4 4T1 breast tumor cells subcutaneously and the tumor volume was monitored every day after by a caliper. After washing in ice-cold PBS for three times, cells were counted using a Bürker counting chamber. 1 x 10^4 cells in 100 µl of the suspension were injected with a 0,4×20 mm (27 G) injection syringe into each flank of shaven abdominal skin of Balb/c mice.

.

IV.6.3. I.v. infection of tumor-bearing mice with *Salmonella* and *Shigella*

Freshly cultured *Shigella* were harvested at mid-logarithmic phase or infection aliquots from stationary phase for *Salmonella* were washed in PBS three times and diluted with PBS prior to i.v. injection. 1 x 10^6 bacteria in 100 µl of the suspension (determined by CFU) were injected with a 0,4×20 mm (27 G) injection syringe into the lateral tail vein of fixed 4T1 induced tumor-bearing Balb/c mice 14 days post cell implantation, or into 6 month old tumor-bearing female MMTV-HER2 mice.
The infected animals were daily observed and if an animal should get sick and suffer, then it was sacrificed immediately and painless.

IV.6.4. Isolation of splenocytes

To isolate and analyze splenocytes, mice were anesthetized under CO_2 atmosphere and killed via cervical dislocation. The abdomen was opened with scissor and forceps to ensure not to damage the main blood vessels. The spleen was isolated and put in PBS/BSA on ice. Then it was transfered in a 100 µm nylon cell strainer and pressed with a 5 ml syringe. The cell

strainer was washed with cold PBS/BSA until all the cells have been washed out. The effluent was collected. PBS/BSA was added up to 50 ml and centrifuged at 300 x g, 5 min and 4 °C. The supernatant was discarded and washing was repeated two times with 50 ml cold PBS/BSA. At the end cells were counted with a Bürker cell chamber.

IV.6.5. Tumor cell isolation and staining procedures for magnetic cell separation (MACS®)

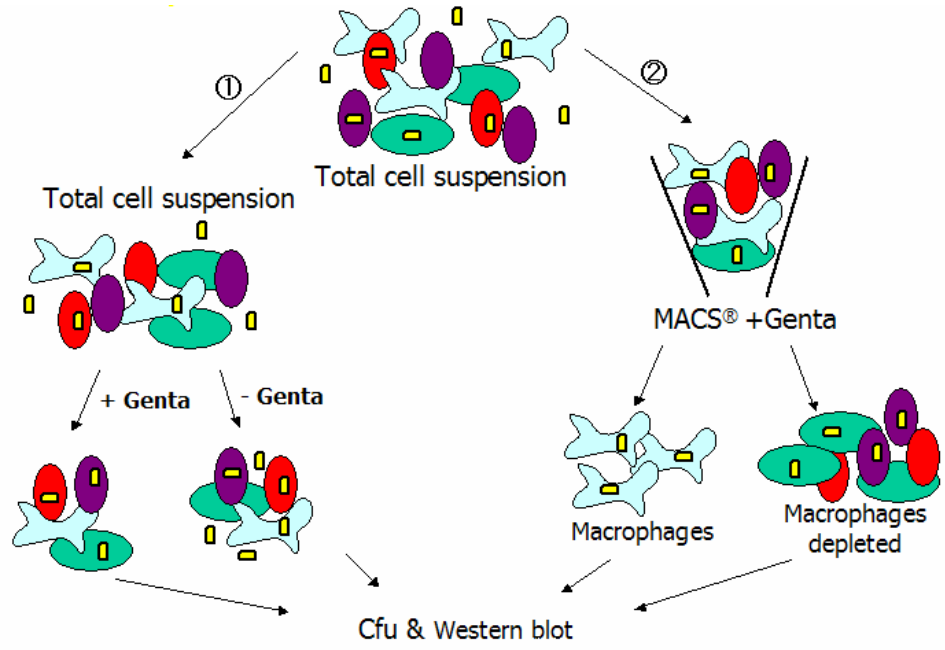

Figure 13: Experimental schedule of cell separation

Mice were sacrificed and tumors were removed, weighed and digested in 0.001 % DNase and 2 µg/ml dispase solution for 30 min at 37 °C. After that they were homogenized with 70 µm and 40 µm cell strainers. Cell numbers of every cell fraction were counted using a Bürker counting chamber. For separation of cellular populations (Fig. 13), parts of the cells were labelled with the pan-macrophage anti-F4/80 (dilution 1:10) antibody for 20 min at 4 °C. Subsequently labelled cells were stained with an anti-IgG antibody conjugated to magnetic beads (10 µl antibody per 10^7 cells) for 10 min at 4 °C. Cell separation was performed with the MACS® Kit according to the manufacturers protocol (Fig. 14). Subsequently every cell fraction was counted using a Bürker cell chamber.

Finally CFU and caspase-1 processing was assessed. For CFU counts, normalization was performed after plating (CFU/cell number, infected cells/cell number). For Western Blot analysis, equivalent cell numbers were loaded.

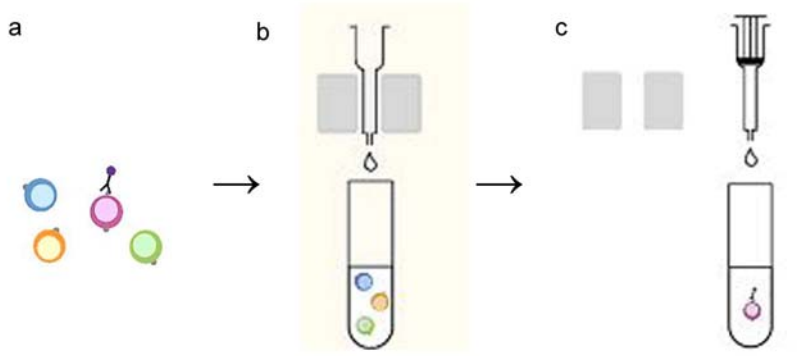

Figure 14: MACS® Technology
a) Magnetic labeling of total tumor cells
b) Magnetic cell separation
c) Elution of the labeled cell fraction (macrophages)

IV.6.6. Fluorescence activated cell sorting (FACS analysis)

Flow cytometry is an analytical tool that allows cells within a heterogeneous population to be discriminated based on their size and different structural features including cell surface molecules. Cell surface antigens can be labeled with specific antibodies coupled to a fluorochrome. The cell suspension containing the labeled cells is directed into a thin stream enabling them to pass single-file through a laser beam. Each cell scatters some of the laser light and also emits fluorescent light at a particular wavelength excited by the laser. This is detected by a photocell and subsequently analyzed.

Single cell suspension was prepared from spleen and tumor tissue as already described. 1 x 10^6 cells in 50 µl PBS/BSA (FACS buffer) were labeled with anti-mouse Fc receptors (FcR, CD16/CD32) block antibodies (final dilution 1:50) in order to reduce FcγII/III receptor-mediated non-specific antibodies binding which could contribute to background staining. The number of macrophages was analyzed following labeling of spleenocytes and tumor cells with a phycoerythrin (PE)-conjugated rat anti-mouse Gr-1 antibody (1:10 in FACS buffer), fluorescein isothiocyanate (FITC)–conjugated rat anti-mouse CD11b (1:10 in FACS buffer) and phycoerythrin (PE)-conjugated rat anti-mouse F4/80 (1:100 in FACS buffer). Except for the anti-F4/80 antibody which needed an incubation time of 30 min the others were incubated 10 min. The incubations were performed at 4 °C and protected from the light. As isotype controls a mouse IgG_{2B} Isotype conjugated with either phycoerythrin or fluorescein was used. Subsequently there is an incubation for 30 min on ice and in the dark. The cells were centrifuged 5 min, 300 x g at 4 °C and the pellets were resuspended in 100 µl FACS buffer.

The amount of macrophages in tumors was detected measuring a minimum of 1 x 10^5 cells. Flow cytometric analysis was performed on a FACSCalibur (BD Immunocytometry Systems) according to the manufacturer instructions.

IV.6.7. H & E staining

Mice with transplanted tumors of approximately 1,5 cm in diameter were sacrified and tumors were aseptically excised. The tumors were fixed in 4 % buffered paraformaldehyde for 24 h at room temperature, paraffin embedded, sectioned, and stained with hematoxylin and eosin.

The staining method involves application of the basic dye hematoxylin, which colors basophilic structures with blue-purple hue, and alcohol-based acidic eosin Y, which colors eosinophilic structures bright pink. The basophilic structures are usually the ones containing nucleic acids, such as the ribosomes and the chromatin-rich cell nucleus, and the cytoplasmatic regions rich in RNA. The eosinophilic structures are generally composed of intracellular or extracellular protein. The staining protocol is as followed:

Step	Reagent	Time	
1	xylol	10 min	
2	xylol	10 min	
3	absolute alcohol I	2-5 min	
4	absolute alcohol II	2-5 min	Deparaffinisation
5	absolute alcohol III	2-5 min	
6	70 % alcohol	5-10 min	
7	dH_2O	5 min	
8	hematoxylin	0,30-2 min	
9	tap Water	5-10 min	
10	dH_2O	2-5 min	
11	eosin	0,30–1 min	
12	dH_2O	2-5 min	
13	70 % alcohol	3 min	
14	absolute alcohol I	3 min	
15	absolute alcohol II	5 min	
16	absolute alcohol III	5 min	
17	xylol	10 min	

Step	Reagent	Time
18	xylol	10 min

At the end slides are mounted in Entellan.

IV.6.8. Immunohistochemical analysis of tumors

To identify macrophages at the tumor site, tissues were fixed in 4 % buffered paraformaldehyde for one day, paraffin embedded, and processed for sectioning. Subsequently sections were immunostained using the pan-macrophage anti-F4/80 antibody and specific reactivity was detected using a peroxidase-based detection kit as described (Vector Laboratories)[69]. The grade of infiltration of lymphocytes was examined by using an anti-CD45 antibody and the peroxidase-based detection kit (Vector Laboratories)[69]. For the identification of epithelial cells an anti-cytokeratin antibody and a biotinylated anti-IgG antibody was used. At the end sections were counter-stained with hematoxylin.

IV.6.8.1. Anti-F4/80 staining of TAMs

The F4/80 antigen is a 160 kDa glycoprotein expressed by most murine macrophages. Expression of F4/80 is heterogeneous and is reported to vary during macrophage maturation and activation. The F4/80 antigen is expressed on a wide range of mature tissue macrophages including Kupffer cells, Langerhans, microglia, macrophages located in the gut lamina propria, peritoneal cavity, lung, thymus, bone marrow stroma, macrophages in the red pulp of the spleen and it is overexpressed on TAMs[81]. The ligands and biological functions of the F4/80 antigen have not yet been determined but recent studies suggest a role for F4/80 in the generation of efferent CD8+ regulatory T cells[125].

Step	Reagent	Time	
1	xylol	10 min	
2	xylol	10 min	
3	absolute alcohol I	2-5 min	
4	absolute alcohol II	2-5 min	Deparaffinisation
5	absolute alcohol III	2-5 min	
6	70 % alcohol	5-10 min	
7	dH_2O	5 min	
8	Proteinase K (20 µg/ml in TE Buffer, pH 8,0),	30 min (RT)	

Step	Reagent	Time
9	1 x PBS	4 min
10	1,5 % H_2O_2 in 1 x PBS	30 min
11	1 x PBS	5 min (3x)
12	5 % rabbit serum, 0,1 % Triton X-100 in 1 x PBS (Blocking)	30 min (37 °C, humidified chamber)
13	Rat anti-mouse F4/80 (1:500) in Blocking solution (100 µl/slide)	Overnight, RT
14	1 x PBS	5 min (3x)
15	Biotinylated rabbit anti-rat (1:200, 100 µl/slide) in 1 x PBS	60 min (RT, humidified chamber)
16	1 x PBS (Preparation of A+B reagents before 30 min)	10 min (3x)
17	ABC Complex Incubation	45 min, RT
18	Diaminobenzidin (DAB) incubation: 1 ml DAB + 0,8 µl 30 % H_2O_2 (watch-out brown color formation, then stop reaction with water for 5 min)	
19	hematoxylin	0,30-1 min
20	tap Water	5-10 min
21	dH_2O	2-5 min
22	70 % alcohol	3 min
23	absolute alcohol I	3 min
24	absolute alcohol II	5 min
25	absolute alcohol III	5 min
26	xylol	10 min
27	xylol	10 min
28	entellan	

IV.6.8.2. Anti-CD45 staining

The CD45 antigen is a protein which was originally called leukocyte common antigen. The protein encoded by this gene is a member of the protein tyrosine phosphatase (PTP) family. PTPs are known to be signaling molecules that regulate a variety of cellular processes including cell growth, differentiation, mitotic cycle, and oncogenic transformation. This gene

is specifically expressed in hematopoietic cells. This PTP has been shown to be an essential regulator of T- and B-cell antigen receptor signaling.

Step	Reagent	Time	
1	xylol	10 min	
2	xylol	10 min	
3	absolute alcohol I	2-5 min	
4	absolute alcohol II	2-5 min	Deparaffinisation
5	absolute alcohol III	2-5 min	
6	70 % alcohol	5-10 min	
7	dH_2O	5 min	
8	Proteinase K (20 µg/ml in TE Buffer, pH 8,0), Cooling Down after Inkubation (25 min, RT)	20 min (37 °C, humidified chamber)	
9	1 x PBS	4 min	
10	2 % rabbit serum, 1 % BSA, 0,1 % Triton X-100 and 0,05 % Tween 20 in 1 x PBS (Blocking)	30 min (RT)	
11	Rat anti-mouse CD45 (1:20) in 1 x PBS containing 1 % BSA (100 µl/slide)	Overnight, RT	
12	1 x PBS	10 min (3x)	
13	Biotinylated rabbit anti-rat (1:200, 100 µl/slide) in 1 x PBS	30 min (RT, humidified chamber)	
14	1 x PBS (Preparation of A+B reagents before 30 min)	10 min (3x)	
15	ABC Complex Incubation	45 min, RT	
16	Diaminobenzidin (DAB) incubation: 1 ml DAB + 0,8 µl 30 % H_2O_2 (watch-out brown color formation, then stop reaction with water for 5 min)		
17	hematoxylin	0.30-1 min	
18	tap Water	5-10 min	
19	dH_2O	2-5 min	
20	70 % alcohol	3 min	

Step	Reagent	Time
21	absolute alcohol I	3 min
22	absolute alcohol II	5 min
23	absolute alcohol III	5 min
24	xylol	10 min
25	xylol	10 min
26	entellan	

IV.6.8.3. Anti-cytokeratin staining

Cytokeratins are intermediate filament keratins found in the intracytoplasmic cytoskeleton of epithelial tissue. There are two types of cytokeratins: the low weight, acidic type I cytokeratins and the high weight, basic or neutral type II cytokeratins. Cytokeratins are usually found in pairs comprising a type I cytokeratin and a type II cytokeratin. Expression of these cytokeratins is frequently organ or tissue specific. The subsets of cytokeratins which an epithelial cell expresses depends mainly on the type of epithelium, the moment in the course of terminal differentiation and the stage of development[126]. Thus this specific cytokeratin fingerprint allows the classification of all epithelia upon their cytokeratin expression profile. Furthermore this applies also to the malignant counterparts of the epithelia (carcinomas), as the cytokeratin profile tends to remain constant when an epithelium undergoes malignant transformation[126]. Therefore staining for cytokeratins could be used for the detection of residual tumor cells.

Step	Reagent	Time	
1	xylol	10 min	
2	xylol	10 min	
3	absolute alcohol I	2-5 min	
4	absolute alcohol II	2-5 min	Deparaffinisation
5	absolute alcohol III	2-5 min	
6	70 % alcohol	5-10 min	
7	dH_2O	5 min	
8	10 mM Citratpuffer, pH 6,0	10 min (microwave)	
9	1 x PBS	5 min (3x)	
10	3 % H_2O_2 in MeOH	30 min (RT)	
11	1 x PBS	5 min (3x)	

Step	Reagent	Time
12	5 % goat serum in 1 x PBS, 0,1 % Triton-X 100, 1 % BSA	30 min (RT)
13	Rabbit anti-cow Cytokeratin (1:400, 100 µl/slide) in Blocking solution	Overnight, 4 °C
14	1 x PBS	10 min (3x)
15	Biotinylated goat anti-rabbit IgG (1:200, 100 µl/slide) in Blocking solution	90 min, RT
16	1 x PBS (Preparation of A+B reagents before 30 min)	10 min (3x)
17	ABC Complex Incubation	30 min, RT
18	1 x PBS	5 min, RT
16	Diaminobenzidin (DAB) incubation: 1 ml DAB + 0,8 µl 30 % H_2O_2 (watch-out brown color formation, then stop reaction with water for 5 min)	
17	hematoxylin	0.30-1 min
18	tap Water	5-10 min
19	dH_2O	2-5 min
20	70 % alcohol	3 min
21	absolute alcohol I	3 min
22	absolute alcohol II	5 min
23	absolute alcohol III	5 min
24	xylol	10 min
25	xylol	10 min
26	entellan	

IV.7. *Ex vivo* experiments

IV.7.1. *Ex vivo* infection of murine cells

Tumor cells were separated and TAMs were isolated via MACS® system like subscribed before. Subsequently cells were seeded in the desirable cell number in 6-well or 12-well plates for 3 h. *Shigellae* grown to logarithmic growth phase were centifuged (2,000 x g, 10 min, 4 °C) and washed with DMEM medium three times. After 1 h of infection at a MOI 100, cells were incubated for 1 h with 300 µg/ml gentamicin. After that 50 µg/ml gentamicin were used. 2 h *p.i.* cells were harvested to determine CFU or were prepared for Western Blot analysis.

IV.7.2. *Ex vivo* infection of murine lung cells

Lung cells of transgenic *S-PC*-c-RAF-BxB-11 lung tumor mice were separated and F4/80+ macrophages were isolated like subscribed before. Subsequently cells were seeded in the desirable cell number in 6-well plates for 3 h. *Shigellae* grown to logarithmic growth phase were centifuged (2,000 x g, 10 min, 4 °C) and washed with DMEM medium three times. After 1 h of infection at a MOI 100, cells were incubated for 1 h with 300 µg/ml gentamicin. After that 50 µg/ml gentamicin were used. 2 h *p.i.* cells were prepared for Western Blot analysis.

IV.7.3. *Ex vivo* infection of human ascites cells

Ovarian cancer ascites were isolated from a patient and kindly provided by Dr. Jörk Wischhusen (Interdisciplinary Center for Clinical Research, University of Würzburg, Medical School, Clinics for Gynecology and Obstetrics, Würzburg, Germany) for this work. Ovarian cancer ascites contains both adherent cancer and non-adherent myeloid cells. Tumor cells were separated and TAMs were isolated with an anti-F4/80 anitbody (100 µg/ml) as described before. The different cell fractions isolated from an ovarian cancer patient were infected *ex vivo* with wt *S. flexneri M90T, S. flexneri M90TΔaroA* and *S. flexneri BS176ΔaroA* that had been grown to logarithmic growth phase, centrifuged (2,000 x g, 10 min, 4 °C) and washed three times with D-MEM medium. After 1 h of infection at a MOI of 100, cells were incubated for 1 h with 300 µg/ml gentamicin. After that, 50 µg/ml gentamicin was used. 2 h *p.i.* cells were harvested to determine CFU or were prepared for Western Blot analysis.

IV.8. Therapeutic approach

IV.8.1. Efficacy studies

Therapeutic efficacy of *Shigella* infection on tumor growth was explored in 28 six- to eight-week-old female Balb/c mice bearing 4T1-induced tumors. Mice were injected subcutaneously with 1 x 10^4 4T1 murine breast tumor cells and tumor growth was determined every two days with a caliper. Tumor volume was calculated as rotation ellipsoid with the formula $V=\pi/6*a*b^2$ with a being the maximal and b the minimal diameter of the tumor. At day 14 post cell implantation, mean tumor volume had reached 170 mm^3 and mice were randomized into three groups of mice (n = 8). 1 x 10^6 *S. flexneri S. flexneri M90TΔaroA*, *S. flexneri BS176ΔaroA* or 100 µl PBS were injected into the lateral tail vein of the tumor-bearing mice. Tumor size was monitored every second day. On day 31 post tumor cell implantation the naïve and the *S. flexneri BS176ΔaroA* group (tumor size) and two *S. flexneri M90TΔaroA* mice (macroscopic comparison of tumors, data not shown) were sacrificed. On day 62 post tumor cell implantation three *S. flexneri M90TΔaroA* mice were sacrified to determine CFU in tumor, liver and spleen. In addition FACS analysis was performed to determine the amount of macrophages in the tumor tissue. On day 66 post tumor cell implantation animals were re-injected with 1 x 10^6 *S. flexneri M90TΔaroA* i.v. On day 82 post tumor cell implantation CFU was again determined in tumor, liver and spleen tissue. In addition, two tumors were prepared for histological and immunohistochemical analysis.

IV.9. *S-PC*-c-RAF-BxB-11 lung tumors

IV.9.1. I.v. infection of C57Bl/6 and *S-PC*-c-Raf-BxB-11 mice with *Shigella*

S. flexneri M90TΔaroA were harvested at mid-logarithmic phase, washed three times and diluted with PBS prior to i.v. injection. 1 x 10^6 bacteria in 100 µl of the suspension were injected with a 0,4×20 mm (27 G) injection syringe into the lateral tail vein of fixed C57Bl/6 or *S-PC*-c-RAF-BxB-11 mice.

IV.9.2. Histological and immunohistochemical analysis of lung tissue

28 days *p.i.* C57Bl/6 or *S-PC*-c-Raf-BxB-11 mice were sacrificed and lungs were fixed under 25 cm water pressure with 4 % PBS buffered formalin. Histology was done on formalin-fixed, paraffin-embedded lung specimen. 6 µm-cut sections were deparaffinized, rehydrated in graded alcohols and haematoxylin-eosin stained.

To identify macrophages, sections were immunostained using the pan-macrophage anti-F4/80 antibody and specific reactivity was detected using a peroxidase-based detection kit as described (Vector Laboratories)[69]. The level of infiltration of lymphocytes was examined by using an anti-CD45 antibody and the peroxidase-based detection kit (Vector Laboratories)[69]. Epithelial cells were detected by an anti-Cytokeratin antibody and a biotinylated anti-IgG antibody. At the end sections were counter-stained with hematoxylin. Staining procedures were performed as described.

IV.9.3. *Shigella flexneri M90TΔaroA* i.v. infection of Balb/c mice

In this animal study we wanted to investigate whether the lung tissue is targeted by *S. flexneri M90TΔaroA* after an intravenous application. Therefore we injected 1 x 10^4 *S. flexneri M90TΔaroA* i.v. and sacrified two mice per time point (1 d, 7 d, 14 d and 28 d *p.i.*) to determine the CFU in the lung tissue.

V. Results

V.1. Analysis for caspase-1 expression in tumor cells

Intracellular bacteria like *Salmonella* and *Shigella* induce apoptosis in macrophages via activation of caspase-1[29]. To determine whether caspase-1 expression is restricted to macrophages and not present in tumor cells, we checked caspase-1 expression in murine J774A.1 macrophages, the 4T1 breast tumor cell line and the transfected B16 cell line B78-D14 melanoma cell line via RT-PCR (Fig. 15 left panel) and Western Blot analysis (Fig. 15 right panel).

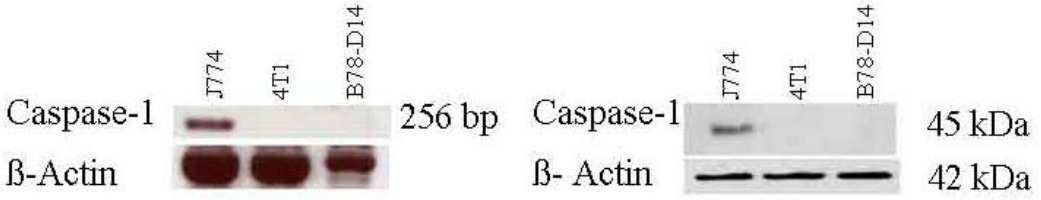

Figure 15: Caspase-1 is exclusively expressed by macrophages

Analysis of caspase-1 expression by RT-PCR (left) and Western Blot analysis (right).

When ICE gene is expressed, there is a product of 250 bp (left). In Western Blot analysis the anti-caspase-1 antibody detects the caspase-1 precursor protein of 45 kDa (right). β-actin was used as loading control.`

So RT-PCR and Western Blot analysis showed that the caspase-1 precursor protein is not expressed in the 4T1 or B78-D14 tumor cell lines (Fig. 15).

Tumors consist of a complex mixture of transformed cells and stroma cells. In addition, stromal cells frequently display a distinct phenotype compared to equivalent cells in their physiological surrounding. In many tumors, tumor-associated macrophages represent a major component of the leucocytic infiltrate.

V.2. Immunohistological examination for infiltration of macrophages in tumor tissue

Macrophage infiltration has been described in several human tumors including breast[78,127,128] and ovarian carcinoma[129]. To determine the level of infiltrated TAMs in different

experimental tumor models we stained macrophages with an anti-F4/80 antibody in paraffin embedded tissues of different tumor models (Fig. 16).

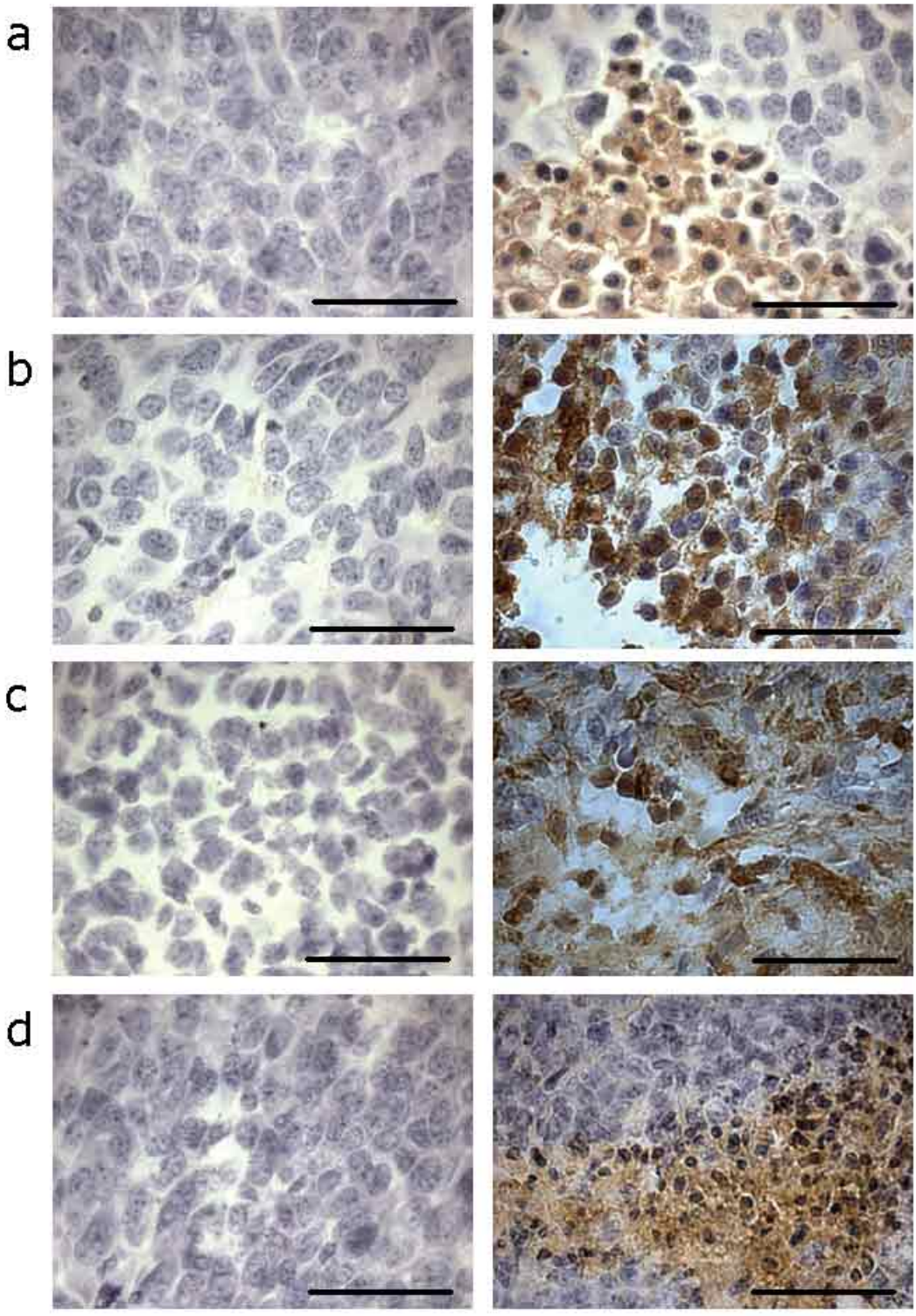

Figure 16: Substantial amounts of TAMs in different mouse tumor models

Tumors with diameters of approximately 1,5 cm were isolated from mice injected s.c. with 1 x 10^6 B78-D14 cells (**a**), 1 x 10^4 4T1 cells (**b**) and 1 x 10^6 P815-PSA cells (**c**). In addition, spontaneous breast tumors from

transgenic MMTV-HER2/new FVB were isolated (**d**). Tumor tissue was fixed and embedded in paraffin. Tumor sections were immunostained with a biotinylated anti-F4/80 monoclonal antibody and subsequently counter-stained with hematoxylin (right panels). Staining with avidin-horseradish peroxidase without F4/80 antibody was performed as a control (left panels). Scale bars represent 50 µm.

In all tumors examined, we detected hotspots of macrophages (Fig. 16, brown staining). Because TAMs are widespread in human breast carcinomas and are associated with negative prognosis, we used the artificial 4T1 model and the transgenic MMTV-HER2 tumor model for further studies[70,74,130,131].

V.3. Tumor targeting by *Shigella flexneri M90T*

We performed at first an experiment to analyse if *Shigella flexneri M90T* is able to infiltrate, replicate and then preferentially accumulate in the tumor tissue. Balb/c mice were transplanted with 1 x 10^4 4T1 breast tumor cells and the tumor volume was monitored every second day (Fig. 17). Tumor volume was determined by following formula:

$$V = \frac{\Pi}{6} \cdot a \cdot b^2 \text{ if a} > \text{b}$$

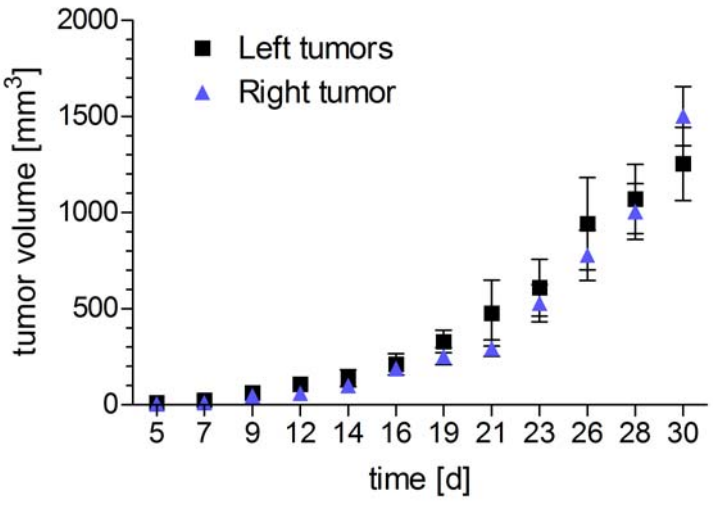

Figure 17: 4T1 cell-induced tumor growth

1 x 10^4 4T1 murine breast tumor cells were applicated s.c. into ten Balb/c mice. Tumor volume was determed every other day by a caliper.

On day 27 (tumor volume 600-800mm^3) 4 x 10^6 *Shigella flexneri M90T* were injected intravenously (Fig. 18).

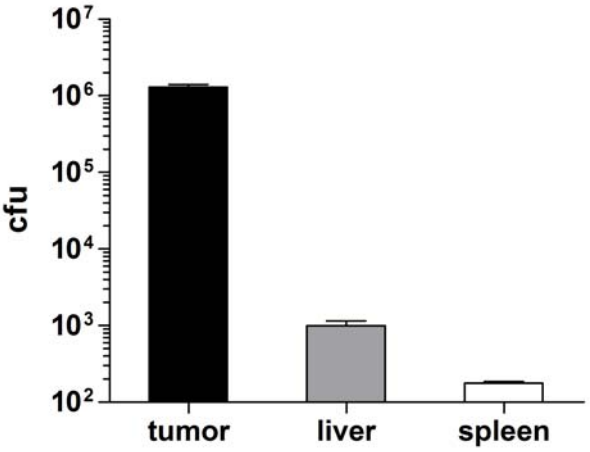

Figure 18: *S. flexneri M90T* accumulates in the tumor tissue

Shigella flexneri M90T is able to infiltrate, replicate and preferentially accumulate in the tumor tissue. On day 7 tumor tissue, liver and spleen were excised and CFUs were determined. Bars represent means +/- SD of ten organs analyzed.

One week later there were 10^5-10^6 bacteria located in the tumor tissue and only 10^2-10^3 bacteria were found in the liver and the spleen tissue. This enrichment is comparabel to results obtained previously in the same model system using *Listeria* and *Salmonella* strains[3].

V.4. Construction of *S. flexneri aroA*-mutants

Because of the high virulence of the *Shigella flexneri M90T* wildtype strain we attempted to create an attenuated *Shigella flexneri* strain, which is still able to induce apoptosis in macrophages by caspase-1 activation.

In this work the *Shigella flexneri* strains *M90T* and *BS176*, which is the plasmidless non-virulent variant, were used. The knockout of the *aroA*-locus in the *Shigella flexneri BS176* strain was performed by using the method of Datsenko and Wanner[115].

To allow a genetically defined comparison of growth-attenuated virulent and non-virulent strains, we first deleted the genomic *aroA*-locus in the avirulent *Shigella flexneri* strain *BS176* using the method of Datsenko and Wanner and subsequently added the virulence plasmid pWR100 by electroporation.

At first we generated a linear PCR-product by using primers AroA_up and AroA_down (=H1, H2; see Fig. 19: step 1) with 36 nucleotid extensions that are homologous to the *AroA* gene. As template we used the pKD3 plasmid which carries an chloramphenicol resistance gene

flanked FRT sites. The next step was the transformation of the PCR product in the competent *Shigella flexneri BS176* strain, which expresses the lambda red recombinase coded by plasmid pKD46 (Fig. 19: step 2). This recombinase is essential for homologous recombination and its expression is regulated by an inducable promoter. The chloramphenicol-resistant transformants were then checked for *aroA*-gene disruption via PCR (Fig. 19: step 3). The last step was the elimination of the resistance cassette by using an helper plasmid, which expressed the FLP recombinase (Fig. 19: step 4).

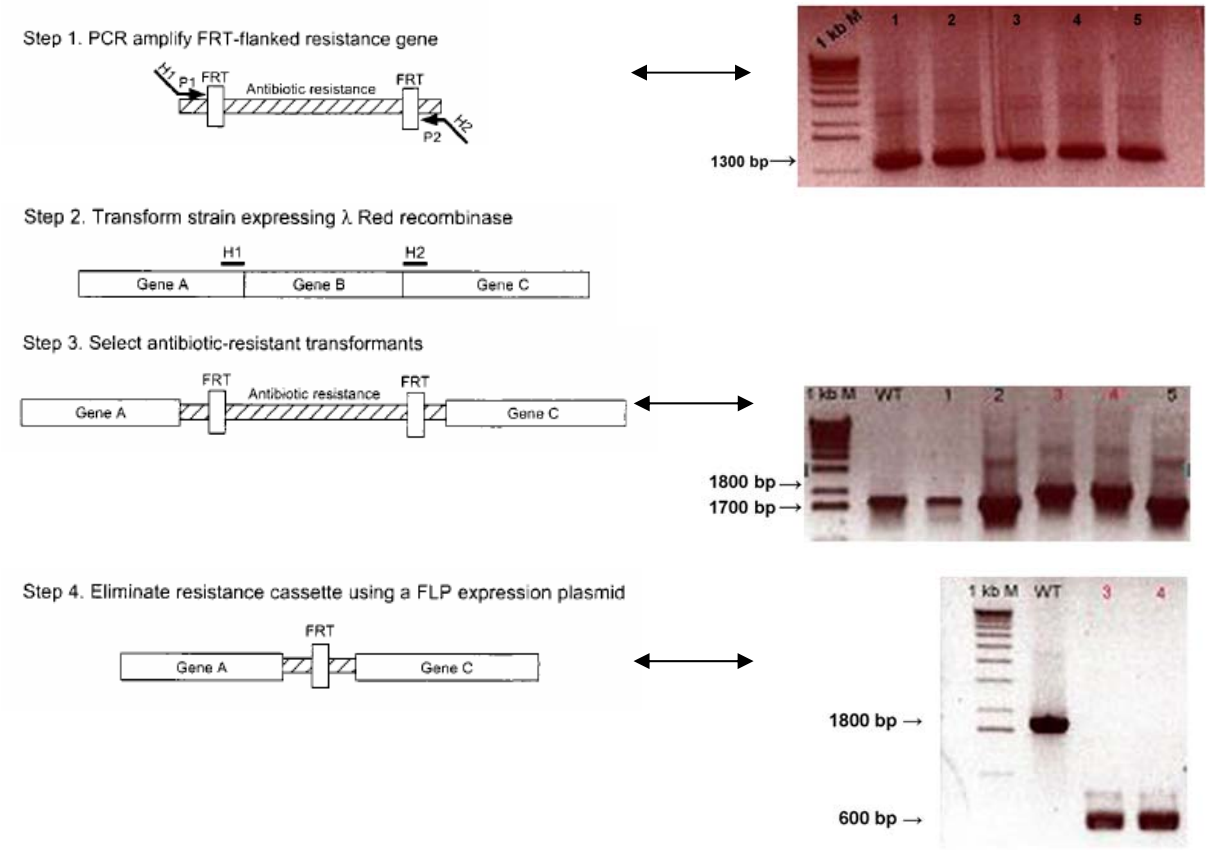

Figure 19: Gene disruption strategy by Datsenko and Wanner in *S. flexneri BS176*[115]

H1 and H2 refer to the homology extensions or regions. P1 and P2 refer to priming sites.

Subsequently the 200 kb virulence plasmid pWR100 of *S. flexneri M90T* was isolated. After that this virulence plasmid and the helperplasmid pCP20[116], carrying an antibiotic-resistance, were transformed in the already constructed *S. flexneri BS176ΔaroA* strain.

After this double transformation the antibiotic-resistant colonies were screened for the virulence plasmid pWR100 (Fig. 20) and for the *aroA*-knockout (Fig. 21). This strain was termed *S. flexneri M90TΔaroA*.

Gel: 1. 1 kb Marker
2. DSM 21058
3. *M90TΔaroA* clone 1
4. *M90TΔaroA* clone 2
5. *M90T*
6. *BS176*
7. *BS176ΔaroA*

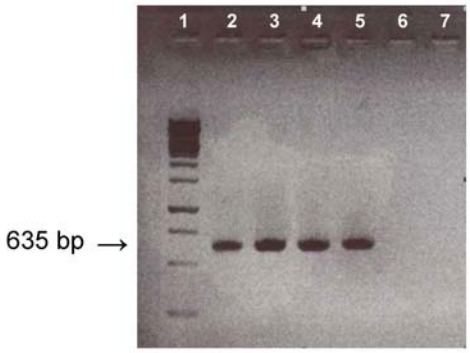

Figure 20: PCR for pWR100

PCR for pWR100 was done with primers pWR100_up and pWR100_down, The two primers are located in the *ics*-Gen, coded by the virulence plasmid pWR100. Strains harboring pWR100 show a 635 bp product (DSM 21058, *M90T, M90TΔaroA*)

A strain haboring the virulence plasmid pWR100 was detected by a 635 bp product as seen for the constructed *S. flexneri M90TΔaroA*, the strain DSM 21058 and the wt *S. flexneri M90T* The latter were used as positive controls (Fig. 20).
Subsequently we performed PCR reactions to detect bacteria with *aroA*-deletion (Fig. 21).

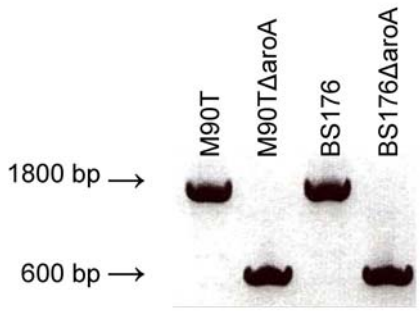

Figure 21: PCR for *aroA* knockout

PCR for *aroA*-gene knockout was done with primers AroAFr_up and AroAFr_down. The product of *aroA* wt gene was 1800 bp (*M90T, BS176*). An *aroA* knockout was detected by a 600 bp product (*M90TΔaroA*, *BS176ΔaroA*)

The product of *aroA* wt gene was 1800 bp detected for *S. flexneri M90T and S. flexneri BS176* (Fig. 21). An *aroA* knockout was detected by a 600 bp product as seen for the constructed *S. flexneri M90TΔaroA*, *S. flexneri BS176ΔaroA* and the strain DSM 21058 (Fig. 21).

V.5. *In vitro* experiments

V.5.1. *In vitro* characterization of *S. flexneri aroA*-mutants

After the construction of the *aroA*-mutants, the strains were characterized with respect to extracellular and intracellular growth, early association, invasion and cell-to-cell spread *in vitro*.

V.5.1.1. Extracellular growth of *aroA*-mutants

Extracellular growth was determined at 37 °C at 180 rpm in LB medium. OD was measured every hour (Fig. 22).

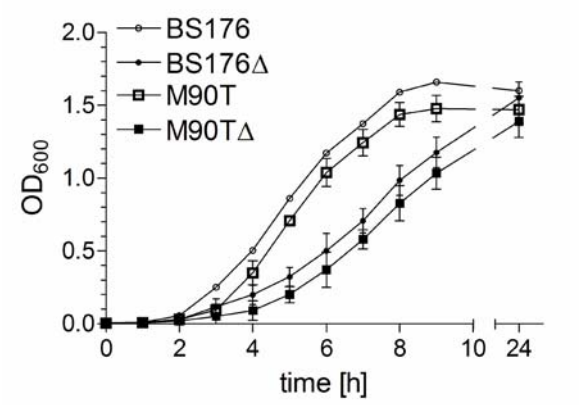

Figure 22: Extracellular growth of *S. flexneri aroA*-mutants

Determination of the growth rates at 37 °C at 180 rpm in LB medium. The overnight-culture was diluted 1:20 for the main culture and OD was measured every hour. Bars represent means +/- SD of three different experiments.

The plasmidless avirulent strain *S. flexneri BS176* was characterized by a maximal growth rate of 0.3 OD/h in LB medium, whereas the virulent strain *S. flexneri M90T* had a slightly reduced maximal growth rate of 0.2 OD/h (Fig. 22), which might be explained by the presence of the large virulence plasmid pWR100. As expected, strains carrying *aroA* mutations had substantially reduced maximal growth rates. *S. flexneri M90TΔaroA* had a 2.5 fold slower maximal growth rate than wt *S. flexneri M90T*. Again, *S. flexneri BS176ΔaroA* had a slightly higher maximal growth rate compared to *S. flexneri M90TΔaroA*.

V.5.1.2. Early association, invasion and intracellular replication of *aroA*-mutants

Subsequently, we investigated the contribution of the *aroA*-mutation with respect to early association, invasion and intracellular replication (Fig. 23).

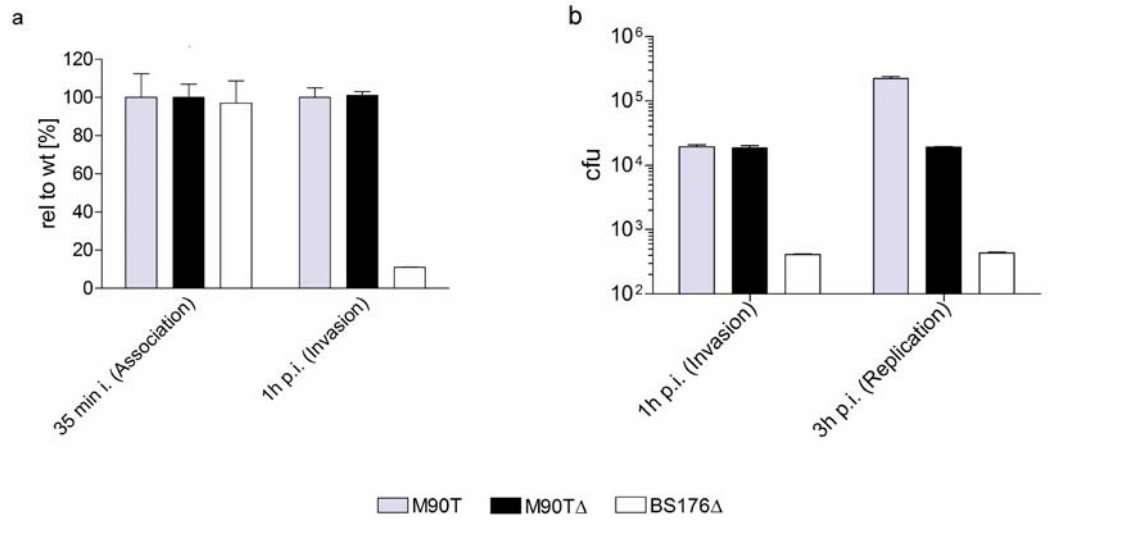

Figure 23: Early association, invasion and intracellular replication of *aroA*-mutants

(**a**) Invasion assay with HeLa cells. Cells were infected at a MOI of 100. 35 min *i.*(association) and 1 h *p.i.* (invasion), the CFUs were determined relative to the wt strain *M90T*. (**b**) To determine the intracellular replicatory potential, cells were infected with an MOI of 100:1 for 1 h. Subsequently, cells were incubated for additional 2 hours in the presence of gentamicin and the CFU of lysed cells was determined. Bars represent means +/- SD of three different experiments. ***: $p < 0{,}001$, Student`s t-test.

As depicted in figure 23a, the strain *S. flexneri M90TΔaroA* showed no significant difference in its rate of association and invasion relative to the wt strain *S. flexneri M90T*. In contrast, *S. flexneri BS176ΔaroA* was attenuated in its invasion behavior as expected. The wt *S. flexneri M90T* showed a 12 fold higher intracellular replication rate than the *aroA*-mutants in the time period of 2 h (Fig. 23b). These data show that the strain *S. flexneri M90TΔaroA* is strongly attenuated in its intracellular replication.

V.5.1.3. Intercellular spreading of *aroA*-mutants

V.5.1.3.1. L-Top agar assay

Because of the defect in intracellular replication of the *aroA*-mutants, cell-to-cell spread is difficult to assess with a conventional assay. Therefore we developed a new spreading assay, which is less sensitive for intracellular replication (Fig. 24).

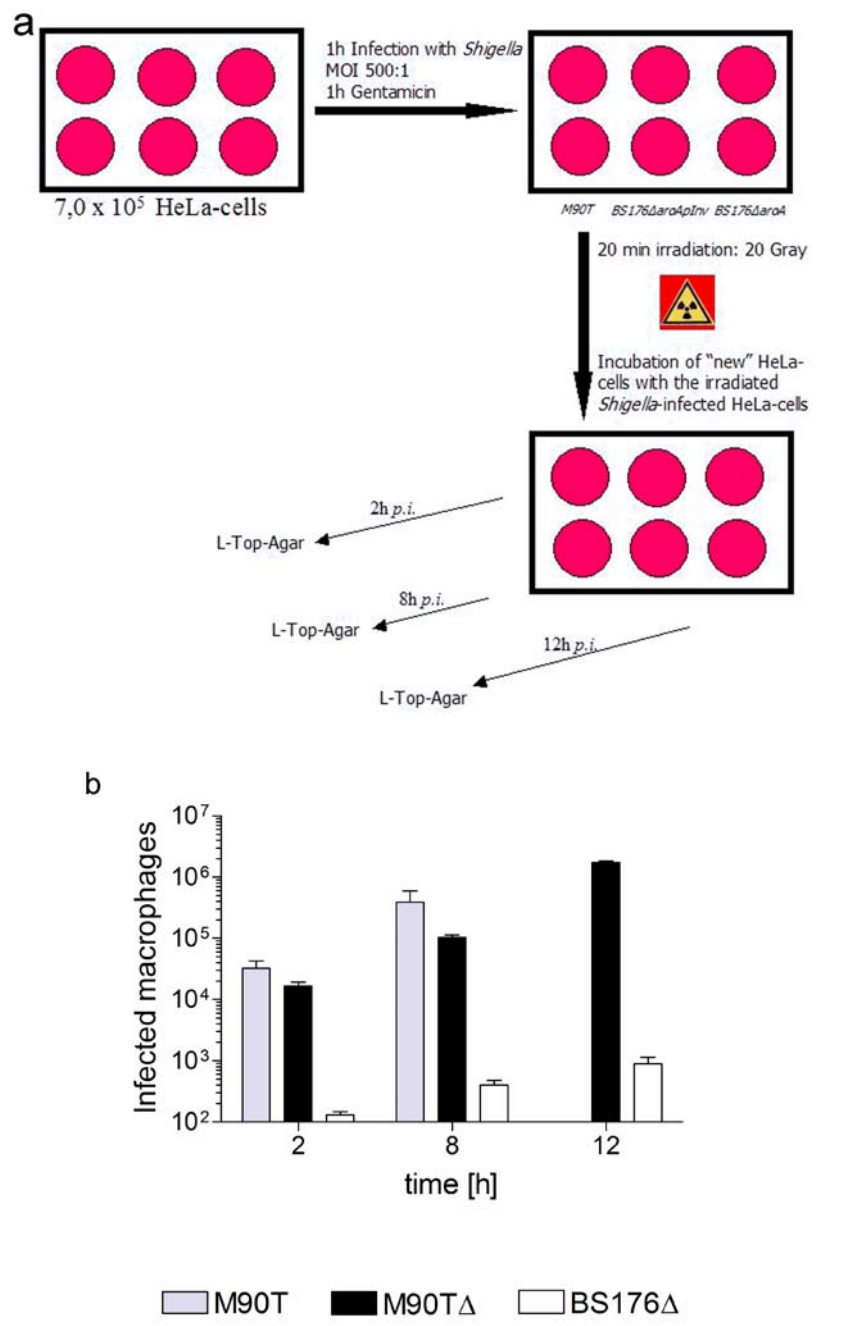

Figure 24: Intercellular spreading of *aroA*-mutants determined by L-Top agar assay

(**a**) Experimental schedule of L-Top agar assay. (**b**) To determine the ability of intercellular spreading, HeLa cells were infected for 1 h at a MOI of 500:1. After that the infected cells were irradiated at 20 Gray to block the replication of the HeLa cells. The infected, irradiated Hela cells were co-incubated with non-infected HeLa cells in a ratio of 70:1 for 2 h, 8 h and 12 h in the presence of gentamicin. Subsequently, serial dilutions of non-lysed cells in SeaPlaque agarose, were plated on BHI agar plates. Due to massive cell death upon infection the 12 h time point could not be assessed for the wt. Bars represent means +/- SD of three different experiments.

In the first step, HeLa-cells were infected for 1 h at a high MOI of 500 (Fig. 24). Subsequently, the infected cells were irradiated to block the replication of the HeLa cells. The

infected, irradiated Hela cells were co-incubated on a monolayer of non-infected HeLa cells in a ratio of 1:70 in the presence of gentamicin. The number of infected cells was determined by plating on SeaPlaque agarose avoiding cell lysis. The wt *S. flexneri M90T* showed an increase in the number of infected cells by a factor of 12 after 8 h. At later time points, the non-attenuated, virulent strain was toxic for the cells and CFU determination was no more possible. In the case of *S. flexneri M90TΔaroA*, the increase of the number of infected cells was 6 fold after 8 h and 17 fold 12 h after co-infection, whereas the number of infected cells for the avirulent strain *S. flexneri BS176ΔaroA* increased by only 3 fold after 8 h and showed no further increase until 12 h. These results suggest a non-impaired potential of *S. flexneri M90TΔaroA* for cell-to-cell spread. The small increase observed for *S. flexneri BS176ΔaroA*, which does not carry the genetic information for cell-to-cell spread might be due to partial cell lysis at early time points of the highly infected irradiated cells with an only partial killing of extracellular bacteria by the rather low gentamicin concentration of only 10 µg/ml for 12 h in order to protect the eukaryotic cells.

V.5.1.3.2. Giemsa staining

To study intracellular multiplication and behavior of cell-to-cell spreading, we also performed Giemsa staining of *Shigella*-infected cells. Briefly, HeLa cells were infected at a MOI of 100 for 1 h. Time points of 1 h and 4 h *p.i.* were examined (Fig. 25).

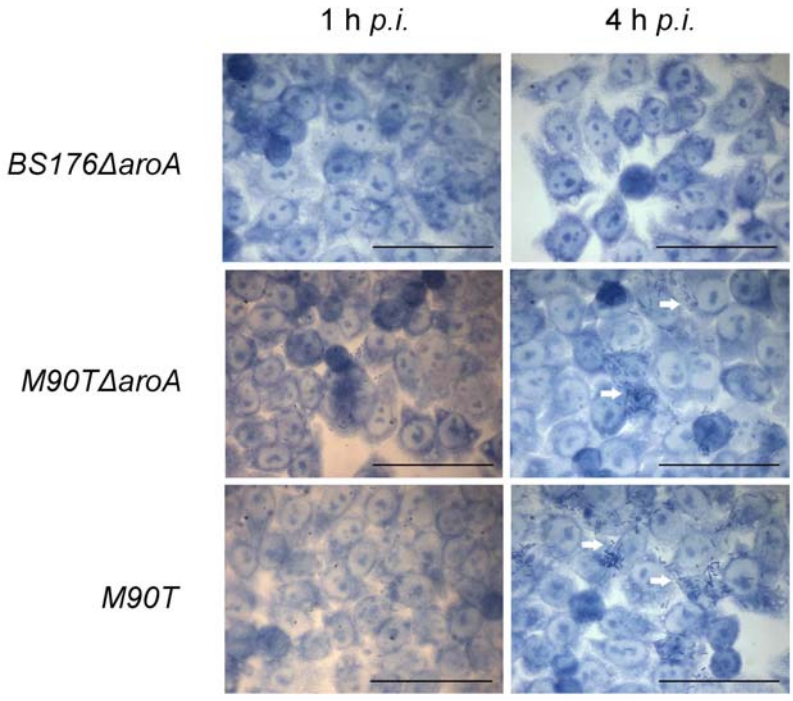

Figure 25: Giemsa staining

HeLa cells were infected with *Shigella flexneri M90T* (M90T), *Shigella flexneri M90TΔaroA* (M90TΔaroA) or *Shigella flexneri BS176ΔaroA* (BS176ΔaroA) for 1 h and 4 h *p.i.* Subsequently cells were fixed and stained with Giemsa dye. Scale bars represent 50 µm.

The Giemsa stainings of HeLa cells infected with wt *S. flexneri M90T* or *S. flexneri M90TΔaroA* 4 h *p.i.* showed regions of cell-to-cell spread (Fig. 25, indicated with arrows) in contrast to HeLa cells infected with *S. flexneri BS176.*

V.5.2. *In vitro* caspase-1 activation and induction of apoptosis by *Shigella aroA*-mutants

V.5.2.1. Western Blot analysis

To determine the capacity of the *aroA*-mutants to activate caspase-1 (Fig. 26a) and to induce apoptosis (Fig. 26b) *in vitro*, J774A.1 mouse macrophages were infected and cellular lysates were analyzed by Western Blotting analysis at different time points using an anti-caspase-1 antibody recognizing the active 20 kDa fragment of activated caspase-1 (Fig. 26a, caspase-1*) and an anti-PARP antibody recognizing the cleaved 85 kDa fragment (Fig. 26b, cPARP).

a

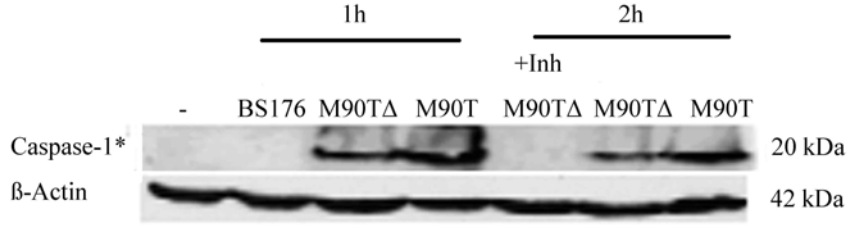

b

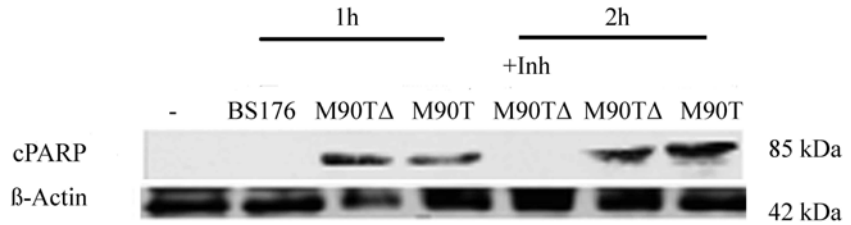

Figure 26: Western Blot analysis of *S. flexneri aroA*-mutants for caspase-1 activation and PARP cleavage

To determine the capacity of the *aroA*-mutants to induce caspase-1 activation and apoptosis, J774A.1 mouse macrophages were infected with *S. flexneri M90T* (M90T), *S. flexneri M90TΔaroA* (M90TΔ) *and S. flexneri BS176* (BS176Δ) for 1 h and 2 h *p.i.* and cellular lysates were analyzed by Western Blot at different time points using an anti-caspase-1 antibody recognizing the active 20 kDa fragment of caspase-1 (**a,** caspase-1*) and an

anti-PARP antibody recognizing the cleaved 85 kDa fragment (**b**, cPARP). Apoptosis induction and caspase-1 processing by *M90TΔ* was completely blocked by the caspase-1 specific inhibitor YVAD-CHO (2,5 mM). B-Actin was used as loading control.

S. flexneri M90TΔaroA, but not *S. flexneri BS176ΔaroA*, was able to induce both caspase-1 processing and apoptosis. Of note, apoptosis induction by *S. flexneri M90TΔaroA* was caspase-1 dependent, as the caspase-1 specific inhibitor YVAD-CHO fully blocked caspase-1 and PARP processing (Fig. 26a, b).

V.5.2.2. Hoechst 33342 staining

For further investigation whether the strain *Shigella flexneri M90TΔaroA* is able to induce apoptosis in macrophages we also performed an infection of J774A.1 mouse macrophages with the *S. flexneri M90TΔaroA* strain for 2 h. After that the cells were stained with Hoechst 33342 dye (Fig. 27).

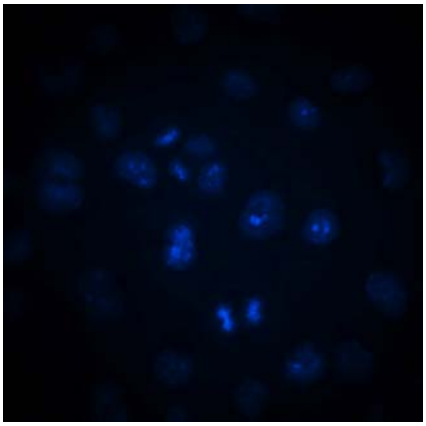

a) Untreated J774A.1 (negative control)

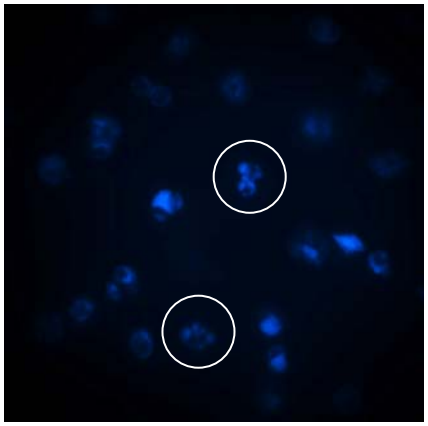

b) J774A.1 treated with staurosporine for 6h (positive control)

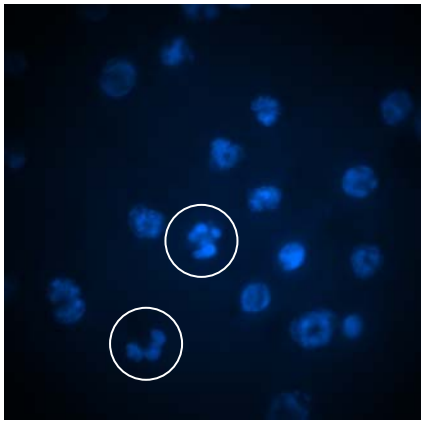

c) J774A.1 infected with *S. flexneri M90TΔaroA* (2 h *p.i.*)

Figure 27: Hoechst 33342 staining of *S. flexneri M90TΔaroA*-infected macrophages

J774A.1 macrophages were infected with *S. flexneri M90TΔaroA* for 1 h at a MOI of 100. After that cells were washed three times with PBS and incubated for 1 h with 100 µg/ml gentamicin. Subsequently macrophages were incubated for 1 h with 50 µg/ml gentamicin. As positiv control for apoptosis induction macrophages were incubated with 4 µmol/l staurosporine for 6 h (**b**). Not infected J774A.1 macrophages were used as negativ control (**a**).

Figure 27a shows healthy untreated macrophages. There are light blue dots which indicate the heterochromatin in the nuclei. In figure 27c the macrophages were infected with the *S. flexneri M90TΔaroA* strain. Phenotypically, *S. flexneri M90TΔaroA*-infected macrophages display common indicators of apoptosis such as nuclear fragmentation (which leads to the replacement of the heterochromatin to the plasma membrane) and cells in the later morphological stages of apoptosis for example with membrane blebbing. So the *S. flexneri M90TΔaroA* strain is able to induce apoptosis in macrophages. In figure 27b the macrophages were treated with staurosporine as a positive control for apoptosis.

V.5.3. *In vitro* activation of caspase-1 by *S. typhimurium ΔaroA* and *S. flexneri* strains

Within macrophages, bacteria like *Salmonella* and *Shigella* can survive using distinct virulence mechanisms and can induce apoptosis of the infected macrophages through activation of caspase-1 mediated by IpaB (*Shigella*) or SipB (*Salmonella*)[17,18]. In our study the strain *S. typhimurium* ΔaroA was used as a control.

RAW 264.7 macrophages were infected at a MOI of 10 with *S. typhimurium* ΔaroA (stationary growth phase), *S. flexneri M90T* and *S. flexneri M90TΔaroA* (both mid-logarithmic growth phase) for different time points. Subsequently, Western Blot analysis for caspase-1 activation of the cell lysate was performed (Fig. 28).

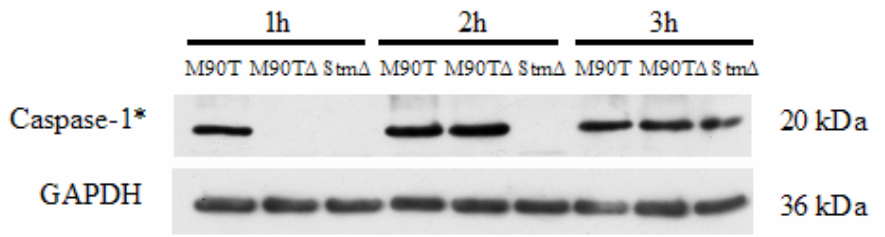

Figure 28: *In vitro* activation of caspase-1 by *S. flexneri M90TΔaroA*

RAW 264.7 macrophages were infected at a MOI of 10 for 1 h with *S. flexneri M90T* (M90T, mid-logarithmic growth phase), *S. flexneri M90TΔaroA* (M90TΔ, mid-logarithmic growth phase) and *S. typhimurium* ΔaroA

(StmΔ, stationary growth phase) for different time points. After an incubation of 1 h with 100 µg/ml gentamicin and additional 1-2 h with 10 µg/ml gentamicin, the different samples were prepared for Western Blot analysis. The antibody detects the activated caspase-1 20 kDa subunit (caspase-1*). GAPDH was used as loading control.

The *Shigella* strain encompassing the *aroA* deletion showed a slight delay in caspase-1 activation but reached the same activity 2 h *p.i.* as compared to the wt *S. flexneri M90T* strain. The *Salmonella* strain induced caspase-1 processing 3 h *p.i.* (Fig. 28).

V.5.3.1. *In vitro* activation of caspase-1 by *S. typhimurium ΔaroA* is growth phase dependent

During an infection with *Salmonella* a gene expression switch from the SPI1 to the SPI2 pathogenicity island occurs, which is the natural sequence after oral infection. One consequence of this switch is the shutdown of the SipB expression and secretion via the SPI1 encoded type 3 secretion system, which leads to a substantial reduction in caspase-1 induced apoptosis at later time points of infection[18].

To investigate that caspase-1 activation by *S. typhimurium* ΔaroA is growth phase dependent, RAW 264.7 macrophages were infected at a MOI of 10 with *S. flexneri M90T*, *S. flexneri M90TΔaroA* (both mid-logarithmic growth phase) and *S. typhimurium* ΔaroA from stationary and from mid-logarithmic growth phase for different time points. Subsequently, Western Blot analysis for caspase-1 activation of the cell lysate was performed (Fig. 29).

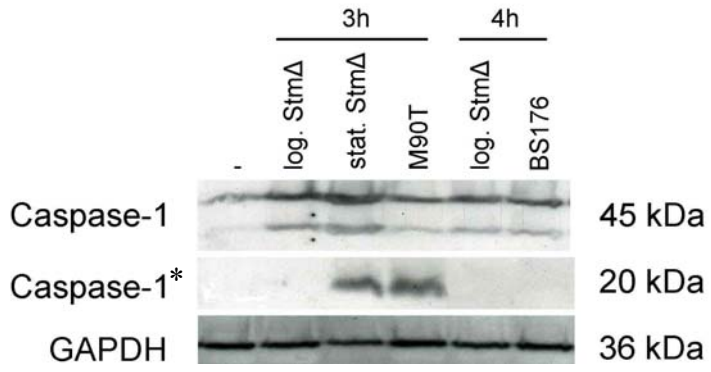

Figure 29: *In vitro* activation of caspase-1 by *S. typhimurium* ΔaroA

RAW 264.7 macrophages were infected at a MOI of 10 for 1 h with *S. flexneri M90T* (M90T, mid-logarithmic growth phase), *S. flexneri BS176* (BS176, mid-logarithmic growth phase), *S. typhimurium* ΔaroA (log. StmΔ: *S. typhimurium* ΔaroA grown to mid-logarithmic growth phase) and *S. typhimurium* ΔaroA (stat. StmΔ: *S. typhimurium* ΔaroA grown to stationary growth phase) for different time points. After an incubation of 1 h with

100 µg/ml gentamicin and additional 2-3 hours with 10 µg/ml gentamicin, the different samples were prepared for Western Blot analysis. The antibody detects caspase-1 zymogen of 45 kDa and the activated caspase-1 20 kDa subunit (caspase-1*). GAPDH was used as loading control.

Salmonella strains harvested in logarithmic phase did not induce caspase-1 processing in this assay even 4 h *p.i.*, in contrast to *Salmonella* strains harvested in stationary growth phase (Fig. 29). For all subsequent infection experiments, *Salmonella* strains harvested in stationary growth phase were used.

V.6. Gentamicin assays

To avoid re-infection of cells during MACS® separation and to assess the number of extracellular bacteria, these have to be killed or substantially reduced during an incubation time of 1 h. To assess the optimal concentration, the gentamicin assay was performed at different concentrations (Fig. 30).

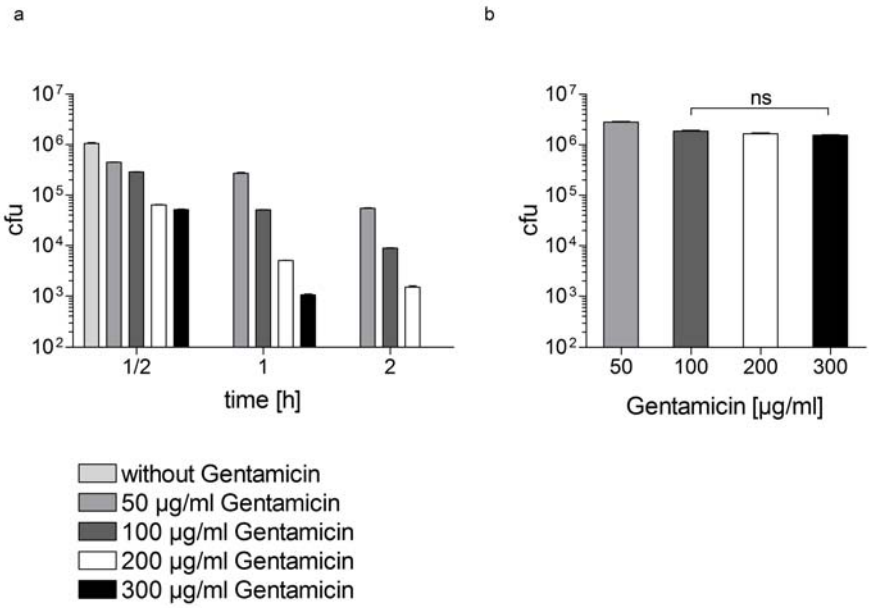

Figure 30: Assays to determine maximal gentamicin concentration

(**a**) In the first assay 1 x 10^6 *S. typhimurium* ΔaroA were treated for ½ h, 1 h and 2 h with 50, 100, 200 and 300 µg/ml gentamicin and CFU was determined by plating serial dilution on LB agar plates. (**b**) In the second gentamicin assay J774A.1 macrophages were infected with 1 x 10^6 *S. typhimurium* ΔaroA (logarithmic growth phase). Bacteria were washed three times with DMEM medium and zetrifuged for 10 min at 20,000 x g at 4 °C. After 1 h infection, cells were incubated for 1 h with 50, 100, 200 and 300 µg/ml gentamicin followed by a 1 h incubation with 10 µg/ml gentamicin after washing with 1 x PBS. CFU was determined after cell lysis by plating serial dilutions on LB agar plates.

As depicted in figure 30a 1 h incubation with 50, 100 or 200 µg/ml gentamicin led to a 3 fold, 10 fold or 100 fold reduction of the CFU compared to untreated control (without gentamicin). In contrast, incubation with 300 µg/ml reduced free bacteria >1000 fold after 1 h incubation and fully eliminated the bacteria after 2 h.

To determine the effect of this concentration on intracellular bacteria, a similar protocol as used for cell separation was employed (Fig. 30b). Macrophages were infected with *S. typhimurium* ΔaroA for 1 h. Subsequently cells were incubated for 1 h with 50, 100, 200 and 300 µg/ml gentamicin followed by 10 µg/ml gentamicin for 1 h. CFU was determined after cell lysis by plating serial dilutions on LB agar plates .

Doses between 100 – 300 µg/ml gentamicin showed a slightly, 1.5 fold increased bactericid activity compared to the 50 µg dose which is marginally active on extracellular bacteria with this short incubation time. In between the doses of 100 – 300 µg/ml gentamicin, there is no significant difference on intracellular CFU. Therefore, the highest dose of 300 µg/ml gentamicin was chosen for future experiments which lead to > 1000 fold reduction of extracellular bacteria in the experimental setting employed for cell separation and did not exhibit a different activity on intracellular bacteria as compared to the dose of 100 µg/ml as suggested in the literature[122,123].

Finally gentamicin activity on *S. typhimurium* ΔaroA was assessed at different temperatures (Fig. 31).

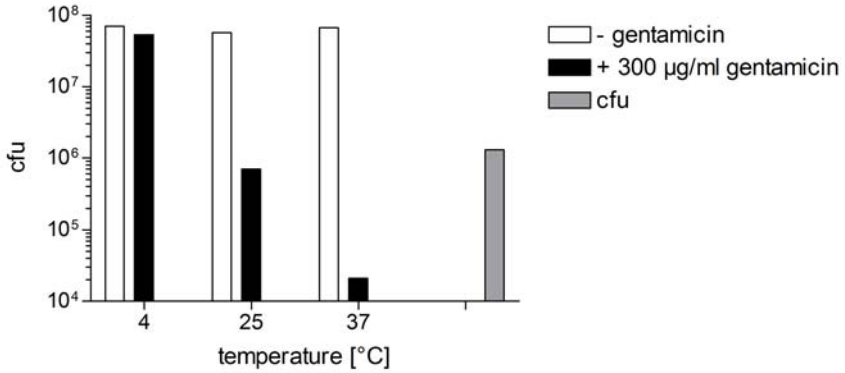

Figure 31: Effect of gentamicin at different temperatures

1 x 10^6 (CFU) *S. typhimurium* ΔaroA were incubated overnight at 4, 25 and 37 °C. Next day CFU was determined by plating serial dilutions on LB agar plates.

As depicted in figure 31, gentamicin had a reduced activity at 25 °C and no activity at 4 °C. Therefore, preparations containing bacteria have to be pre-incubated at 37 °C for 1 h to effectively kill the major part of extracellular bacteria.

V.7. Purity control of cell separation schedule

V.7.1. Light microscopic analysis

To evaluate the efficacy of the cell separation which could influence the results with respect to the number of infected cells, light microscopic analysis of the three different cell fractions were performed (Fig. 32).

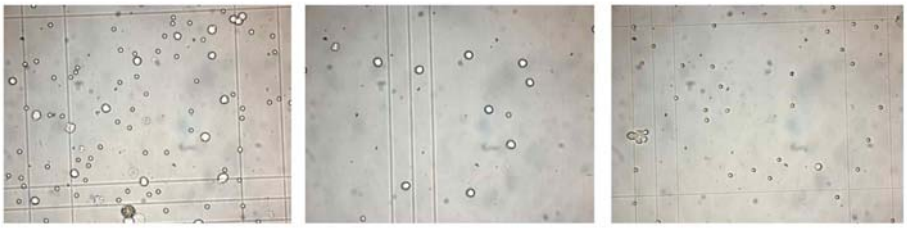

Figure 32: Light microscopic analysis of the three cell fractions after cell separation

The left panel in figure 32 shows the total tumor cell fraction. In the middle the separated macrophages are depicted. The right panel represents the macrophage-depleted fraction. The cells of all fractions mainly appear as single cells.

V.7.2. FACS analysis

After tumor removal and separating of total tumor cells by 0,001 % DNAse and 2 µg/ml dispase treatment, cell separation was performed using MACS®. To control the purity of the three cell fractions FACS analysis were performed (Fig. 33). Therefore cells were stained with an anti-CD11b-FITC, anti-F4/80-PE (Fig. 33) and anti-Gr-1-PE antibody (Fig. 34).

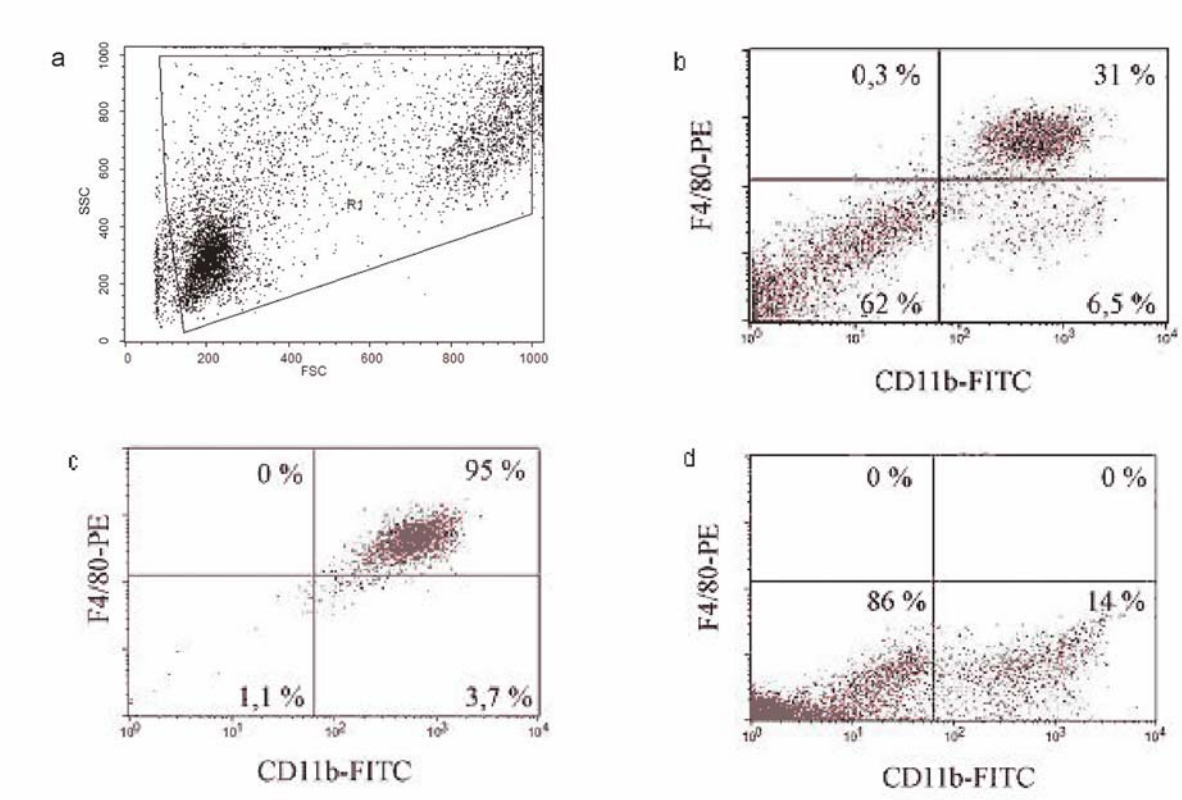

Figure 33: Control of cell fraction purity by FACS analysis

(**a**) FSC (forward scatter) – SSC (side scatter) dot blot of tumor cell suspension. Gating of tumor cell suspension and classification of live cells as population R1. Cell size and complexity affect the relative forward scatter and side scatter of incident light, respectively, which are presented in arbitrary units on a linear scale. Each dot represents the FSC and SSC value for a single tumor cell. (**b**, **c**, **d**) To control the purity of cell fractions after MACSing, cells were double stained with an anti-CD11b-FITC and anti-F4/80-PE antibody. Subsequently FACS analysis were performed. This figure shows one representative experiment out of seven. Up to 31 % macrophages were detected in the total cell fraction classified as R1 (**b**). After MACS® separation, the macrophage fraction showed a purity of 95 % (**c**) and no macrophages were detectable in the macrophage-depleted fraction (**d**).

The purity of the macrophages fraction is between 95–99 % (n = 7). Note that the macrophage fraction (Fig. 33c) contains a substantially lower amount of cells compared to the macrophage depleted (Fig. 33d) fraction.

For purity control the macrophage fraction and the magrophage-depleted fraction were also stained by an anti-CD11b-FITC and an anti-Gr-1-PE antibody, because we define our TAMs as F4/80$^+$, CD11b$^+$ and Gr-1$^-$ (Fig. 34). Gr-1 is a cell surface marker of granulocytes.

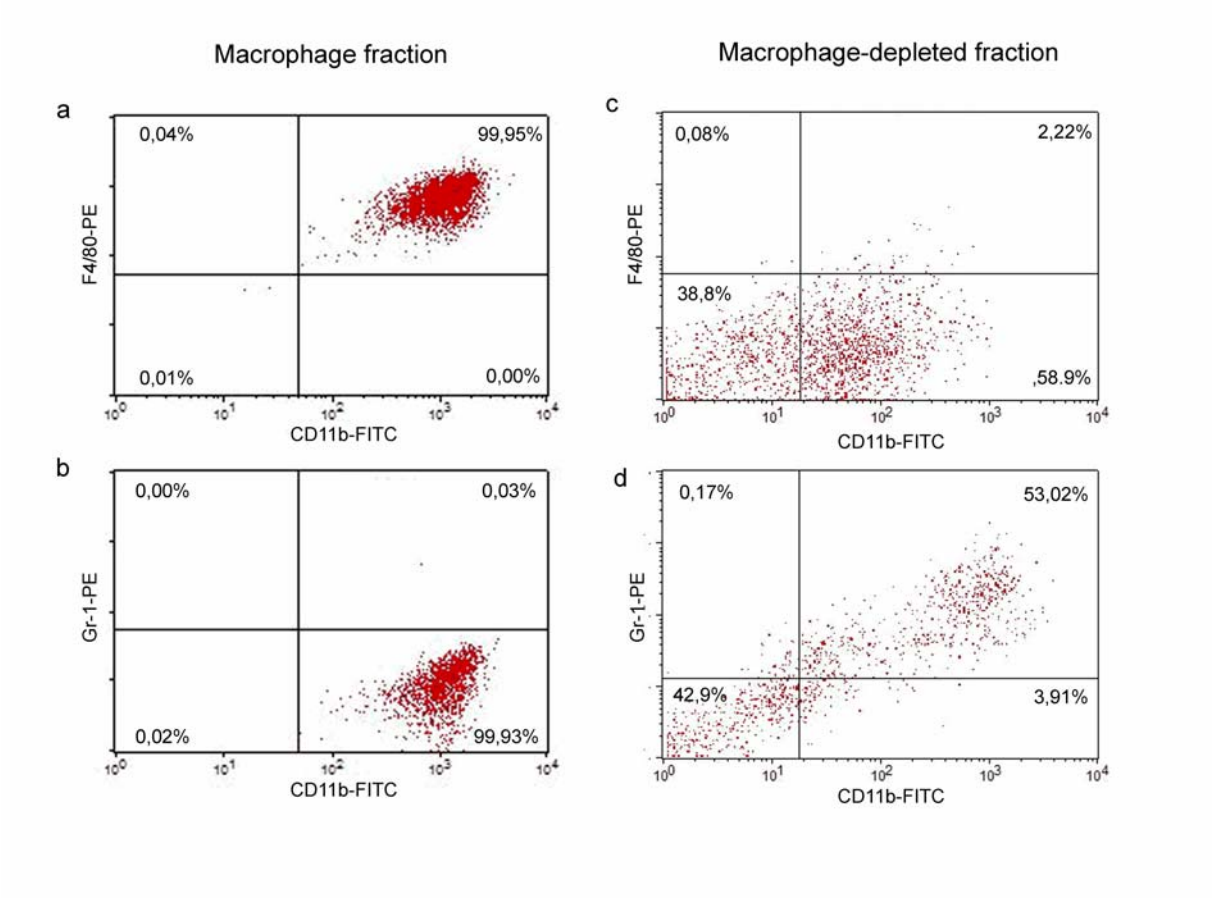

Fiure 34: Purity control of the macrophages fraction

For purity control the macrophages fraction (**a**, **b**) and the macrophage-depleted fraction (**c**, **d**) were also stained by an anti-CD11b-FITC and an anti-Gr-1-PE antibody (bottom panels). This figure shows one representative experiment out of seven.

As figure 34 shows, the number of Gr-1$^+$ cells in the macrophages fraction was between 0,01 – 0,03 % (Fig. 34b). So the degree of purity in the macrophages fraction was around 99 %. In addition we showed that TAMs do not express Gr-1 (Fig. 34b). In the macrophage-depleted fraction we detected up to 53 % Gr-1 and CD-11b double positive granulocytes (Fig. 34d). Whereas only few macrophages (around 2 %) were detectable in this fraction (Fig. 34c).

V.8. *Ex vivo* experiments

In this experimental setup tumor tissue from tumor-bearing Balb/c (Fig. 35a, b), or female MMTV-HER2 mice (Fig. 36a, b) were excised and separated. 1 x 10^6 cells per fraction were seeded in a 6-well-plate. After 3 h the different cell fractions were infected with the three different *Shigella* strains: *S. flexneri M90T*, *S. flexneri M90TΔaroA* and *S. flexneri BS176ΔaroA*. After an incubation of 1 h with 300 µg/ml gentamicin some samples were

prepared for Western Blot analysis (Fig. 35 and 36) and serial dilutions of the other samples were plated onto agar plates to determine CFU (Fig. 37).

V.8.1. *Ex vivo* activation of caspase-1

To investigate whether there is an activation of caspase-1 and an induction of apoptosis after an *ex vivo* infection, the three different cell fractions isolation from tumor-bearing Balb/c (Fig. 35) or MMTV-HER2 mice (Fig. 36) were infected with *S. flexneri M90T, S. flexneri M90TΔaroA* and *S. flexneri BS176ΔaroA* at a MOI of 100 for 1 h and Western Blot analysis was performed (Fig. 35 and 36).

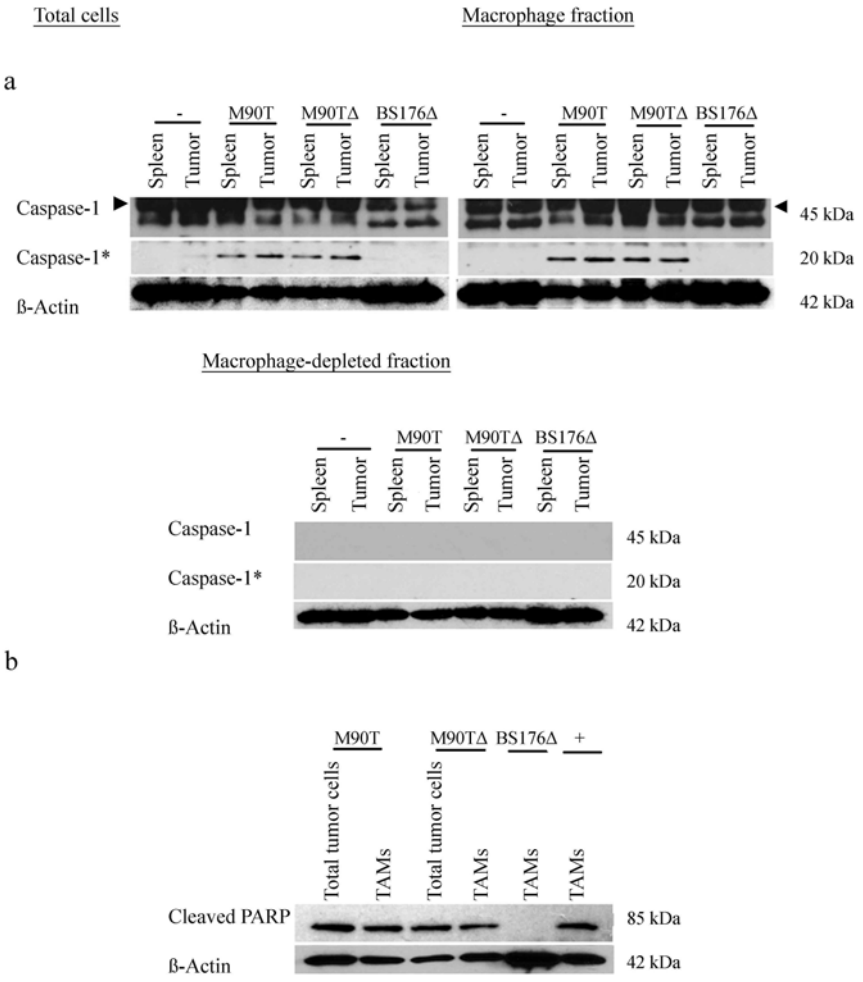

Figure 35: *Ex vivo* infection of separated 4T1-induced tumor cell fractions with *Shigella* strains

(**a**, **b**) *Ex vivo* infection of the three different cell fractions after cell isolation from tumor-bearing Balb/c mice with *S. flexneri M90T, S. flexneri M90TΔaroA* and *S. flexneri BS176ΔaroA* at a MOI of 100 for 1 h. After an incubation of 1 h with 300 µg/ml gentamicin the different samples were prepared for Western Blot analysis. The

antibody detects the procaspase-1 (45 kDa) and the activated caspase-1 20 kDa subunit (**a**, caspase-1*). The PARP antibody detects the cleaved PARP fragment of 85 kDa (**b**, cPARP). Cells were incubated with staurosporine (4 µM) for 6 h as positive control for apoptosis induction. β-Actin was used as loading control.

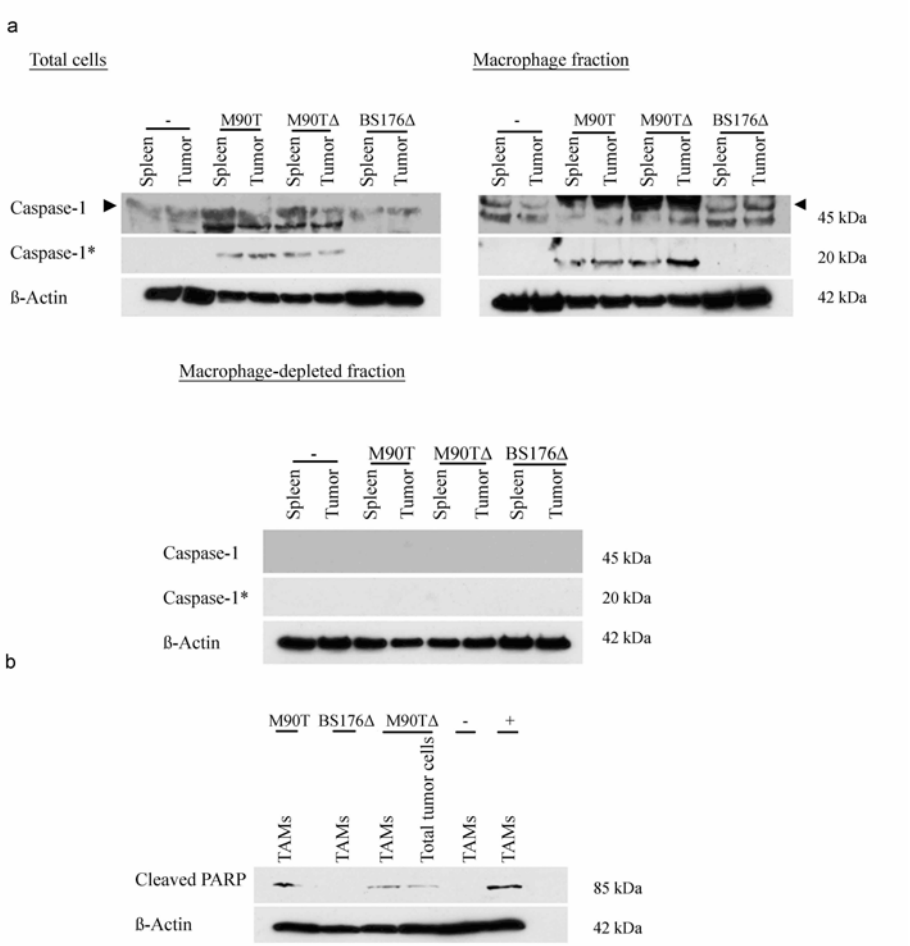

Figure 36: *Ex vivo* infection of separated MMTV-HER2 breast tumor cell fractions with *Shigella* strains

(**a**, **b**) *Ex vivo* infection of the three different cell fractions after cell isolation from MMTV-HER2 mice (**c**, **d**) with *S. flexneri M90T, S. flexneri M90TΔaroA* and *S. flexneri BS176ΔaroA* at a MOI of 100 for 1 h. After an incubation of 1 h with 300 µg/ml gentamicin the different samples were prepared for Western Blot analysis. The antibody detects the procaspase-1 (45 kDa) and the activated caspase-1 20 kDa subunit (**a**, caspase-1*). The PARP antibody detects the cleaved PARP fragment of 85 kDa (**b**, cPARP). Cells were incubated with staurosporine (4 µM) for 6 h as positive control for apoptosis induction. β-Actin was used as loading control.

M90T, *M90TΔaroA* (M90TΔ) but not *BS176ΔaroA* (BS176Δ) induced caspase-1 processing and apoptosis in macrophages isolated from 4T1-induced Balb/c breast tumors (Fig. 35) and spontaneous breast adenocarcinomas from transgenic MMTV-HER2/new FVB mice (Fig. 36) *ex vivo*. The macrophage-depleted fractions do not contain procaspase-1 in detectable levels.

V.8.2. Determination of CFU after *ex vivo* infection with *Shigella*

In the next experiment we wanted to investigate whether *Shigella flexneri M90TΔaroA* predominantly infects TAMs derived from freshly isolated breast tumors from 4T1-induced tumor-bearing Balb/c mice *ex vivo* (Fig. 37).

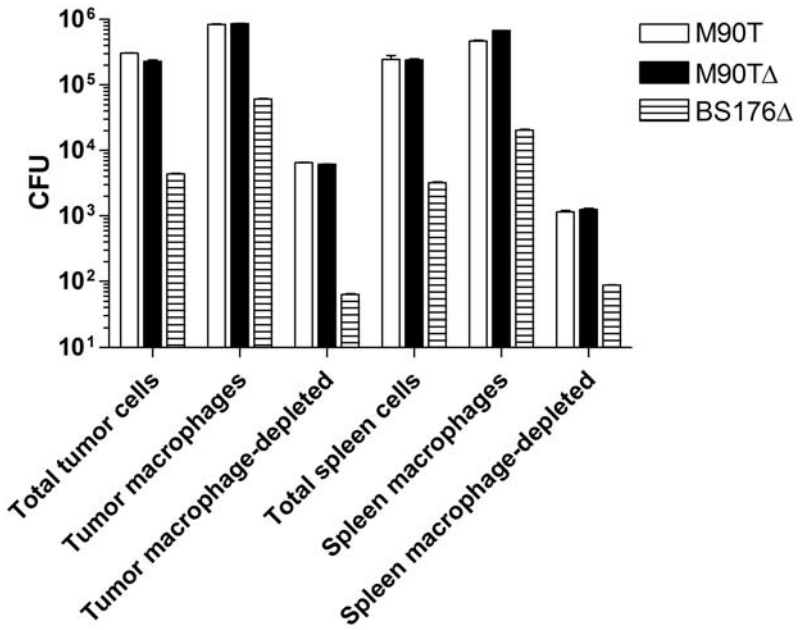

Figure 37: Determination of CFU after *ex vivo* infection of separated tumor cell fractions with *Shigella* strains

Tumor cells were separated and TAMs were isolated as described before. 1 x 10^6 cells of each cell fraction were seeded for 3 h. Subsequently the different cell fractions were infected *ex vivo* with wt *S. flexneri M90T* (M90T), *S. flexneri M90TΔaroA* (M90TΔ) and *S. flexneri BS176ΔaroA* (BS176Δ) at a MOI of 100. After 1 hour of infection, cells were incubated for 1 h with 300 µg/ml gentamicin followed by 1 h incubation with 50 µg/ml gentamicin. Subsequently, CFU was determined. All results shown are mean ± SD of two samples. Splenocytes were used as a control.

S. flexneri M90TΔaroA effectively infected TAMs isolated from 4T1-induced tumor-bearing Balb/c mice (Fig. 37). Again, infection of TAMs was at least 100 fold more efficient compared to the macrophage-depleted fraction. These results lead to the question whether 4T1 breast tumor cells generally can be infected by *S. flexneri M90TΔaroA*.

V.8.3. Determination of CFU after *in vitro* infection of 4T1 cells with *Shigella*

To investigate the ability of *S. flexneri M90T* to infect and invade 4T1 epithelial cells *in vitro*, we performed some invasion and survival assays (Fig. 38)

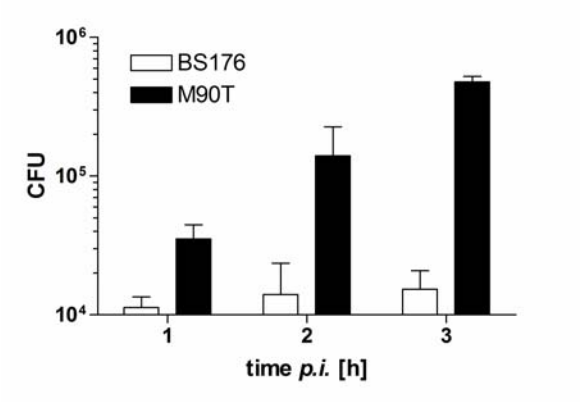

Figure 38: *In vitro* infection of 4T1 cells with *S. flexneri M90T*

Invasion and survival assay with 4T1 cells to determine the grade of infection. 2 x 10^5 cells were infected at a MOI of 100 with *S. flexneri M90T* and *S. flexneri BS176* for 1 h *p.i.* (invasion), 2 h *p.i.* and 3 h *p.i.* (survival). Subsequently CFUs and the grade of infection were determined. Bars represent means +/- SD of four different experiments.

As depicted in figure 38, the strain *S. flexneri M90T* showed at 1 h *p.i.* about 3 fold higher grade of infection in comparison to the non-invasive strain *S. flexneri BS176*. These data show that the strain *S. flexneri M90T* is able to invade non-phagocytic epithelial cells like 4T1 breast cancer cells. Moreover *S. flexneri M90T* is able to survive and replicate intracellularly.

V.9. *In vivo* experiments

After our *ex vivo* experiments we wanted to determine whether *S. flexneri M90TΔaroA* also effectively infects TAMs and activates caspase-1 *in vivo*.

V.9.1. Determination of CFU and infected cell number

In this set of experiments, we wanted to investigate the quantitative distribution of *Shigella* and *Salmonella* in the extracellular and intracellular compartment of different breast tumor models, as well as different cell types of the tumor tissue. Therefore 1 x 10^6 *Salmonella typhimurium* ΔaroA (*Salmonella typhimurium* ΔaroA, StmΔ), *Shigella flexneri BS176ΔaroA*

(BS176Δ) and *Shigella flexneri M90TΔaroA* (M90TΔ) were applied intravenously in mice with established 4T1 tumors (Fig. 39 and 40) or spontaneous MMTV-HER2/new breast carcinoma (Fig. 41 and 42).

Therefore tumors were removed at different time points after infection. Tumor cells were separated to obtain a tumor cell suspension. Pools of the tumor cell suspension were treated with gentamicin to distinguish extra- and intracellular bacteria. In parallel, cells were separated in macrophages and macrophage-depleted fractions to analyze the bacterial content. The cell number of every cell fraction was determined by a Bürker cell chamber. Plating was performed either after lysis of the eukaryotic cells to determine total CFU titers, or by plating in L-Top agar avoiding cell lysis to determine the number of infected cells (Fig. 39, 40, 41 and 42).

V.9.1.1. Determination of CFU and infected cell number after infection with *S. typhimurium* ΔaroA in the 4T1-induced tumor model

1 x 10^6 *Salmonella typhimurium* ΔaroA (*Salmonella typhimurium* ΔaroA, StmΔ) were applied intravenously in mice with established 4T1 tumors and quantitative distribution of these bacteria was investigated in the extracellular and intracellular compartment of this breast tumor model (Fig. 39).

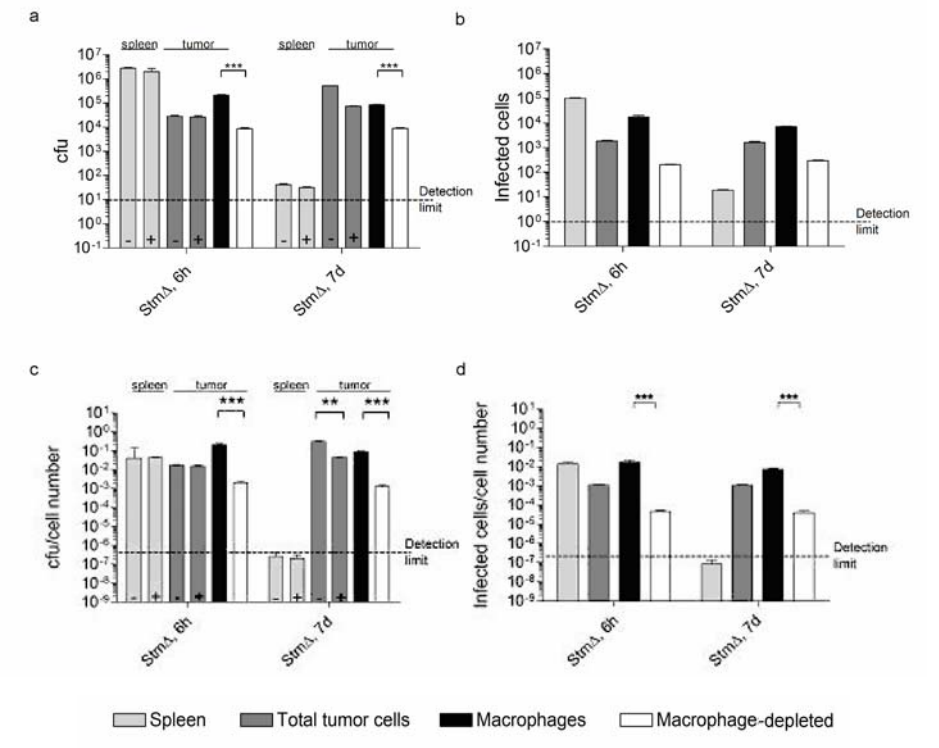

Figure 39: *Salmonella* predominantly target TAMs in Balb/c mice at early time points

Determination of CFU (**a**), infected cell number (**b**), CFU/cell number (**c**) and infected cells/cell number (**d**) of separated tumor cells and splenocytes as a control 6 h and 7 d after i.v. infection of tumor-bearing mice (n = 3 mice per group and time point) with 1 x 10^6 *S. typhimurium* ΔaroA (StmΔ) . CFU was determined by plating serial dilutions of cell lysate. Infected cell number were determined by plating non-lysed, gentamicin treated cells, in L-Top agar. + describes gentamicin treatment in contrast to – (without gentamicin treatment). All results shown are mean ± SD; **: $p < 0,01$, ***: $p < 0,001$, Student`s t-test. Detection limits are set up at the highest values of counted tumor cell number.

As shown in figure 39, the strain *Salmonella typhimurium* ΔaroA predominantly targets TAMs *in vivo* after 6 h *p.i*. 7 d after infection there were only few bacteria detected in the spleen, which is in line with previous works[132]. After 6 h and 7 d significantly more bacteria are found in the macrophages fraction compared to macrophage-depleted tumor cells. 4 h and 6 h after infection, most bacteria are intracellular, whereas 7 d after infection more bacteria are found extracellularly as determined by CFU numbers derived from gentamicin treated compared to untreated total tumor cells.

V.9.1.2. Determination of CFU and infected cell number after infection with *Shigella* in the 4T1-induced tumor model

Subsequently we analysed whether *Shigella* shows a similar preferred targeting of macrophages as observed for *Salmonella.* Therefore, we injected *Shigella* i.v. in Balb/c mice with established 4T1-tumors in a similar setting as performed before for *Salmonella* (Fig. 40).

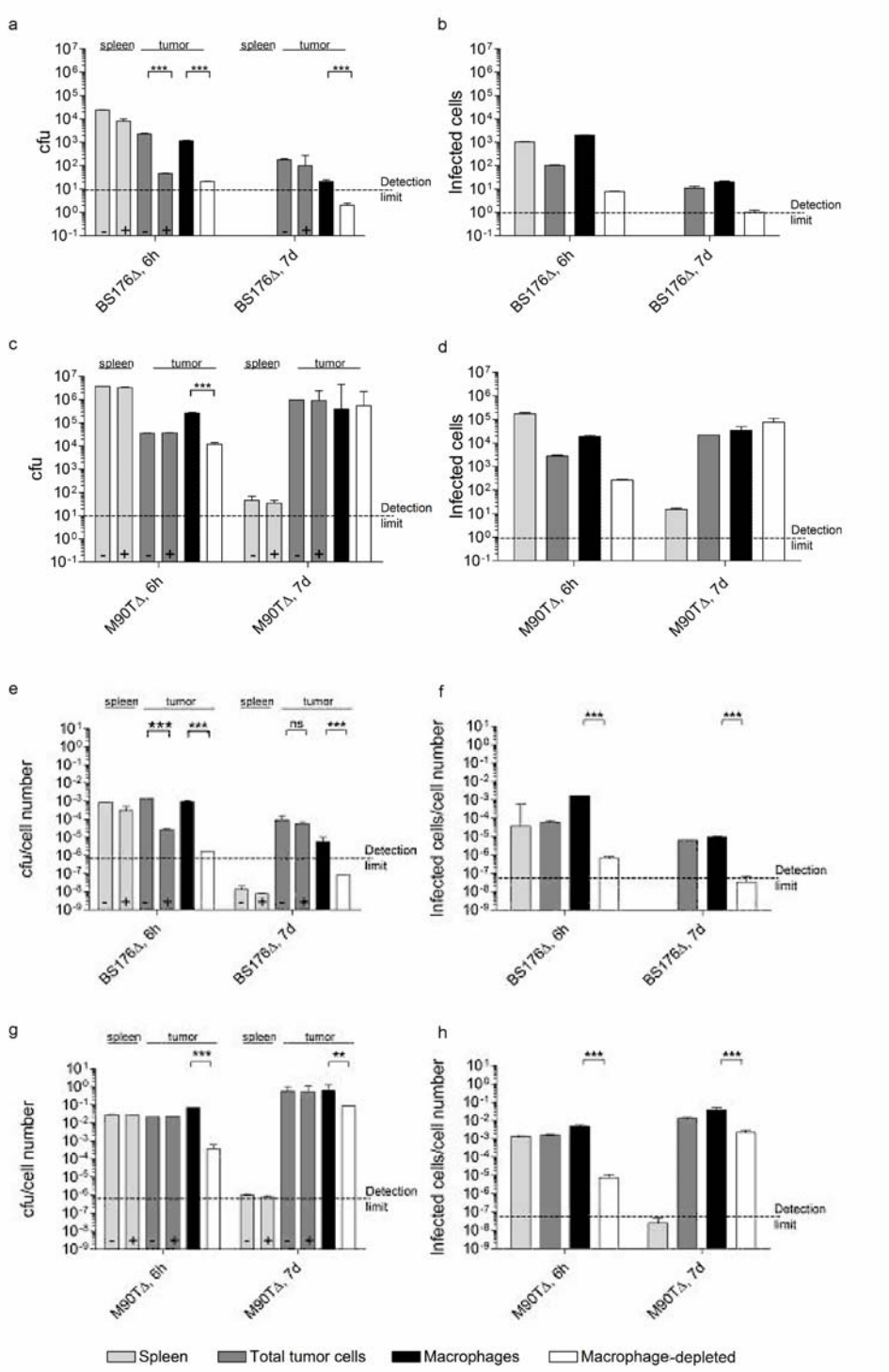

Figure 40: *S. flexneri M90TΔaroA* predominantly target TAMs in Balb/c mice

Determination of CFU (**a**, **c**), infected cell number (**b**, **d**), CFU/cell number (**e**, **g**) and infected cells/cell number (**f**, **h**) of separated tumor cells and splenocytes as a control 6 h and 7 d after i.v. infection of tumor-bearing Balb/c mice (n = 3 mice per group and timepoint) with *S. flexneri BS176ΔaroA* (BS176Δ) (**a**, **b**, **e**, **f**) and *M90TΔaroA* (M90TΔ) (**c**, **d**, **g**, **h**). + describes gentamicin treatment in contrast to – (without gentamicin treatment). All results shown are mean ± SD; **: $p < 0,01$, ***: $p < 0,001$, Student`s t-test. Detection limits are set up at the highest values of counted tumor cell number.

Again, significantly more bacteria per cell (Fig. 40e, g) and more infected cells (Fig. 40f, h) were found in the macrophages fraction at any time point. Furthermore, the major part of *S. flexneri M90TΔaroA* is found intracellularly (Fig. 40g), whereas 50 fold more bacteria were found extracellularly 6 h after infection with the avirulent strain *S. flexneri BS176ΔaroA* (Fig. 40e).

V.9.1.3. Determination of CFU and infected cell number after infection with *S. typhimurium* ΔaroA in the MMTV-HER2/new tumor model

To investigate the exact location of bacteria like *Salmonella* in a spontaneous tumor model, we performed the same experimental setup with transgenic MMTV-HER2/new mice (Fig. 41).

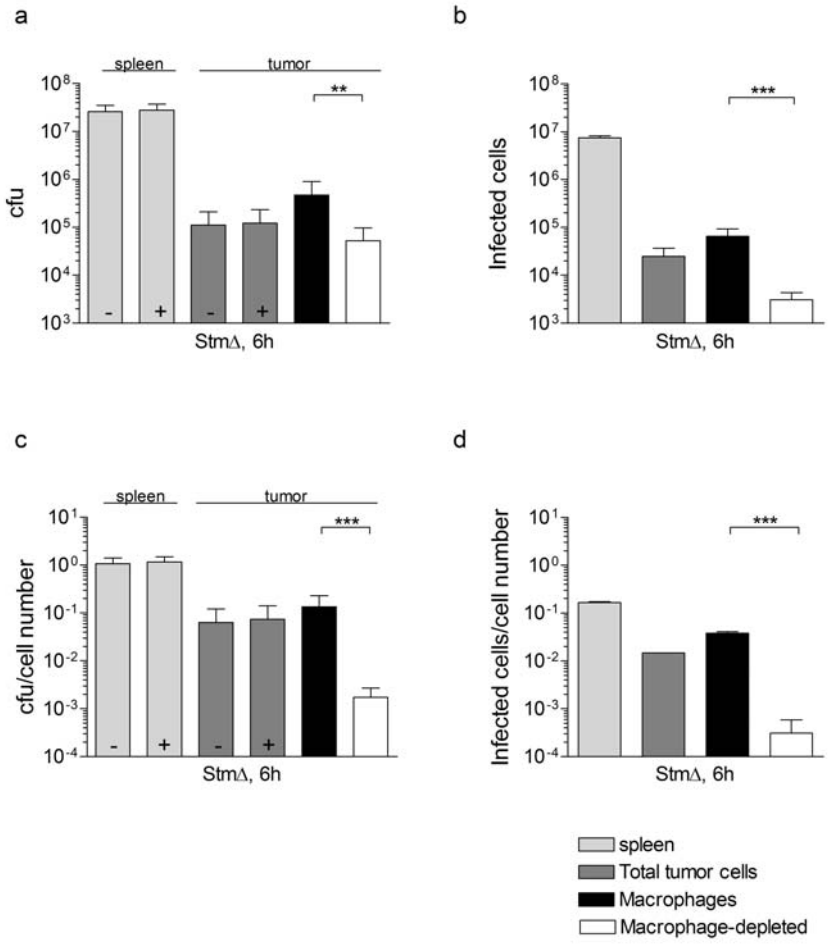

Figure 41: *S. typhimurium* ΔaroA (StmΔ) predominantly targets TAMs in transgenic MMTV-HER2/new FVB mice

In vivo infection of tumor-bearing MMTV-HER2/new FVB mice with 1 x 10^6 *Salmonella typhimurium* ΔaroA (StmΔ) and determination of CFU (**a**, **c**) and the number of infected cells (**b**, **d**) by L-top agar assay after 6 h. Tumor-bearing MMTV-HER2/new FVB mice (n = 4) were infected with *Salmonella typhimurium* ΔaroA (1 x

10^6). 6 h *p.i.* spleens and tumors were removed, cells were separated and gentamicin-treated (+) or not (-). Total CFU was determined by plating serial dilutions of lysed cells and the number of infected cells was determined by plating of serial dilutions of intact cells in L-Top agar. All results shown are mean ± SD; **: $p < 0,01$, ***: $p < 0,001$, Student`s t-test.

Similar to the results obtained with transplanted tumors (Fig. 39), *Salmonella* infected TAMs with approximately 100 fold higher efficiency as compared to macrophage-depleted tumor cells in a transgenic animal model bearing spontaneous breast adenocarcinoma (Fig. 41a-d). Also in this model, the majority of bacteria was intracellular.

V.9.1.4. Determination of CFU and infected cell number after infection with *Shigella* in the MMTV-HER2/new tumor model

To investigate the exact location of bacteria like *Shigella* in a spontaneous tumor model, we performed the same experimental setup with transgenic MMTV-HER2/new FVB mice (Fig. 42).

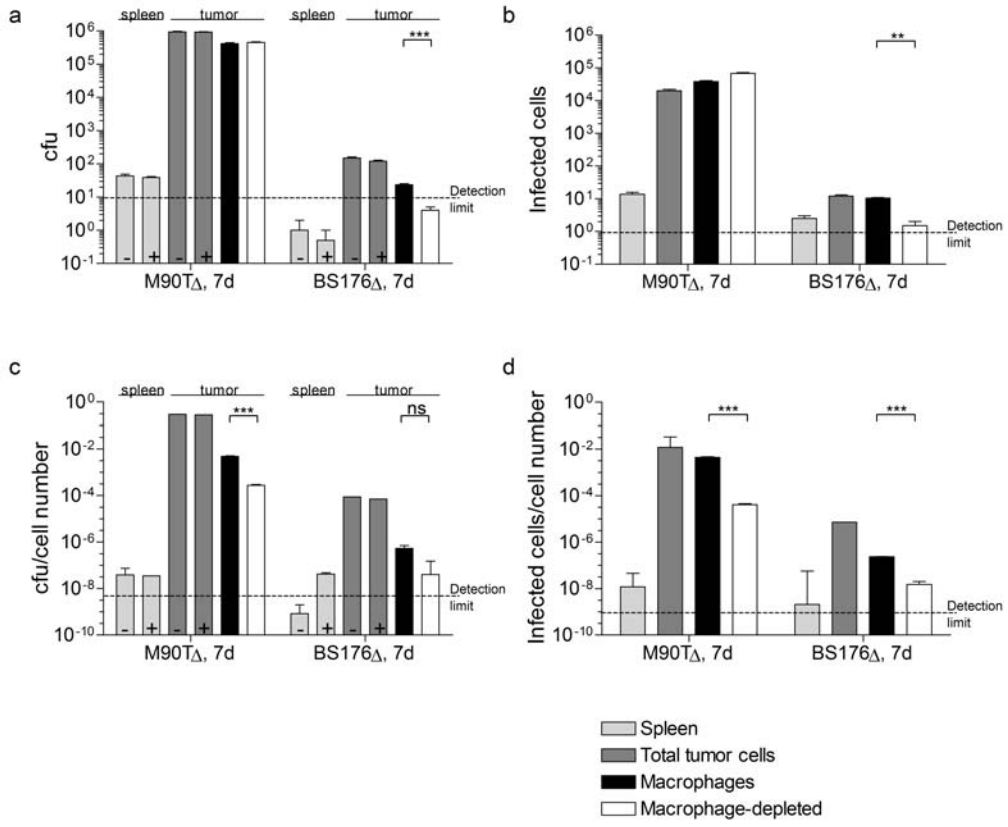

Figure 42: *S. flexneri M90TΔaroA* (M90TΔ) predominantly targets TAMs in transgenic MMTV-HER2 mice

Determination of CFU (**a**, **c**) and the number of infected cells (**b**, **d**) by L-Top agar assay after 7 d. Tumor-

bearing MMTV-HER2/new FVB mice (n = 4) were infected with *S. flexneri M90TΔaroA* and *BS176ΔaroA* (1 x 10^6). After 7 d *p.i.* spleens and tumors were removed, and cells were separated. Total CFU was determined by plating of serial dilutions of lysed cells and the number of infected cells was determined by plating serial dilutions of intact cells in L-Top agar. All results shown are mean ± SD; **: $p < 0,01$, ***: $p < 0,001$, Student`s t-test. Detection limits are set up at the highest values of counted tumor cell number.

S. flexneri M90TΔaroA predominantly resided in macrophages of tumor-bearing mice with spontaneous breast adenocarcinoma (5 fold difference compared to macrophage-depleted fraction) 7 d *p.i.* (Fig. 42). The non-invasive *S. flexneri BS176ΔaroA* strain was still present in the tumors with very low bacteria numbers and also found predominantly in macrophages.

V.9.2. Kinetics of bacterial tumor colonization

To determine the kinetics of tumor colonization 1 x 10^6 *S. flexneri M90TΔaroA* and *S. flexneri BS176ΔaroA* were applied intravenously in mice with established 4T1 tumors and quantitative distribution of these bacteria was investigated in the extracellular and intracellular compartment of this breast tumor model after 1 d, 3 d and 7 d *p.i.* (Fig. 43).

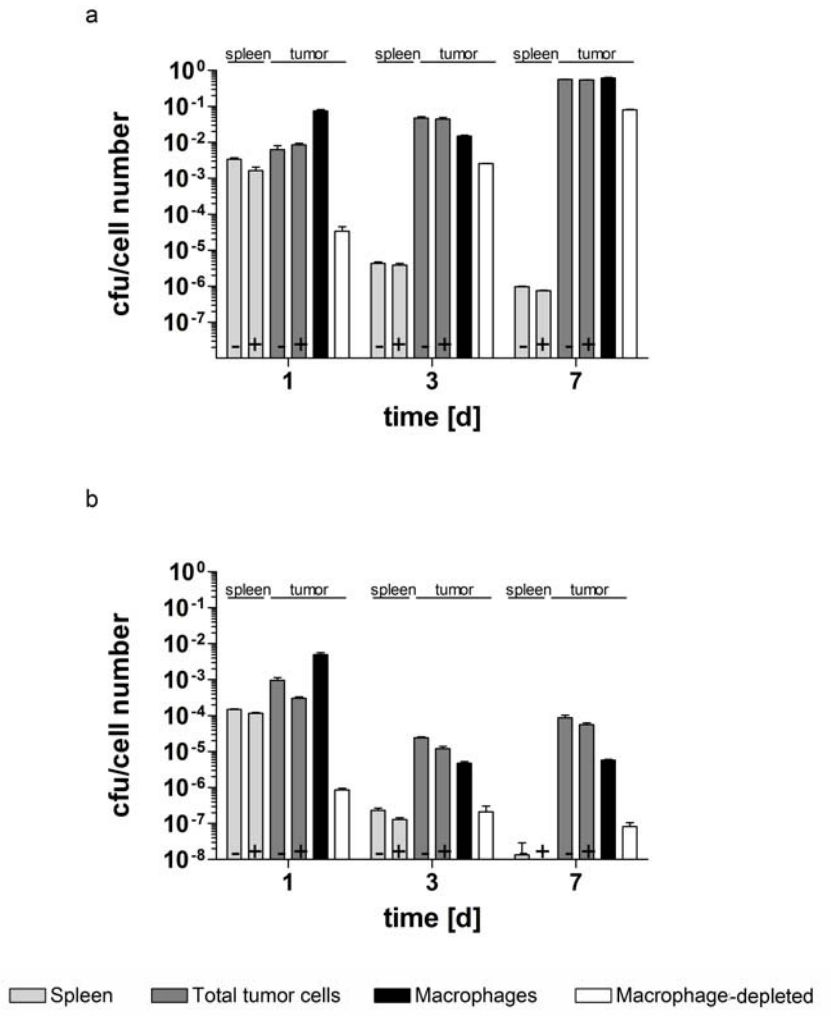

Figure 43: Kinetics of tumor targeting by *Shigella* in tumor-bearing Balb/c mice

Determination of CFU/cell number after 1 d, 3 d and 7 d *p.i.* 4T1-induced tumor-bearing Balb/c mice (n = 4) were infected with 1 x 10^6 *S. flexneri M90TΔaroA* (**a**) and *BS176ΔaroA* (**b**). After 1 d, 3 d and 7 d *p.i.* spleens and tumors were removed, and cells were separated. Total CFU was determined by plating of serial dilutions of lysed cells. + describes gentamicin treatment in contrast to – (without gentamicin treatment). All results shown are mean ± SD.

Again, significantly more bacteria per cell were found in the macrophages fraction at any time point (Fig. 43a, b). Furthermore, the major part of *S. flexneri M90TΔaroA* is found intracellularly at 1 d, 3 d and 7 d *p.i.* (Fig. 43a), whereas some bacteria were found extracellularly at all time points after infection with the avirulent strain *S. flexneri BS176ΔaroA* (Fig. 43b).

V.9.3. Caspase-1 activation and induction of apoptosis *in vivo*

Afterwards we asked whether there is an induction of apoptosis in the macrophages via caspase-1 activation by secreted SipB (*Salmonella*) or IpaB (*Shigella*) *in vivo*. Therefore we analysed the cell populations for caspase-1 activation and induction of apoptosis after infection with *Salmonella typhimurium* ΔaroA (Fig. 44) and *Shigella* (Fig. 45 and 46).

V.9.3.1. Caspase-1 activation and induction of apoptosis by *S. typhimurium ΔaroA* in the 4T1-induced tumor model

After infection of 4T1-induced tumor-bearing mice with *Salmonella*, caspase-1 activation and PARP cleavage of separated and lysed tumor cells was analyzed by Western Blot (Fig. 44).

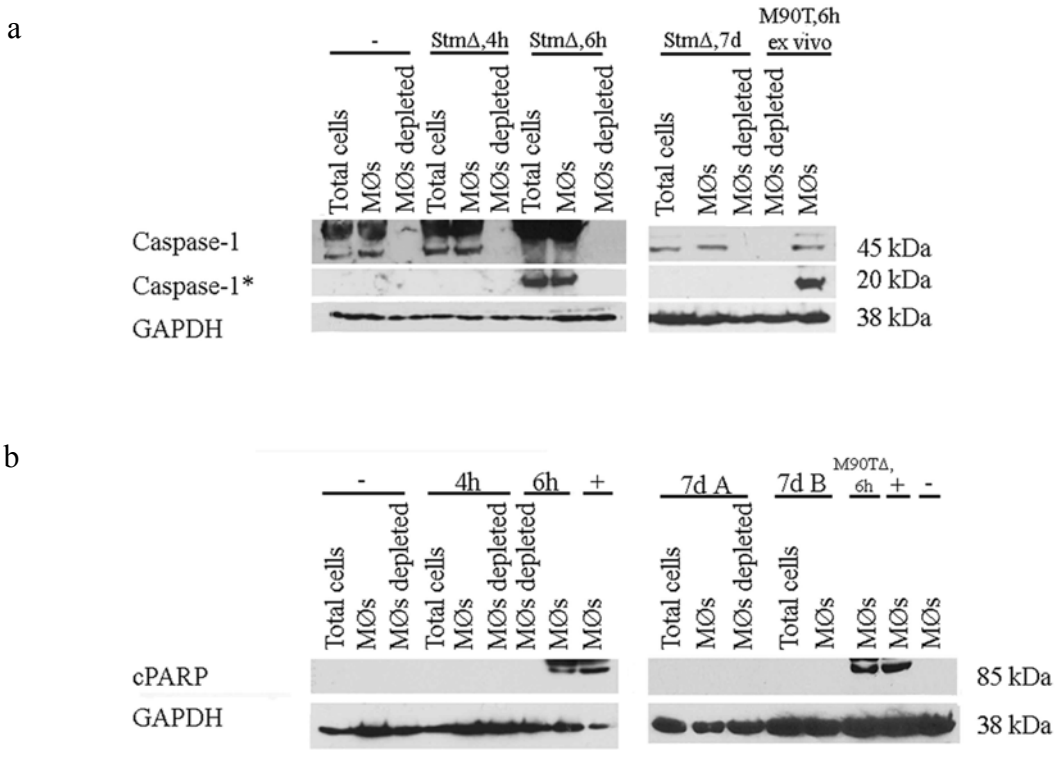

Figure 44: Caspase-1 activation and induction of apoptosis 6 h after infection with *S. typhimurium* ΔaroA

In vivo infection of tumor-bearing Balb/c mice with 1 x 10^6 *S. typhimurium* ΔaroA (StmΔ), tumor cell isolation and analysis for caspase-1 activation (**a**) and induction of apotosis (**b**). *Ex vivo* infection with *S. flexneri M90T* for 2 h in tumor-bearing Balb/c isolated TAMs was used as positive control for caspase-1 activation. Incubation of tumor-bearing Balb/c isolated TAMs with staurosporine (4 µM) for 6 h was taken as positive control for PARP cleavage. The caspase-1 antibody detects the caspase-1 zymogen of 45 kDa and the active 20 kDa subunits of caspase-1 (caspase-1*). The PARP antibody detects the cleaved PARP fragment (cPARP) of 85 kDa. GAPDH was used as loading control.

Caspase-1 activation and PARP cleavage was detected in total cells and macrophages fraction of tumors from mice 6 h after infection, but not from 4 h infected mice (Fig. 44). Caspase-1 activation and PARP cleavage was not detected in the macrophage-depleted fraction, where neither caspase-1 processing nor caspase-1 expression was detectable. Caspase-1 induction was not detected in any fraction 7 d after *Salmonella* infection.

V.9.3.2. Caspase-1 activation and induction of apoptosis by *S. flexneri M90TΔaroA*

V.9.3.2.1. Caspase-1 activation and induction of apoptosis in the 4T1-induced tumor model

In this experimental setup 4T1-induced tumor-bearing Balb/c mice were infected with *Shigella aroA*-mutants for 4 h, 6 h and 7 d. Subsequently caspase-1 activation and PARP cleavage of separated and lysed tumor cells was analyzed by Western Blot (Fig. 45).

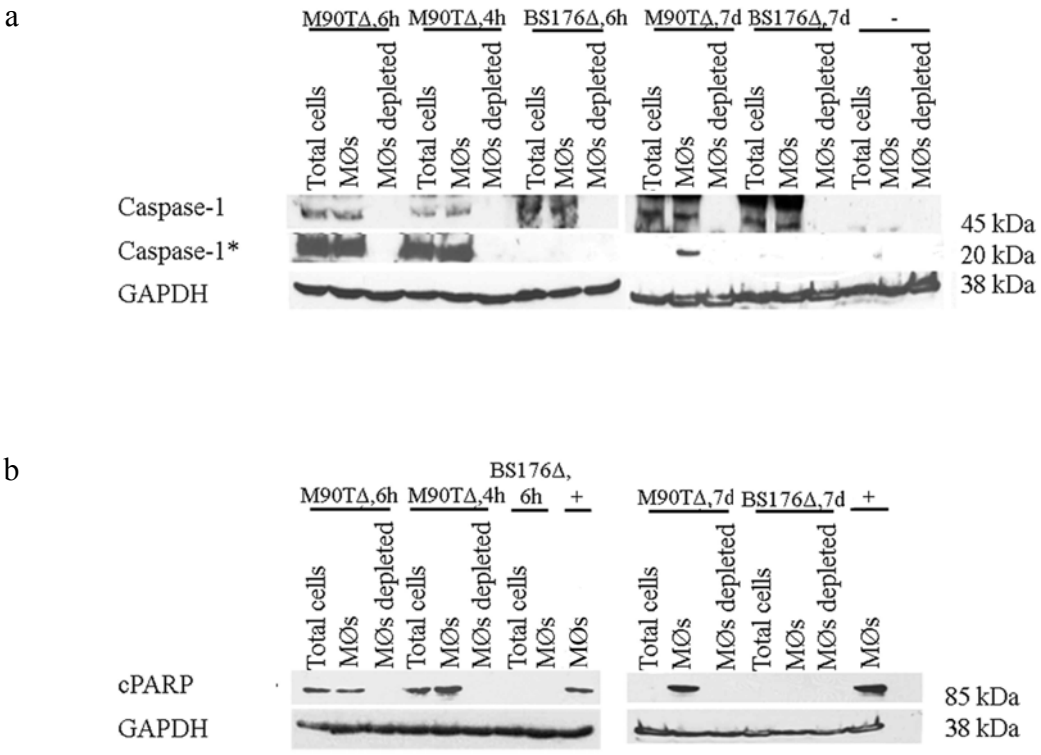

Figure 45: Caspase-1 activation and induction of apoptosis 4 h, 6 h and 7 d after infection with *S. flexneri M90TΔaroA* in tumor-bearing Balb/c mice

In vivo infection of tumor-bearing Balb/c mice with 1 x 10^6 *S. flexneri M90TΔaroA* (M90TΔ) or *S. flexneri BS176ΔaroA* (BS176Δ), tumor cell isolation and analysis for caspase-1 activation (**a**) and induction of apotosis (**b**). The caspase-1 antibody detects the caspase-1 zymogen of 45 kDa and the active 20 kDa subunits of caspase-1 (caspase-1*). The PARP antibody detects the cleaved PARP fragment (cPARP) of 85 kDa. GAPDH was used

as loading control. Incubation of tumor-bearing Balb/c isolated TAMs with staurosporine (4 µM) for 6 h was taken as positive control for PARP cleavage.

Caspase-1 activation (Fig. 45a) and PARP cleavage (Fig. 45b) was detectable in total cells and macrophages fraction of tumors taken from mice 4 h and 6 h after *S. flexneri M90TΔaroA* infection, and in the macrophages fraction 7 d after infection with *S. flexneri M90TΔaroA*, but not *S. flexneri BS176ΔaroA*.

V.9.3.2.1. Caspase-1 activation and induction of apoptosis in the MMTV-HER2/new tumor model

In this experimental setup tumor-bearing MMTV-HER2/new FVB mice were infected with *Shigella aroA*-mutants for 6 h and 7 d. Subsequently caspase-1 activation and PARP cleavage of separated and lysed tumor cells was analyzed by Western Blot (Fig. 46).

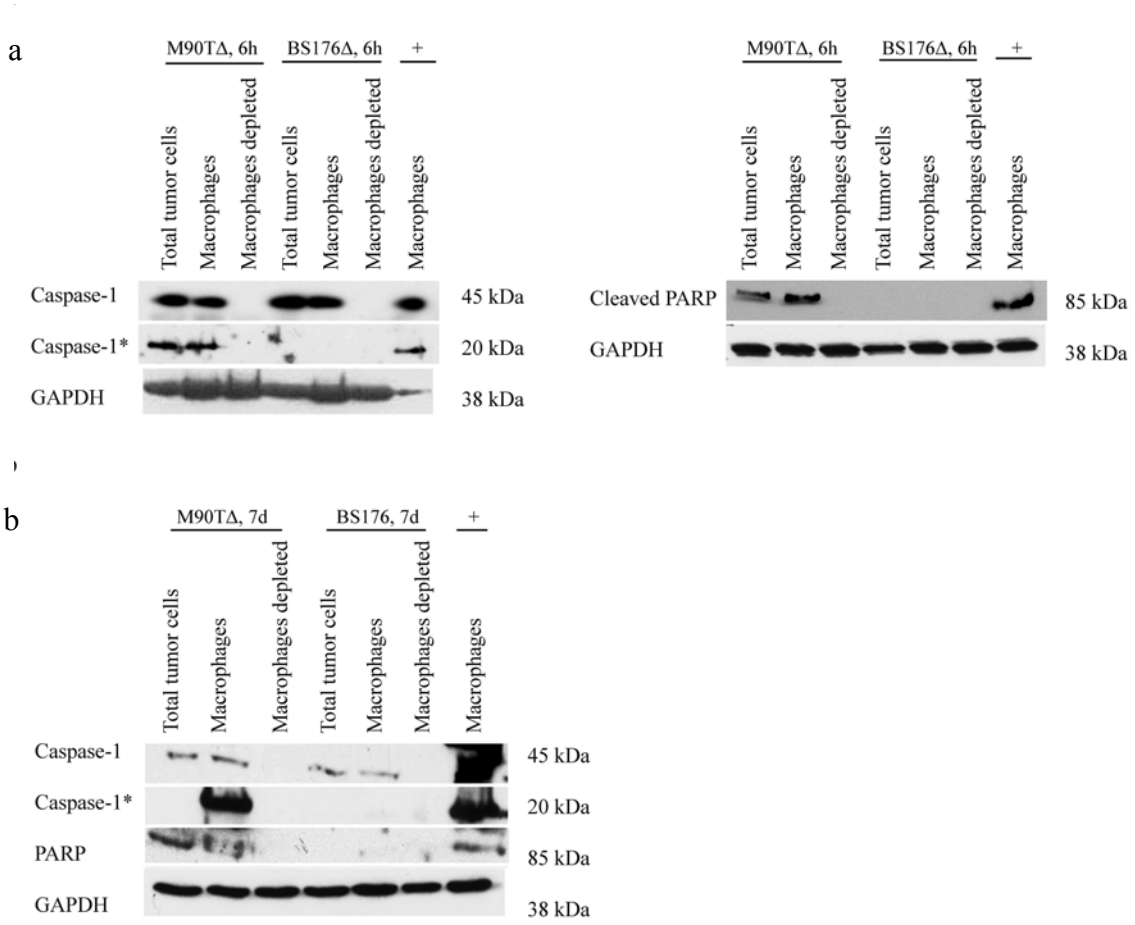

Figure 46: Caspase-1 activation and induction of apoptosis 4 h, 6 h and 7 d after infection with *S. flexneri M90TΔaroA* in MMTV-HER2/new FVB mice

In vivo infection of tumor-bearing MMTV-HER2/new mice with 1 x 10^6 *S. flexneri M90TΔaroA* (M90TΔ) or *S.*

flexneri BS176ΔaroA (BS176Δ), tumor cell isolation and analysis for caspase-1 activation (**a**) and induction of apotosis (**b**). The caspase-1 antibody detects the caspase-1 zymogen of 45 kDa and the active 20 kDa subunits of caspase-1 (caspase-1*). The PARP antibody detects the cleaved PARP fragment (cPARP) of 85 kDa. GAPDH was used as loading control. *Ex vivo* infection with *S. flexneri M90T* for 2 h in tumor-bearing Balb/c isolated TAMs was used as positive control for caspase-1 activation. Incubation of tumor-bearing Balb/c isolated TAMs with staurosporine (4 µM) for 6 h was taken as positive control for PARP cleavage.

Similar to the results obtained with transplanted tumors (Fig. 39), caspase-1 activation and induction of apoptosis by *Shigella flexneri M90TΔaroA* was detected in the total cell fraction and in macrophages fraction 4 h, 6 h and 7 d *p.i*. in transgenic MMTV-HER2 breast tumor mice (Fig. 46). In addition caspase-1 activation and PARP cleavage was not detected in the macrophage-depleted fraction, where neither caspase-1 processing nor caspase-1 expression was detectable. Also caspase-1 induction was not detected in any fraction after infection with *Shigella flexneri BS176ΔaroA*.

V.10. Determination of TAMs number by FACS analysis

In the next set of experiments, 1 x 10^6 *S. typhimurium* ΔaroA (StmΔ), *S. flexneri BS176ΔaroA* (BS176Δ) and *S. flexneri M90TΔaroA* (M90TΔ) were applied intravenously in mice with established 4T1 tumors (Fig. 48) or spontaneous breast carcinoma (Fig. 49). 7 d post infection the relative amount of TAMs was determined by FACS analysis (Fig. 47).

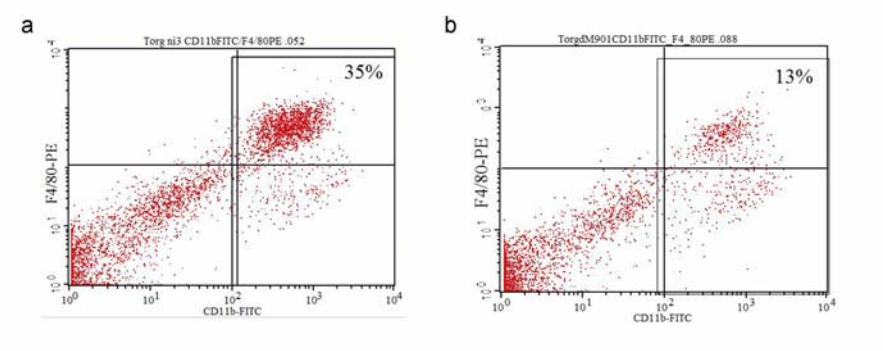

Figure 47: Determination of TAMs number by FACS analysis

To control the the number of TAMs 7 d after infection with *S. typhimurium* ΔaroA (StmΔ), *S. flexneri BS176ΔaroA* (BS176Δ) and *S. flexneri M90TΔaroA* (M90TΔ) in tumor-bearing Balb/c (Fig. 48) and transgenic MMTV-HER2/new FVB (Fig. 49), the relative amount of TAMs was determined by FACS. Cells were double stained with an anti-CD11b-FITC and anti-F4/80-PE antibody. Subsequently FACS analysis were performed. This figure shows one representative experiment of infection with not infected tumor tissue (**a**) and tumor tissue 7 d infected with *S. flexneri M90TΔaroA* (**b**).

The number of macrophages in the tumor tissue of naïve mice was between 27-35 % (n = 4, in the 4T1-induced tumor model) and 30-45 % (n = 3, in the MMTV-HER2/new tumor model). Note that the reduction of macrophage number in 7d *M90TΔaroA*-infected tumor tissue was up to 70 % in both breast tumor models (Fig. 47b).

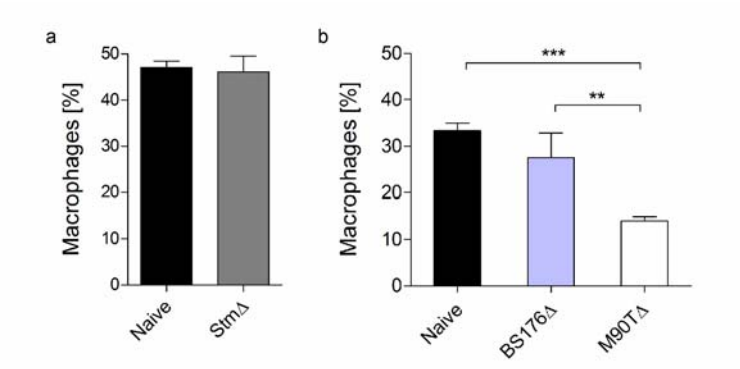

Figure 48: Determination of TAMs number in the 4T1-induced tumor model by FACS analysis

7 d after infection with *S. typhimurium* ΔaroA (**a**, StmΔ), *S. flexneri BS176ΔaroA* (**b**, BS176Δ) and *S. flexneri M90TΔaroA* (**b**, M90TΔ) in tumor-bearing Balb/c mice, the relative amount of TAMs was determined by FACS. Bars represent means +/- SD of four (M90TΔ , BS176Δ) alternatively three (StmΔ) tumors analyzed per group, **: $p < 0.01$, ***: $p < 0.001$, Students t-test.

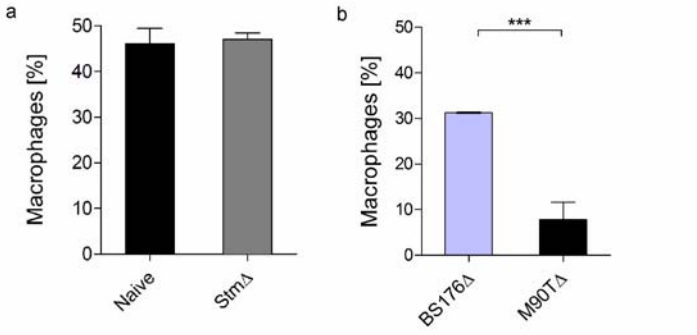

Figure 49: Determination of TAMs number in the MMTV-HER2/new tumor model by FACS analysis

7 d after infection with *S. typhimurium* ΔaroA (**a**, StmΔ), *S. flexneri BS176ΔaroA* (**b**, BS176Δ) and *S. flexneri M90TΔaroA* (**b**, M90TΔ) in tumor-bearing MMTV-HER2/new FVB mice the relative amount of TAMs was determined by FACS. Bars represent means +/- SD of four (M90TΔ , BS176Δ) alternatively three (StmΔ) tumors analyzed per group, **: $p < 0.01$, ***: $p < 0.001$, Students t-test.

S. flexneri M90TΔaroA, but not *S. flexneri BS176ΔaroA* infection resulted in a substantial reduction in macrophage numbers 7 d after infection in both breast tumor models (Fig. 47b,

48 and 49). In addition an infection with *S. typhimurium* ΔaroA did not affect macrophage numbers 7 d after infection in both breast tumor models (Fig. 48 and 49).

V.11. Fluorescence staining for cytokeratin

To confirm that epithelial 4T1 cells are positive for cytokeratin we performed some *in vitro* fluorescence staining (Fig. 50).

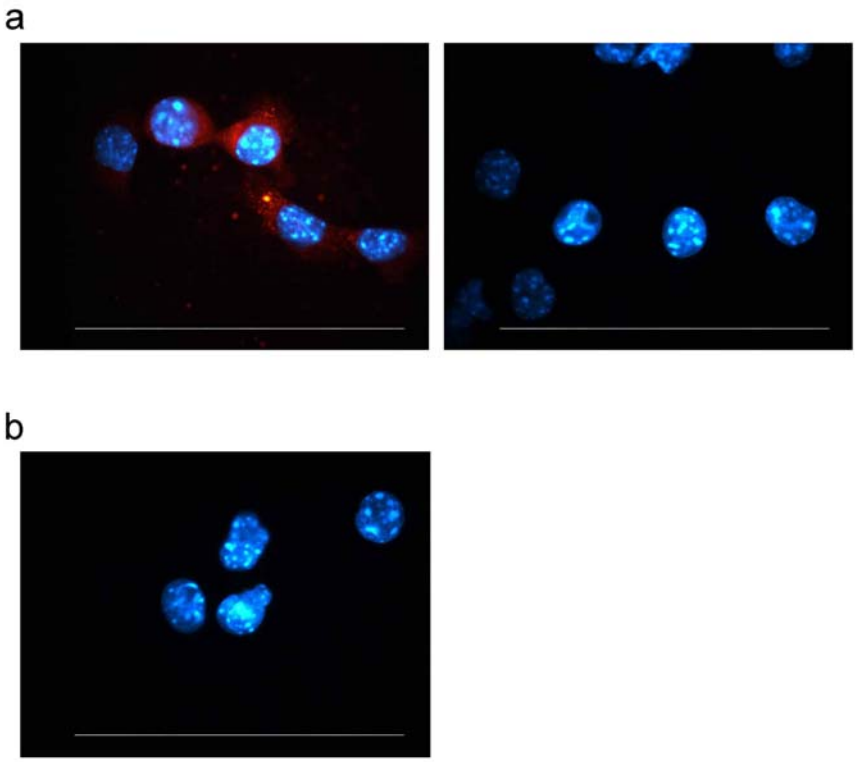

Figure 50: Fluorescence staining for cytokeratin of 4T1 cells *in vitro*

4T1 cells (**a**) and RAW 264.7 (**b**) macrophages were grown on coverslips for 36 h. Then cells were fixed with 3.7 % paraformaldehyde and quenched with 10 mM NH_4Cl in PBS. The primary antibody anti cytokeratin was incubated for 30 min with cells. After several washes with PBS, Tetramethyl Rhodamine Iso-Thiocyanate (TRITC)-labeled secondary antibody were diluted in PBS/BSA and incubated with cells for 30 min. Then the cells were treated with 0.1 µg/ml Hoechst 33342 dye. At the end cells were covered with Mowiol and subjected to fluorescence microscopy. In 4T1 case right panel is the antibody control. Scale bars represent 50 µm.

Staining for cytokeratin revealed that 4T1 breast cancer cells exhibit a characteristic epithelial structure (Fig. 50a, red staining) in contrast to RAW 264.7 macrophages, which are cytokeratin-negative (Fig. 50b).

V.12. Histological examinations 7 d post *in vivo* infection

To confirm the substantial reduction of macrophage number, which was detected by FACS analysis, immunohistological examination of naïve, 7 days *S. flexneri BS176ΔaroA*- or *S. flexneri M90TΔaroA*-infected Balb/c mice were performed (Fig. 51).

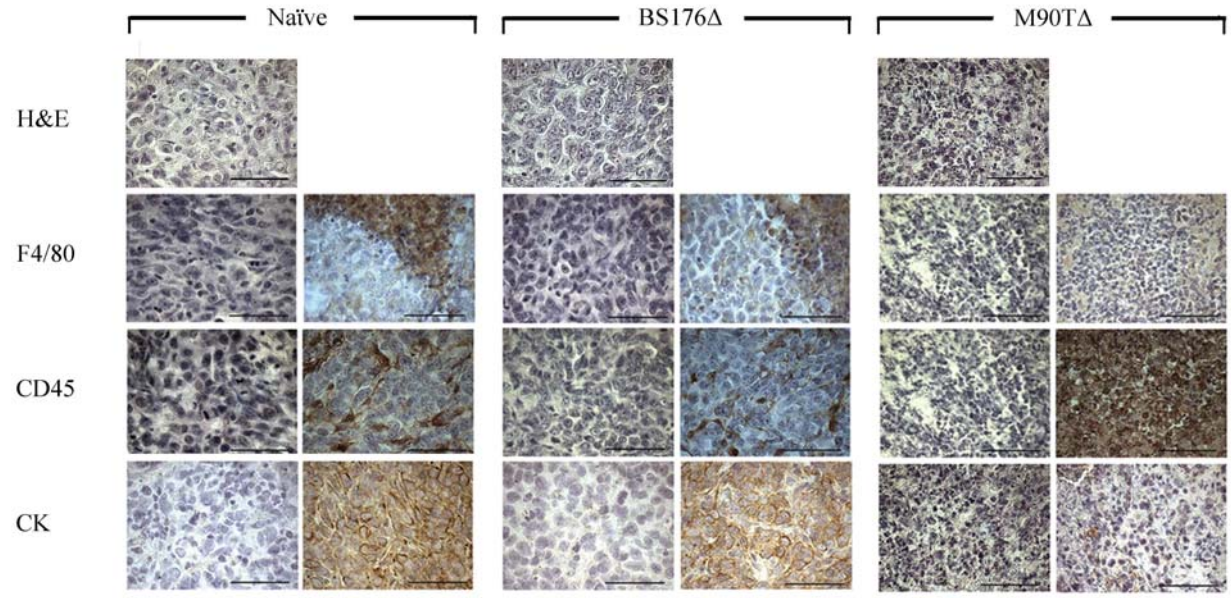

Figure 51: Histological examinations of tumor tissue 7 d after infection

Histological examination of naïve (left panels), *S. flexneri BS176ΔaroA* (BS176Δ, middle panels) and *S. flexneri* M90T*ΔaroA* (M90TΔ, right panels). Besides H&E staining, immunohistological stainings were performed to detect macrophages (anti-F4/80 antibody), infiltration of inflammatory cells (anti-CD45 antibody) and cytokeratin (anti-cytokeratin (CK) antibody) In each case left panels are the antibody controls. Scale bars represent 50 µm.

7d infected mice revealed a substantial reduction of macrophages (Fig. 51, anti-F480 staining) and an intense infiltration of inflammatory cells (Fig. 51, anti-CD45 staining). Furthermore, cytokeratin staining (Fig. 51, anti-CK staining) of tumors derived from *M90TΔaroA*-infected mice showed a marked reduction in positive cells indicating that cytokeratin positive epithelial 4T1 tumor cells are depleted along with the depletion of macrophages. In the naïve and *BS176ΔaroA*-infected tissue no tissue degeneration was detectable and a normal tumor rim structure was observed.

V.13. Therapeutic approach

To investigate whether this substantial reduction in macrophage numbers and infiltration of inflammatory cells induced by *S. flexneri M90TΔaroA* is associated with a therapeutic effect,

S. flexneri M90TΔaroA or *S. flexneri BS176ΔaroA* were applied to 4T1-induced tumor-bearing Balb/c mice and tumor growth was assessed every second day (Fig. 52).

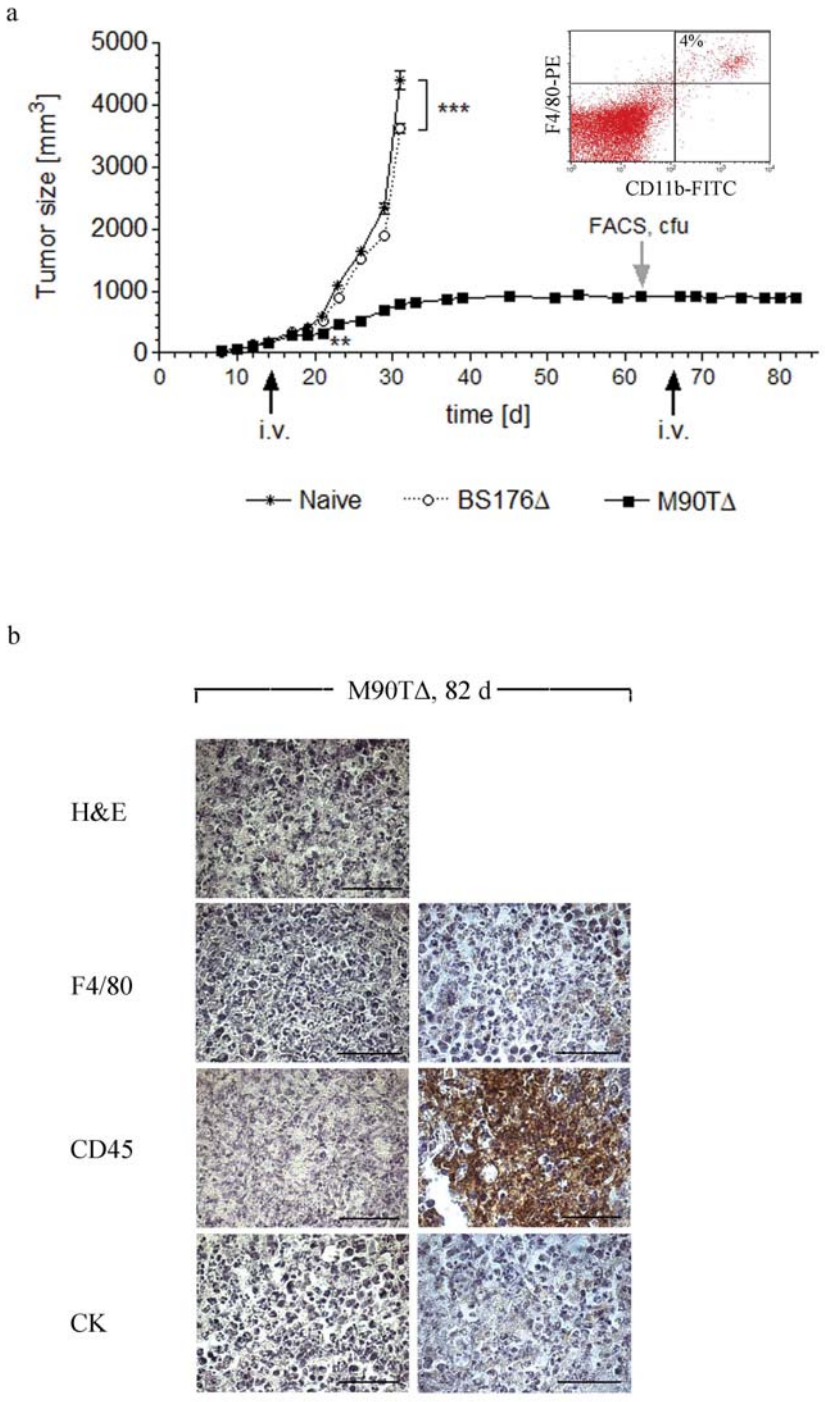

Figure 52: Infection with *S. flexneri M90TΔaroA* blocks tumor growth

(**a**) 14 days after tumor cell inoculation at a mean tumor volume of 187 mm^3, 1 x 10^6 bacteria were applied i.v. to n = 8 mice per group. Naïve and *S. flexneri BS176ΔaroA* (BS176Δ) infected mice were sacrificed 31 days after tumor cell inoculation due to animal welfare reasons. From the *S. flexneri M90TΔaroA* (M90TΔ)-infected group, two mice were sacrificed at day 31 for macroscopic comparison of tumors and 3 mice at day 62 to determine CFU and macrophage numbers. ** $P < 0.01$, *** $P < 0.001$. At day 66 after tumor cell inoculation, 1 x 10^6 *S.*

flexneri M90TΔaroA (M90TΔ) were applied i.v. into the remaining 3 mice. On day 82 after tumor cell inoculation, CFU in tumor, liver and spleen was determined and the tumor was assessed histologically. (**b**) Histology of tumor tissue from *S. flexneri M90TΔaroA* (M90TΔ)-infected mice at 82 days after tumor cell inoculation (68 days after the first infection). For untreated controls, see Fig. 40. Left panels represent antibody controls. Scale bars represent 50 µm. CK: Cytokeratin.

There was a substantial reduction in tumor growth after infection with *S. flexneri M90TΔaroA* (Fig. 52). Of note, tumor growth was completely blocked 19 days after treatment. Infection with *S. flexneri BS176ΔaroA* resulted in a small, albeit significant reduction of tumor growth. At day 62 after tumor cell inoculation the non-growing tumors exhibited very low macrophage numbers (~4 %) and bacteria were not detectable after CFU determination. At day 66 after tumor cell inoculation 1 x 10^6 *S. flexneri M90TΔaroA* were applied i.v. to the remaining 3 mice. No reduction of tumor size was detected. On day 82 after tumor cell inoculation CFU was determined. Bacteria were not detectable in tumor, liver and spleen any more. Histological examination of *S. flexneri M90TΔaroA* 68 d infected mice (at day 82 after tumor cell inoculation) revealed still a substantial reduction of macrophages, an intense infiltration of inflammatory cells (Fig. 52, anti-CD45 staining) and a complete depletion of 4T1 tumor cells (Fig. 52, anti-CK staining).

V.14. *S. flexneri* infection of transgenic *SP-C-c-raf* BxB-11 mice

V.14.1. Histological examinations of lung tissue

To investigate whether a treatment with *S. flexneri M90TΔaroA* would be applicable in transgenic *SP-C*-c-Raf BxB-11 mice with lung tumors, we applied 1 x 10^6 *S. flexneri M90TΔaroA* i.v. Subsequently we performed histological analysis of lung tissues from control C57Bl/6 mice and mice transgenic for lung-targeted expression of *SP-C*-c-Raf-1-BxB-11 protein of different age infected with *M90TΔaroA* i.v. for 28 d (Fig. 53 – 56).

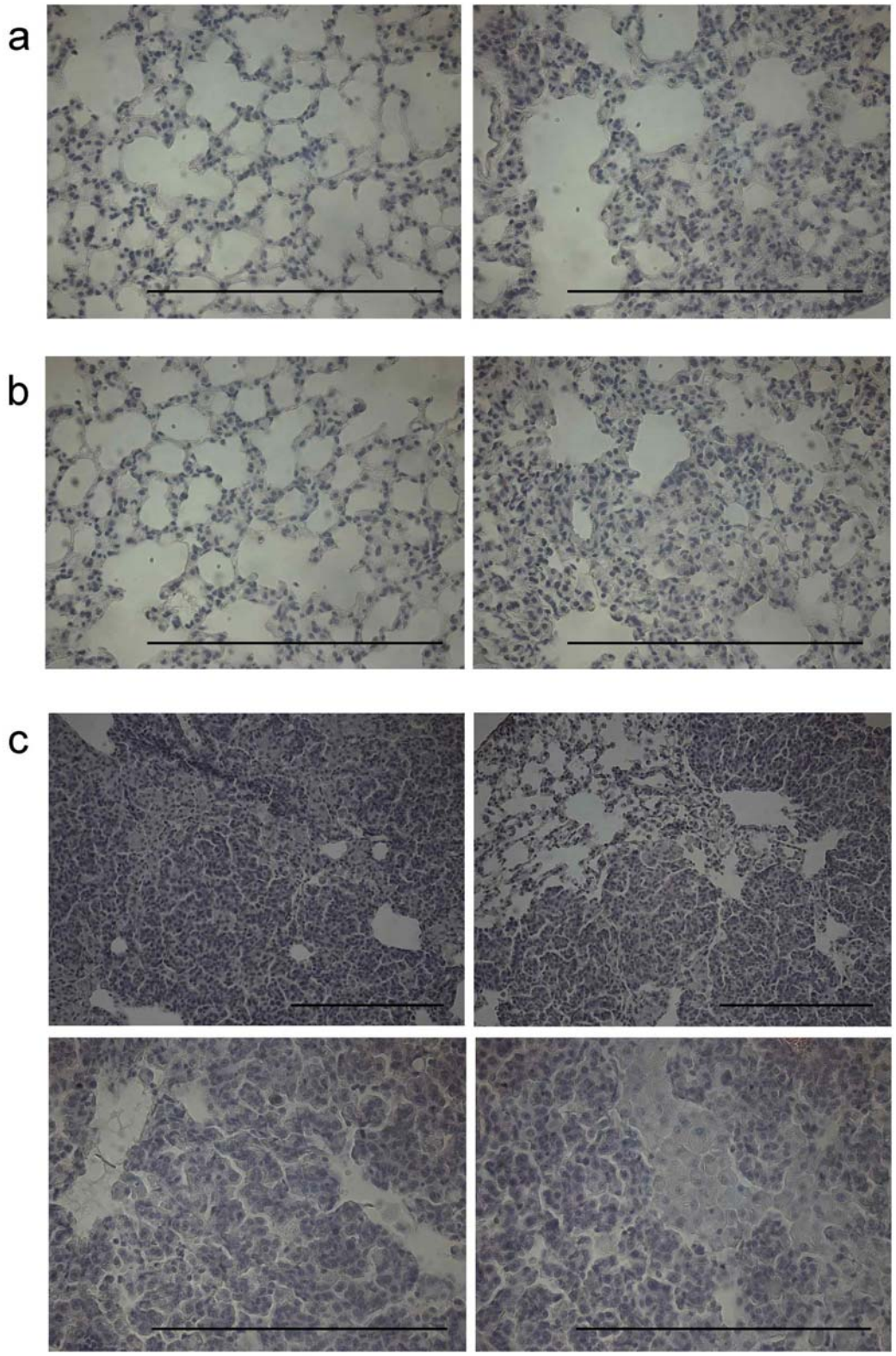

Figure 53: Histological examination of lung tissue

Lung tissues from naïve 8-month-old C57Bl/6 mouse (**a**), a 8-month-old C57Bl/6 mouse infected with *S. flexneri M90TΔaroA* (**b**) and a *S. flexneri M90TΔaroA*-infected 6-month-old *SP-C*-c-Raf-1-BxB-11 mouse (**c**) were fixed in paraformaldehyde, embedded in paraffin, sectioned at 4 µm, and stained with H&E after an infection with *S. flexneri M90TΔaroA* for 28 d. Scale bars represent 50 µm.

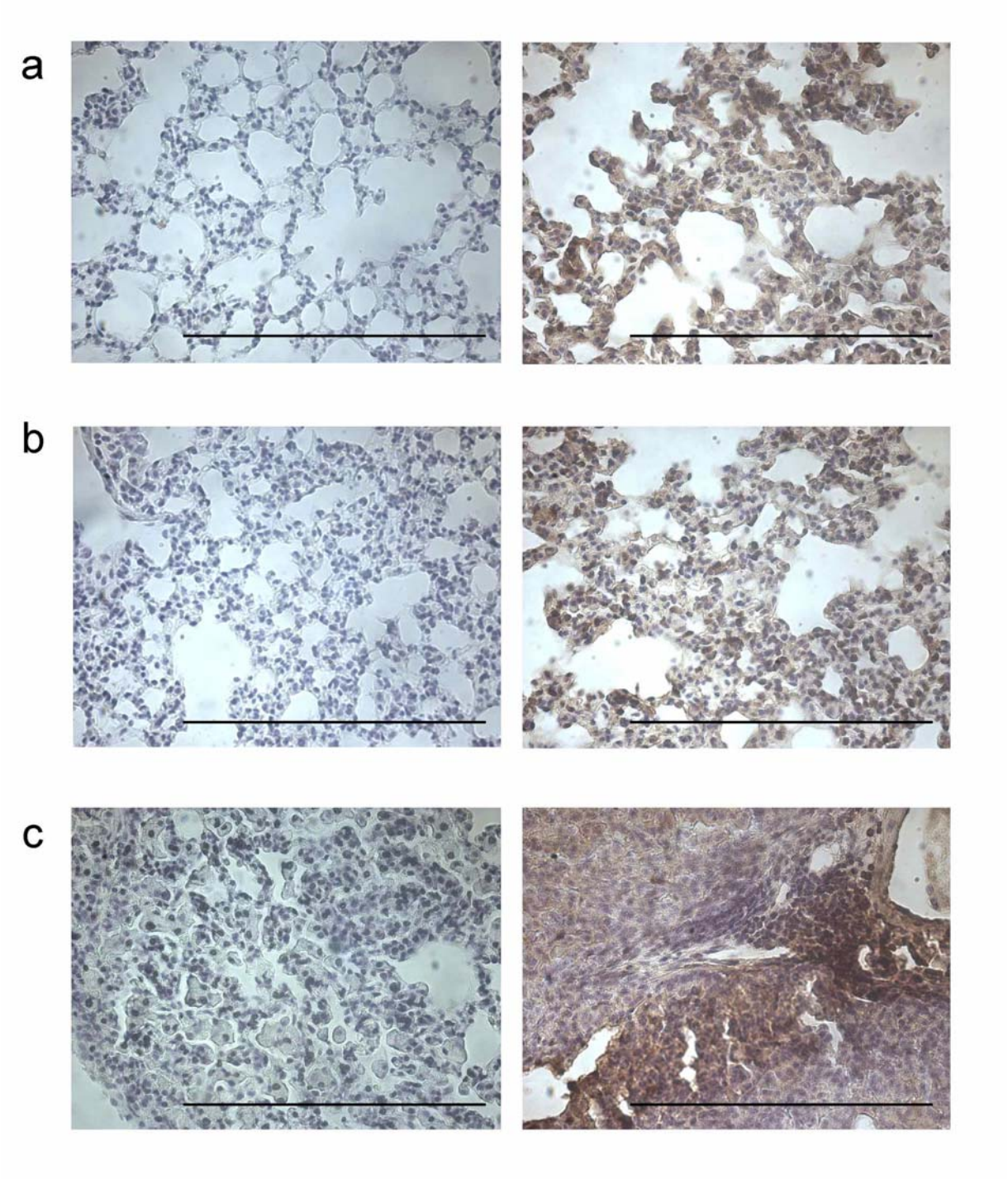

Figure 54: Immunohistological staining of CD45+ cells in lung tissue

Lung tissues from naïve 8-month-old C57Bl/6 mouse (**a**), a 8-month-old C57Bl/6 mouse infected with *S. flexneri M90TΔaroA* (**b**) and a *S. flexneri M90TΔaroA*-infected 6-month-old *SP-C*-c-Raf-1-BxB-11 mouse (**c**) were fixed in paraformaldehyde, embedded in paraffin, sectioned at 4 µm, and immunostained with an anti-CD45 antibody after an infection with *S. flexneri M90TΔaroA* for 28 d. In each case left panels represent antibody controls. Scale bars represent 50 µm.

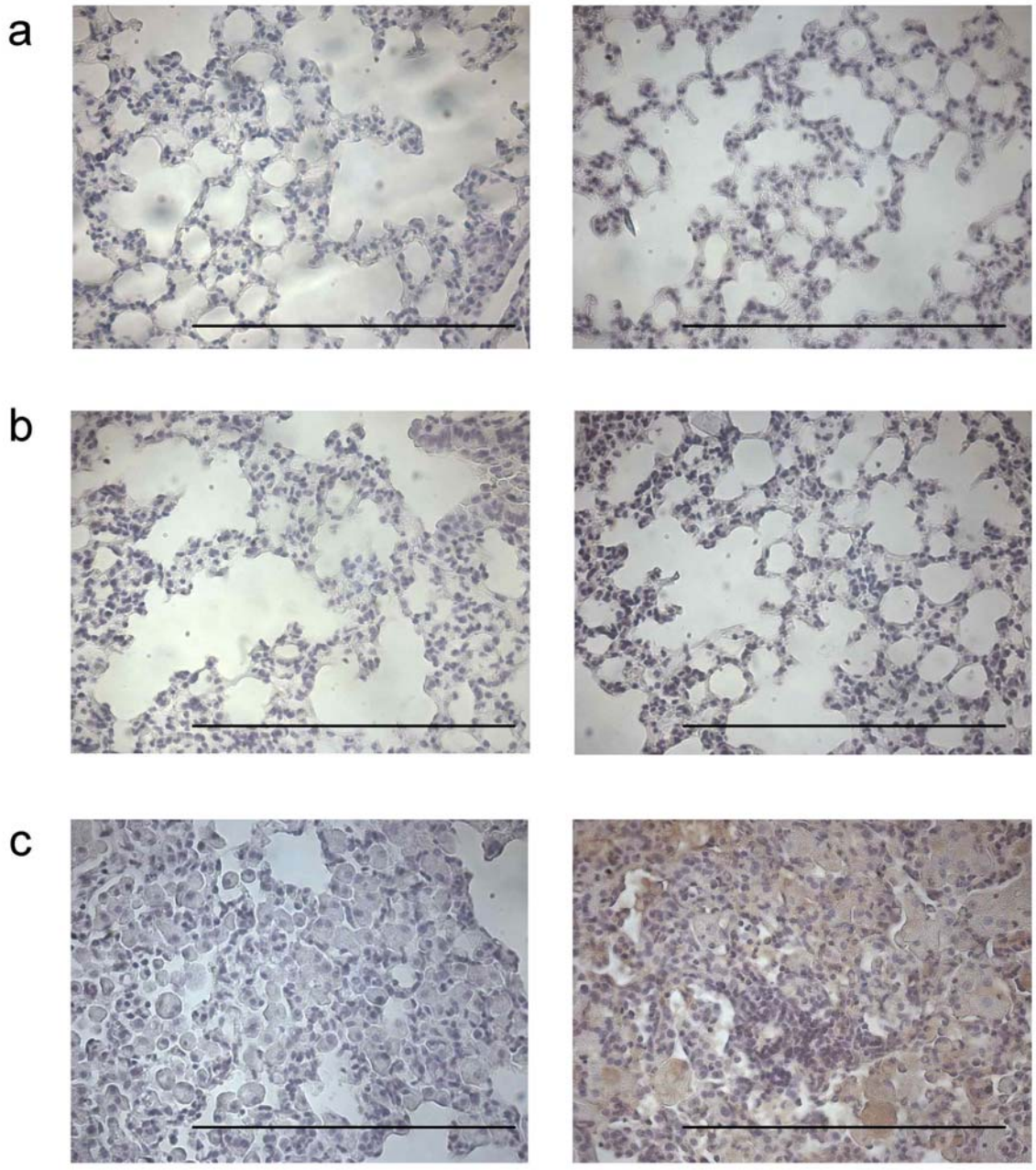

Figure 55: Immunohistological staining of F4/80+ macrophages in lung tissue

Lung tissues from naïve 8-month-old C57Bl/6 mouse (**a**), a 8-month-old C57Bl/6 mouse infected with *S. flexneri M90TΔaroA* (**b**) and a *S. flexneri M90TΔaroA*-infected 6-month-old *SP-C*-c-Raf-1-BxB-11 mouse (**c**) were fixed in paraformaldehyde, embedded in paraffin, sectioned at 4 µm, and immunostained with an anti-F4/80 antibody after an infection with *S. flexneri M90TΔaroA* for 28 d. In each case left panels represent antibody controls. Scale bars represent 50 µm.

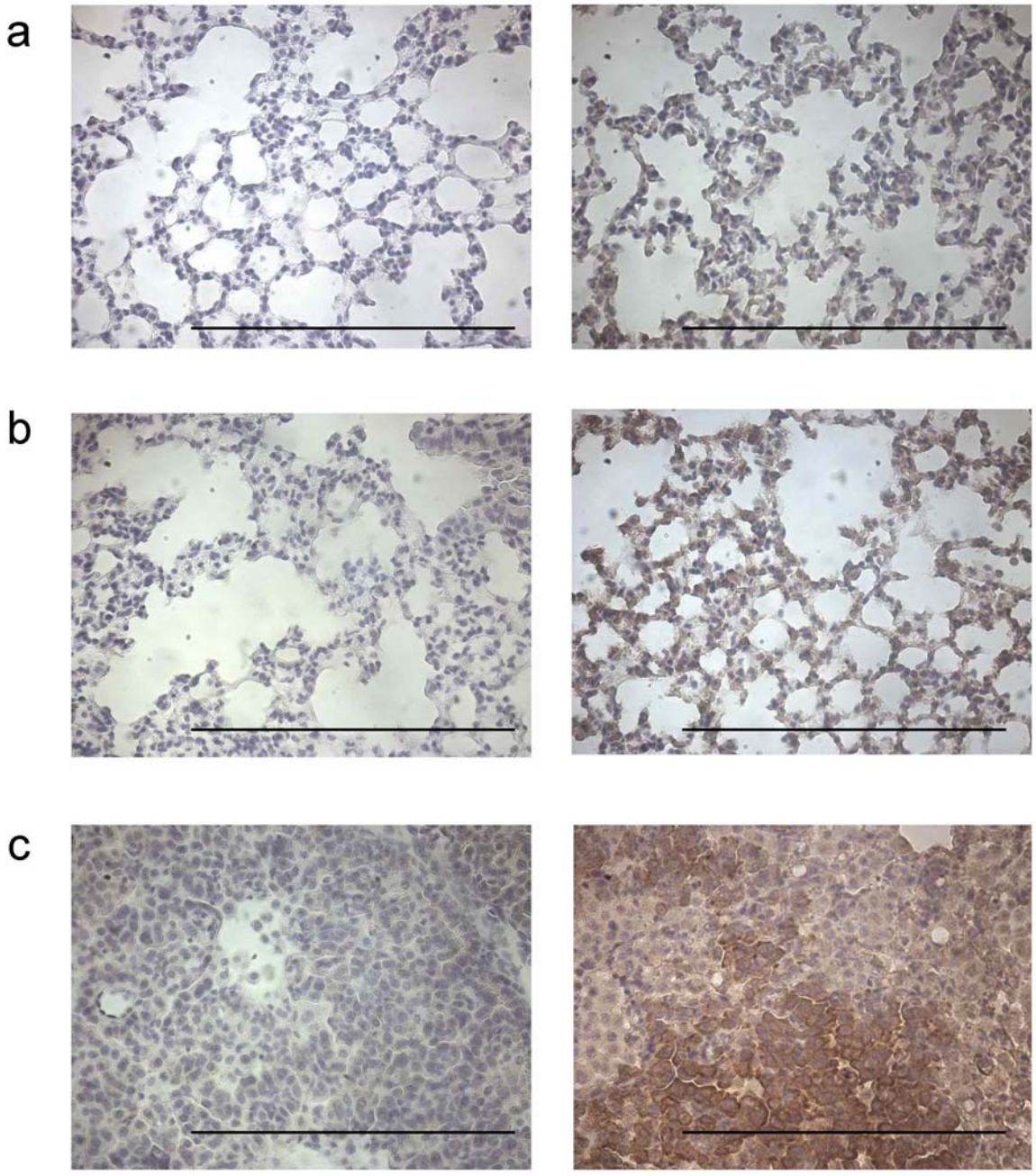

Figure 56: Immunohistological staining of cytokeratin in lung tissue

Lung tissues from naïve 8-month-old C57Bl/6 mouse (**a**), a 8-month-old C57Bl/6 mouse infected with *S. flexneri M90TΔaroA* (**b**) and a *S. flexneri M90TΔaroA*-infected 6-month-old *SP-C*-c-Raf-1-BxB-11 mouse (**c**) were fixed in paraformaldehyde, embedded in paraffin, sectioned at 4 µm, and immunostained with an anti-cytokeratin antibody after an infection with *S. flexneri M90TΔaroA* for 28 d. In each case left panels represent antibody controls. Scale bars represent 50 µm.

The lung of the C57Bl/6 control mice both, naïve or *S. flexneri M90TΔaroA*-infected, exhibited no tumor tissue (Fig. 53a, b). We observed normal lung tissue containing type I and type II pneumocytes and a small number of alveolar macrophages, whereas a small number of

infiltrated cells were detectable in the lung of *S. flexneri M90TΔaroA*-infected C57Bl/6 control mouse. In addition we detected vascular smooth muscle cells. Here all normal lung specimens had a similar staining pattern and a normal structure of bronchial gland cells and epithelial cells (surface epithelium, globlet cells). In contrast to that for the 6-month-old *SP-C*-c-Raf-1-BxB-11 mouse, the tumor incidence was much higher, resulting in multiple tumor foci (Fig. 53 and 56) and immune cell infiltration (Fig. 54). We could not detect any F4/80+ macrophages in the lung tissues by F4/80+ staining (Fig. 55).

In addition we determined the CFU in the lung tissue at 1 d, 7 d, 14 d and 28 d after infection. At this time points we did not detect any bateria in the lung.

V.14.2. Infection of *SP-C*-c-Raf-1-BxB-11 lung cells *ex vivo*

To investigate whether a treatment with *Shigella flexneri M90TΔaroA* would be applicable in macrophages of *SP-C*-c-Raf-1-BxB-11 lung tumors we infected cells derived from freshly isolated lung from a *SP-C*-c-Raf-1-BxB-11 mouse with *S. flexneri M90TΔaroA ex vivo* (Fig. 57).

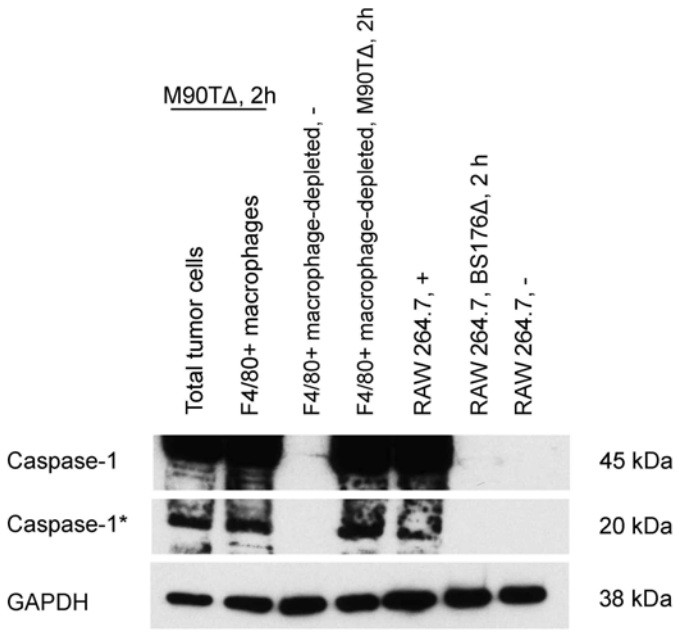

Figure 57: Caspase-1 activation in cell fractions isolated from *SP-C*-c-Raf-1-BxB-11 tumor lung cells

Caspase-1 activation in infected cells was analysed by Western Blot analysis. The antibody detects the procaspase-1 (45 kDa) and the activated 20 kDa subunit (caspase-1*). RAW 264.7 macrophages were used as positive control. Incubation of RAW 264.7 macrophages with staurosporine (4 µM) for 6 h was used as positive control (+). GAPDH was used as loading control.

S. flexneri M90TΔaroA effectively induced caspase-1 processing in the total cell fraction, in the F4/80+ macrophage-fraction and in the F4/80+ macrophage-depleted fraction (Fig. 57). Note that there were less than 0,5 % F4/80+ macrophages detected in *SP-C*-c-Raf-1-BxB-11 lung tissue. In the F4/80+ macrophage-depleted cell fraction we also detected procaspase-1 and activated caspase-1 (caspase-1*) suggesting the remaining of F4/80 weak or F4/80 negative macrophages in the F4/80+ macrophage-depleted cell fraction.

V.15. *S. flexneri* infection of human cancer ascites cells

V.15.1. Infection of human cancer ascites cells *ex vivo*

To investigate whether a treatment with *Shigella flexneri M90TΔaroA* would be applicable in humans we infected cells derived from freshly isolated ascites from an ovarian carcinoma patient with *S. flexneri M90TΔaroA ex vivo* (Fig. 58).

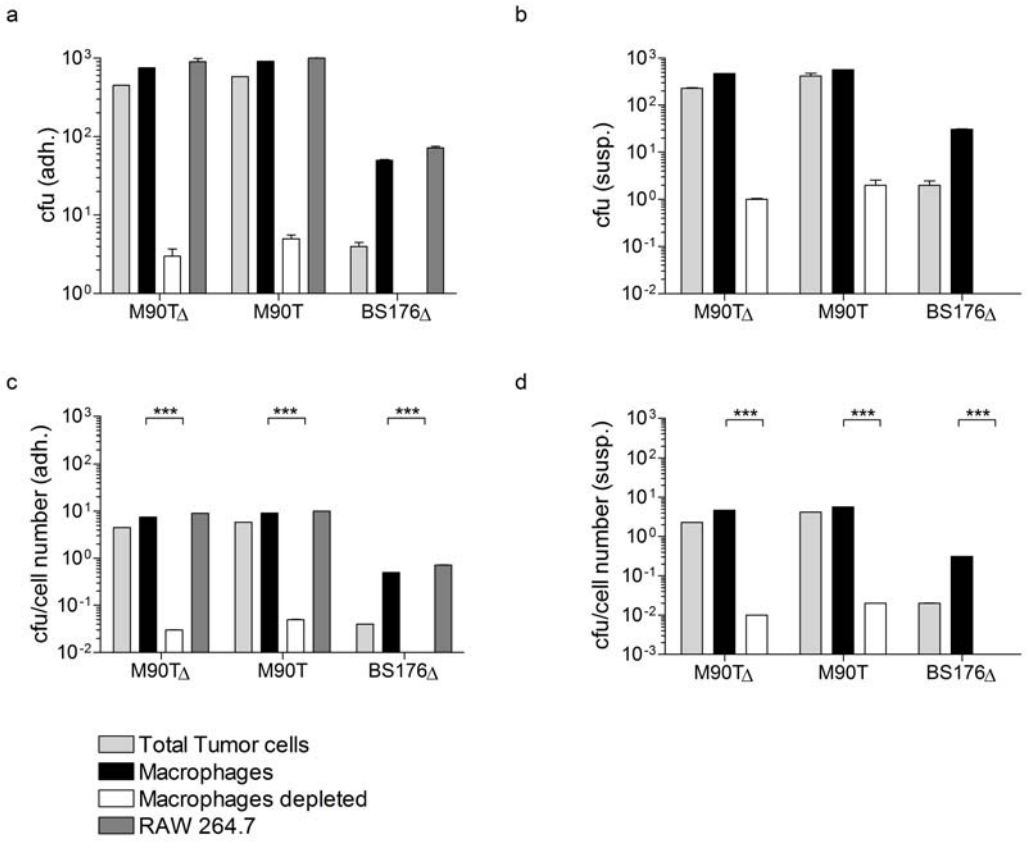

Figure 58: *S. flexneri M90TΔaroA* (M90TΔ) predominantly targets TAMs isolated from human ascites cells *ex vivo*

Ovarian cancer ascites contain an adherent (adh.) and a non-adherent (susp.) cellular fraction. Both fractions were treated separately with the following protocol. Tumor cells were separated and TAMs were isolated as

described before. The different cell fractions were infected *ex vivo* with wt *S. flexneri M90T* (M90T)*, S. flexneri M90TΔaroA* (M90TΔ) and *S. flexneri BS176ΔaroA* (BS176Δ) at a MOI of 100. After 1 h of infection, cells were incubated for 1 h with 300 µg/ml gentamicin followed by 1 h incubation with 50 µg/ml gentamicin. Subsequently, CFU was determined. All results shown are mean ± SD of three samples. ***: $p < 0{,}001$, Student`s t-test.

S. flexneri M90TΔaroA effectively infected TAMs isolated from human tumors (Fig. 58). Again, infection of TAMs derived from a human tumor isolate was at least 100 fold more efficient compared to the macrophage-depleted fraction.

V.14.2. Caspase-1 activation and apoptosis induction in human cancer ascites cells

In addition separated cell fractions from isolated human cancer ascites cells were used for Western Blot analysis to investigate caspase-1 expression, activation and induction of apoptosis (Fig. 59).

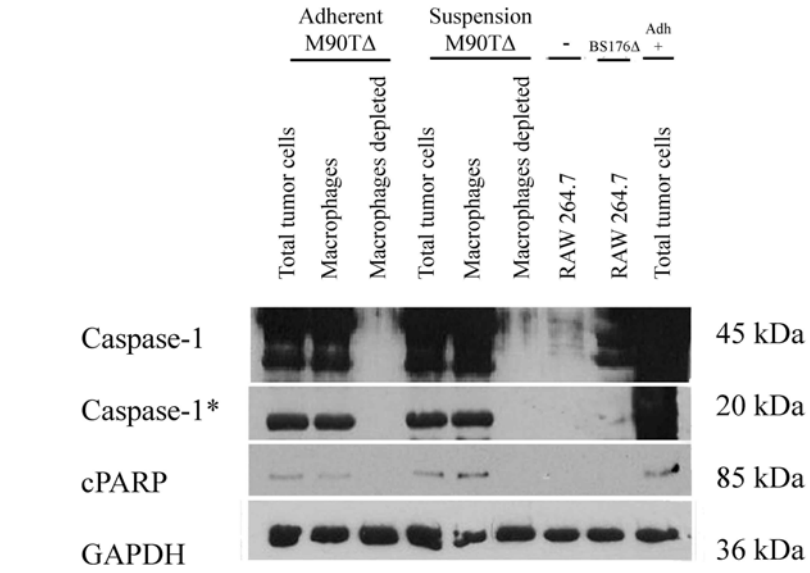

Figure 59: Caspase-1 activation and apoptosis induction in TAMs isolated from human cancer ascites cells

Caspase-1 activation and PARP processing in infected cells was analysed by Western Blot analysis. The antibody detects the procaspase-1 (45 kDa) and the activated 20 kDa subunit. The PARP antibody detects the cleaved PARP (cPARP) fragment of 85 kDa. RAW 264.7 macrophages were used as positive control. Incubation of total tumor cells isolated from tumor-bearing Balb/c mice with staurosporine (4 µM) for 6 hours was used as positive control for cleaved PARP. GAPDH was used as loading control.

S. flexneri M90TΔaroA effectively infected TAMs isolated from human tumors (Fig. 58) and induced caspase-1 processing and apoptosis in the total cell fraction and in the macrophages fraction (Fig. 59). Note that the macrophage-depleted fraction does not contain procaspase-1 in detectable levels.

VI. Discussion

In this work we have demonstrated that pathogenic intracellular bacteria like *Salmonella* and *Shigella* primarily target TAMs after i.v. infection of tumor-bearing mice both in a 4T1 graft and a MMTV-HER2/new transgenic breast cancer model. To determine the behavior of *Shigella*, we constructed an attenuated strain termed *S. flexneri M90TΔaroA*. This strain primarily targeted TAMs in tumor-bearing 4T1 grafted or transgenic MMTV-HER2/new mice. In contrast to *Salmonella*, the *Shigella* strain was predominantly intracellular at all time points and showed a caspase-1 activation and apoptosis induction over the whole observation period of 7 days. The sustained apoptosis induction led to a substantial depletion of the TAMs and a disruption of TAM clusters in tumors. In contrast, the avirulent strain *S. flexneri BS176ΔaroA* and *Salmonella* had no effect on the macrophage population. Most importantly, the macrophage depletion translated into a pronounced therapeutic effect in the 4T1 graft model. A single injection of the *S. flexneri M90TΔaroA* strain resulted in a complete block of tumor growth. Approximately two months after treatment, *Shigella* were no longer detectable in the non-growing tumors, whereas TAM numbers were still substantially reduced by a factor of 10 compared to values of non-treated animals with similar tumor sizes. Finally, the *M90TΔaroA* strain also efficiently infected TAMs freshly isolated from ascites of a human ovarian carcinoma, induced caspase-1 processing and apoptosis in these cells. Therefore, a therapy based on the i.v. injection of intracellular bacteria which are capable of sustained apoptosis induction might be a worthwhile strategy to follow in future tumor therapy.

Extracellular bacteria were repeatedly used for experimental tumor therapy[1]. Their effect in different tumor models was explained by the preferential replication in tumors, toxic effects on tumor cells by bacterial products and an induction of inflammation[1]. In our model, we aimed primarily at studying intracellular bacteria. However, the avirulent *Shigella* strain *S. flexneri BS176ΔaroA* basically behaves like an extracellular bacterium as it cannot actively infect host cells. Our results principally confirm the observation described by others[1]. At early time points like 4 h and 6 h *p.i.*, most of the bacteria are found extracellularly in the tumor. In contrast, bacteria isolated from the spleen are found mainly intracellularly. Although we did not separate the splenic cell populations, the elimination of systemic bacteria in the spleen is normally mediated by phagocytic cells including macrophages[133]. Our data therefore confirms the hypothesis that TAMs have a defect in phagocytosis[134,135]. At later time points like 7 d *p.i.*, *S. flexneri BS176ΔaroA* is also found mainly within macrophages. However, the overall number of these metabolically highly attenuated bacteria is very low. These data suggest that

phagocytosis in TAMs might still occur, albeit at a much slower rate. Alternatively, different TAM populations might exist, including some that have retained the capacity of phagocytosis. Interestingly, the treatment with *S. flexneri BS176ΔaroA* resulted in a small, albeit significant, therapeutic effect which is in line with recent observations for *E. coli* strains, that induced a measurable inflammatory response but failed to exert a relevant anti-tumor response[8]. Compared to experiments with extracellular bacteria by other authors[8,136], our strain carried a mutation which blocked intra- and strongly reduced extracellular growth already in rich culture medium. Therefore, bacterial numbers were very low seven days after treatment. Strong attenuation of bacterial growth may not be the method of choice for a therapy based on extracellular bacteria, as it will only result in small numbers of bacteria populating the tumor. In addition, bacterial growth could be coupled with impaired phagocytic activity of TAMs resulting in the presence of extracellular bacteria at all time points. Such a situation might pose the risk of systemic release and consequent septic shock, especially in case of Gram-negative bacteria.

For intracellular bacteria, the demonstration that they can transfer DNA into eukaryotic cells opened the possibility to deliver therapeutic proteins[137]. For tumor therapy, it is critical to know the target population and the quantitative efficacy of this process. Here we showed for the first time, that TAMs are the primary target of intracellular bacteria like *Shigella* and *Salmonella* in tumors with high numbers of TAMs. In contrast, only a very low portion of tumor cells depleted of TAMs are infected. These results question approaches which depend on delivering a toxic payload into tumor cells, as it will be difficult to target relevant numbers of cells. A possible circumvention might be the use of recombinant bacteria expressing molecules allowing a specific uptake of the bacteria by tumor cells. Of note, *Salmonella*, but not *Shigella* were found mainly extracellularly 7 days after infection, which is in line with the qualitative observation from others[8]. A possible explanation would be a gene expression switch from the SPI1 to the SPI2 pathogenicity island within the tumor, which is the natural sequence after oral infection[60]. One consequence of this switch is the shutdown of the SipB expression and secretion via the SPI1 encoded type 3 secretion system, which would lead to the observed substantial reduction in apoptosis induction at later time points as shown also *in vitro*. In addition, the switch might reduce the induction of active uptake which would result in the observed higher numbers of extracellular bacteria in the presence of TAMs with impaired phagocytic capacities.

Our data suggest that the therapeutic effect observed by others using *Salmonella*[7,12,138] may be best explained by the induction of inflammation, but not by a depletion or modification of

TAMs. One trigger for inflammation might be LPS or bacterial DNA[139,140], which could also explain the observed limited therapeutic efficacy of the avirulent *Shigella* strain *BS176*Δ on cancer stem cells. In addition, the physiological consequence of caspase-1 activation is the release of IL-1 and IL-18, which are strong pro-inflammatory cytokines. As *Salmonella* activates caspase-1 at early time points (6 h *p.i.*) , this caspase-1 mediated inflammation might contribute to the therapeutic efficacy described by others. However, the clinical efficacy of *Salmonella* was limited, but we can only speculate about the possible reasons. Others have already suggested that faster elimination of bacteria from the blood stream in humans leads to less efficient tumor targeting of the bacteria limiting the therapeutic efficacy[141,142]. Based on our data, we suggest that a failure to induce relevant levels of caspase-1 triggering an inflammatory response might add to the limited efficacy in humans. One of the reasons might be the treatment of patients with tumors encompassing only low numbers of TAMs. Another reason might be the use of bacteria harvested in the log-phase of growth, which is standard for bacteria produced with fermentation. Indeed, *Salmonella* harvested in the log phase do not express the SPI1 pathogenicity island and, as a consequence, do not induce caspase-1 in macrophages[18]. Examining macrophages infected with *Salmonella* harvested in the log and in the stationary phase *in vitro*, we could confirm that only stationary phase *Salmonella* induce caspase-1 processing.

In contrast to *Salmonella*, *Shigella* do not downregulate their machinery required for caspase-1 induction after infection. It is well conceivable that virulent *Shigella* are not suitable for therapeutic approaches. In contrast to conventional vaccines, we rely on a fully functional virulence apparatus and therefore decided to delete the *aroA*-locus without modifying virulence genes. This *Shigella* strain showed an apoptosis induction in TAMs at all time points like 4 h and 6 h *p.i.* and resulted in a profound reduction of TAMs which was associated with a substantial therapeutic effect in our model. At this point it is difficult to decide, whether the observed therapeutic effect was caused by the depletion of TAMs or a consequence of inflammation induced by IL-1 and IL-18. However, others have already shown that depletion of TAMs is sufficient to block tumor growth in several tumor models [143]. Therefore both factors might contribute to the therapeutic efficacy. Of note, the depletion of TAMs is long lasting and persists at late time points, when no more bacteria are present. This might be an important factor for a sustained therapeutic efficacy also in the human setting, as inflammation will be dependent on the presence of bacteria and therefore transient.

In this respect it is interesting to compare our data with a most recent work assessing tumor targeting in a colon carcinoma model[15]. In colon carcinoma, macrophages do not seem to play

a relevant role in tumor progression and the experimental tumor was instead associated with neutrophil invasion, which is in contrast to the 4T1 and HER2/new breast cancer model, where Gr-1+ neutrophil numbers were quite low. In this model, the attenuated *Shigella* strain did not reach the tumor after i.v. infection, only intratumoral injection resulted in partial necrosis which only had a therapeutic effect after depletion of neutrophils. Therefore, our data suggest that both, for targeting and therapeutic efficacy of *Shigella*, the presence of and the dependence on TAMs is important rather than the limited pathogenicity of *Shigella* in mice, as postulated by Weiss.

Although our data suggest that targeting of tumor cells with *Salmonella* or *Shigella* will be difficult in tumors with high numbers of TAMs, we consider selective targeting of TAMs as a potential advantage. First, TAMs are associated with tumor progression and negative prognosis in several human tumors and in mouse models depletion of TAMs has resulted in a therapeutic effect. Therefore, TAMs represent a valid target for tumor therapy. Second, although TAMs might have a different phenotype compared to macrophages residing outside the tumor, they are genetically stable and not transformed[144]. Therefore, targeting TAMs as a part of a tumor-stroma oriented therapy will not face the problems of therapies targeting transformed cells bearing a large genetic heterogenity with the risk of escape mutants. Third, the data obtained with *Shigella* imply that already a relatively small number of bacteria in the tumor are sufficient for a substantial therapeutic effect which would minimize the risk of severe side effects resulting from the systemic release of the bacteria.

The central question is whether depletion of TAMs by *S. flexneri M90TΔaroA* resulting in tumor growth inhibition can be confered on other tumor models. Tumor-associated macrophages in breast cancer have been associated with poor prognosis[70]. The association between TAM and reduced survival has also been shown in renal cell carcinoma[145], bladder cancer[146], prostate cancer[147] and lymphoma[148]. In lung cancer, TAMs may favor tumor progression by contributing to stroma formation and angiogenesis through their release of PDGF, in conjunction with TGF-ß1 production by cancer cells[149]. Studies in M-CSF-deficient mice (*op*/*op*) have provided strong support to the concept of the protumor function of the mononuclear phagocyte system. M-CSF deficiency in *op*/*op* mice diminishes macrophage recruitment, stroma formation and tumor growth in the Lewis lung carcinoma model[150]. However, after i.v. application we could show that *S. flexneri M90TΔaroA* is not able to target the lung tissue of transgenic lung tumor mice. The *ex vivo* infection showed caspase-1 activation not only in F4/80+ macrophages isolated from lung tumor tissue but also in F4/80+ macrophage-depleted cell fraction after infection with *S. flexneri M90TΔaroA*. This indicates

lung macrophages freshly isolated from transgenic lung tumor mice express mainly other surface markers than the F4/80 antigen. It has been reported that an anti-F4/80 antibody did not stain lung macrophages in normal mice[151]. This was in agreement with our results, but differs from the results of other authors[152,153]. The predominant surface phenotype of lung macrophages is described as F4/80 weak, Ml/70-, MOMA-2+, NLDC-145+, MOMA-I+, SER-4+, which resembles the pattern of expression by lymphoid macrophages rather than representative tissue macrophages such as those found in the peritoneal cavity[151]. This indicates that in our F4/80+ macrophage-depleted cell fraction are still F4/80 weak or F4/80- macrophages left in which caspase-1 could be activated.

To our knowledge, immunological studies illustrated the potential of the mouse intranasal challenge model for characterization of cellular and humoral immune responses protecting against *Shigella* infection in mucosal epithelia[154]. The mouse lung can be considered a simplified model for the study of the pathogenesis and immunobiology of *Shigella* infection. For example, the pulmonary epithelium in the tracheobronchial tree is simple ciliated columnar epithelium with transition to simple cuboidal epithelium in the alveolar sacs[155]. In addition, the bronchial wall contains occasional lymphoid follicles or aggregates of follicles that are similar to the Peyer's patches of the intestine[156]. Thus, the bronchus constitutes a mucosal surface with some characteristics of the intestinal epithelium. Like the intestine, the lung is a lymphoid organ with antigen-presenting cells, T helper and suppresser lymphocytes, and B lymphocytes[156]. For this reason intranasal application of *Shigella flexneri M90TΔaroA* might be the best way of application to study the effect of *Shigella* infection on TAMs of lung tumors and their effect on lung tumor growth.

In summary, we suggest that targeting TAMs using attenuated *Shigella* or *Salmonella* with additional modification (e.g. a constitutive expression of SPI1) is a promising option for future breast tumor therapy. Further studies are required with respect to the safety of the *Shigella* strain and the efficacy of tumor targeting in humans. Furthermore, other intracellular bacteria like *Listeria*[157] might be suitable for a macrophage targeted bacterial tumor therapy.

VII. References

1. Van Mellaert, L., Barbe, S. & Anne, J. Clostridium spores as anti-tumour agents. *Trends Microbiol* **14**, 190-6 (2006).
2. Coley, W.B. The treatment of malignant tumors by repeated inoculations of erysipelas. With a report of ten original cases. 1893. *Clin Orthop Relat Res*, 3-11 (1991).
3. Yu, Y.A. et al. Visualization of tumors and metastases in live animals with bacteria and vaccinia virus encoding light-emitting proteins. *Nat Biotechnol* **22**, 313-20 (2004).
4. Brown, J.M. The Hypoxic Cell: A Target for Selective Cancer Therapy--Eighteenth Bruce F. Cain Memorial Award Lecture. *Cancer Res* **59**, 5863-5870 (1999).
5. Vaupel, P.W. *Tumour Oxygenation.* , 219–232 (Germany: Gustav Fischer Verlag, 1995).
6. Ryan, R.M., Green, J. & Lewis, C.E. Use of bacteria in anti-cancer therapies. *Bioessays* **28**, 84-94 (2006).
7. Agrawal, N. et al. Bacteriolytic therapy can generate a potent immune response against experimental tumors. *Proc Natl Acad Sci U S A* **101**, 15172-7 (2004).
8. Weibel, S., Stritzker, J., Eck, M., Goebel, W. & Szalay, A.A. Colonization of experimental murine breast tumours by Escherichia coli K-12 significantly alters the tumour microenvironment. *Cell Microbiol* (2008).
9. Forbes, N.S., Munn, L.L., Fukumura, D. & Jain, R.K. Sparse initial entrapment of systemically injected Salmonella typhimurium leads to heterogeneous accumulation within tumors. *Cancer Res* **63**, 5188-93 (2003).
10. Kasinskas, R.W. & Forbes, N.S. Salmonella typhimurium specifically chemotax and proliferate in heterogeneous tumor tissue in vitro. *Biotechnol Bioeng* **94**, 710-21 (2006).
11. Carmeliet, P. & Jain, R.K. Angiogenesis in cancer and other diseases. *Nature* **407**, 249-57 (2000).
12. Zhao, M. et al. Tumor-targeting bacterial therapy with amino acid auxotrophs of GFP-expressing Salmonella typhimurium. *Proc Natl Acad Sci U S A* **102**, 755-60 (2005).
13. Vassaux, G., Nitcheu J., Jezzard S. & Lemoine N.R. Bacterial gene therapy strategies. *The Journal of Pathology* **208**, 290-298 (2006).
14. Pawelek, J.M., Low, K.B. & Bermudes, D. Tumor-targeted Salmonella as a novel anticancer vector. *Cancer Res* **57**, 4537-44 (1997).
15. Westphal, K., Leschner, S., Jablonska, J., Loessner, H. & Weiss, S. Containment of tumor-colonizing bacteria by host neutrophils. *Cancer Res* **68**, 2952-60 (2008).
16. Pilgrim, S. et al. Bactofection of mammalian cells by Listeria monocytogenes: improvement and mechanism of DNA delivery. *Gene Ther* **10**, 2036-45 (2003).
17. Zychlinsky, A. et al. IpaB mediates macrophage apoptosis induced by Shigella flexneri. *Mol Microbiol* **11**, 619-27 (1994).
18. Monack, D.M., Navarre, W.W. & Falkow, S. Salmonella-induced macrophage death: the role of caspase-1 in death and inflammation. *Microbes Infect* **3**, 1201-12 (2001).
19. Jennison, A.V. & Verma, N.K. Shigella flexneri infection: pathogenesis and vaccine development. *FEMS Microbiol Rev* **28**, 43-58 (2004).
20. DuPont, H.L., Levine, M.M., Hornick, R.B. & Formal, S.B. Inoculum size in shigellosis and implications for expected mode of transmission. *J Infect Dis* **159**, 1126-8 (1989).

21. Small, P., Blankenhorn, D., Welty, D., Zinser, E. & Slonczewski, J.L. Acid and base resistance in Escherichia coli and Shigella flexneri: role of rpoS and growth pH. *J Bacteriol* **176**, 1729-37 (1994).
22. Niebuhr, K. et al. Conversion of PtdIns(4,5)P(2) into PtdIns(5)P by the S.flexneri effector IpgD reorganizes host cell morphology. *Embo J* **21**, 5069-78 (2002).
23. Buchrieser, C. et al. The virulence plasmid pWR100 and the repertoire of proteins secreted by the type III secretion apparatus of Shigella flexneri. *Mol Microbiol* **38**, 760-71 (2000).
24. Hueck, C.J. Type III protein secretion systems in bacterial pathogens of animals and plants. *Microbiol Mol Biol Rev* **62**, 379-433 (1998).
25. Menard, R., Sansonetti, P.J. & Parsot, C. Nonpolar mutagenesis of the ipa genes defines IpaB, IpaC, and IpaD as effectors of Shigella flexneri entry into epithelial cells. *J Bacteriol* **175**, 5899-906 (1993).
26. Sakai, T., Sasakawa, C. & Yoshikawa, M. Expression of four virulence antigens of Shigella flexneri is positively regulated at the transcriptional level by the 30 kiloDalton virF protein. *Mol Microbiol* **2**, 589-97 (1988).
27. Page, A.L., Sansonetti, P. & Parsot, C. Spa15 of Shigella flexneri, a third type of chaperone in the type III secretion pathway. *Mol Microbiol* **43**, 1533-42 (2002).
28. Menard, R., Sansonetti, P. & Parsot, C. The secretion of the Shigella flexneri Ipa invasins is activated by epithelial cells and controlled by IpaB and IpaD. *Embo J* **13**, 5293-302 (1994).
29. Blocker, A. et al. The tripartite type III secreton of Shigella flexneri inserts IpaB and IpaC into host membranes. *J Cell Biol* **147**, 683-93 (1999).
30. Tran Van Nhieu, G., Ben-Ze'ev, A. & Sansonetti, P.J. Modulation of bacterial entry into epithelial cells by association between vinculin and the Shigella IpaA invasin. *Embo J* **16**, 2717-29 (1997).
31. Bourdet, G.L. & Lescroart, G. Theoretical Modeling and Design of a Tm, Ho:YLiF(4) Microchip Laser. *Appl Opt* **38**, 3275-81 (1999).
32. High, N., Mounier, J., Prevost, M.C. & Sansonetti, P.J. IpaB of Shigella flexneri causes entry into epithelial cells and escape from the phagocytic vacuole. *Embo J* **11**, 1991-9 (1992).
33. Mantis, N., Prevost, M.C. & Sansonetti, P. Analysis of epithelial cell stress response during infection by Shigella flexneri. *Infect Immun* **64**, 2474-82 (1996).
34. Bernardini, M.L., Mounier, J., d'Hauteville, H., Coquis-Rondon, M. & Sansonetti, P.J. Identification of icsA, a plasmid locus of Shigella flexneri that governs bacterial intra- and intercellular spread through interaction with F-actin. *Proc Natl Acad Sci U S A* **86**, 3867-71 (1989).
35. Lett, M.C. et al. virG, a plasmid-coded virulence gene of Shigella flexneri: identification of the virG protein and determination of the complete coding sequence. *J Bacteriol* **171**, 353-9 (1989).
36. Sansonetti, P.J., Arondel, J., Fontaine, A., d'Hauteville, H. & Bernardini, M.L. OmpB (osmo-regulation) and icsA (cell-to-cell spread) mutants of Shigella flexneri: vaccine candidates and probes to study the pathogenesis of shigellosis. *Vaccine* **9**, 416-22 (1991).
37. Monack, D.M. & Theriot, J.A. Actin-based motility is sufficient for bacterial membrane protrusion formation and host cell uptake. *Cell Microbiol* **3**, 633-47 (2001).
38. Page, A.L., Ohayon, H., Sansonetti, P.J. & Parsot, C. The secreted IpaB and IpaC invasins and their cytoplasmic chaperone IpgC are required for intercellular dissemination of Shigella flexneri. *Cell Microbiol* **1**, 183-93 (1999).
39. Alnemri, E.S. et al. Human ICE/CED-3 protease nomenclature. *Cell* **87**, 171 (1996).

40. Riedl, S.J. & Shi, Y. Molecular mechanisms of caspase regulation during apoptosis. *Nat Rev Mol Cell Biol* **5**, 897-907 (2004).
41. Solary, E., Eymin, B., Droin, N. & Haugg, M. Proteases, proteolysis, and apoptosis. *Cell Biol Toxicol* **14**, 121-32 (1998).
42. O'Brien, S., Tefferi, A. & Valent, P. Chronic myelogenous leukemia and myeloproliferative disease. *Hematology Am Soc Hematol Educ Program*, 146-62 (2004).
43. Cerretti, D.P. et al. Molecular cloning of the interleukin-1 beta converting enzyme. *Science* **256**, 97-100 (1992).
44. Howard, A.D. et al. IL-1-converting enzyme requires aspartic acid residues for processing of the IL-1 beta precursor at two distinct sites and does not cleave 31-kDa IL-1 alpha. *J Immunol* **147**, 2964-9 (1991).
45. Thornberry, N.A. et al. A novel heterodimeric cysteine protease is required for interleukin-1 beta processing in monocytes. *Nature* **356**, 768-74 (1992).
46. Dinarello, C.A. Interleukin-1 beta, interleukin-18, and the interleukin-1 beta converting enzyme. *Ann N Y Acad Sci* **856**, 1-11 (1998).
47. Chang, H.Y., Yang, X. & Baltimore, D. Dissecting Fas signaling with an altered-specificity death-domain mutant: requirement of FADD binding for apoptosis but not Jun N-terminal kinase activation. *Proc Natl Acad Sci U S A* **96**, 1252-6 (1999).
48. Kang, S.J. et al. Dual role of caspase-11 in mediating activation of caspase-1 and caspase-3 under pathological conditions. *J Cell Biol* **149**, 613-22 (2000).
49. Martinon, F., Burns, K. & Tschopp, J. The inflammasome: a molecular platform triggering activation of inflammatory caspases and processing of proIL-beta. *Mol Cell* **10**, 417-26 (2002).
50. Wang, S. et al. Murine caspase-11, an ICE-interacting protease, is essential for the activation of ICE. *Cell* **92**, 501-9 (1998).
51. Ramage, P. et al. Expression, refolding, and autocatalytic proteolytic processing of the interleukin-1 beta-converting enzyme precursor. *J Biol Chem* **270**, 9378-83 (1995).
52. Gu, Y. et al. Interleukin-1 beta converting enzyme requires oligomerization for activity of processed forms in vivo. *Embo J* **14**, 1923-31 (1995).
53. Wilson, K.P. et al. Structure and mechanism of interleukin-1 beta converting enzyme. *Nature* **370**, 270-5 (1994).
54. Ramadani, M. et al. Overexpression of caspase-1 in pancreatic disorders: implications for a function besides apoptosis. *J Gastrointest Surg* **5**, 352-8 (2001).
55. Martinon, F. & Tschopp, J. Inflammatory caspases: linking an intracellular innate immune system to autoinflammatory diseases. *Cell* **117**, 561-74 (2004).
56. Damiano, J.S., Stehlik, C., Pio, F., Godzik, A. & Reed, J.C. CLAN, a novel human CED-4-like gene. *Genomics* **75**, 77-83 (2001).
57. Geddes, B.J. et al. Human CARD12 is a novel CED4/Apaf-1 family member that induces apoptosis. *Biochem Biophys Res Commun* **284**, 77-82 (2001).
58. Poyet, J.L. et al. Identification of Ipaf, a human caspase-1-activating protein related to Apaf-1. *J Biol Chem* **276**, 28309-13 (2001).
59. Kuwae, A. et al. Shigella invasion of macrophage requires the insertion of IpaC into the host plasma membrane. Functional analysis of IpaC. *J Biol Chem* **276**, 32230-9 (2001).
60. Chen, L.M., Kaniga, K. & Galan, J.E. Salmonella spp. are cytotoxic for cultured macrophages. *Mol Microbiol* **21**, 1101-15 (1996).
61. Yamin, T.T., Ayala, J.M. & Miller, D.K. Activation of the native 45-kDa precursor form of interleukin-1-converting enzyme. *J Biol Chem* **271**, 13273-82 (1996).
62. Zychlinsky, A. et al. In vivo apoptosis in Shigella flexneri infections. *Infect Immun* **64**, 5357-65 (1996).

63. Coussens, L.M. & Werb, Z. Inflammation and cancer. *Nature* **420**, 860-7 (2002).
64. Balkwill, F. & Mantovani, A. Inflammation and cancer: back to Virchow? *Lancet* **357**, 539-45 (2001).
65. Lin, E.Y., Gouon-Evans, V., Nguyen, A.V. & Pollard, J.W. The macrophage growth factor CSF-1 in mammary gland development and tumor progression. *J Mammary Gland Biol Neoplasia* **7**, 147-62 (2002).
66. Leek, R.D. & Harris, A.L. Tumor-associated macrophages in breast cancer. *J Mammary Gland Biol Neoplasia* **7**, 177-89 (2002).
67. Brigati, C., Noonan, D.M., Albini, A. & Benelli, R. Tumors and inflammatory infiltrates: friends or foes? *Clin Exp Metastasis* **19**, 247-58 (2002).
68. Pollard, J.W. Tumour-educated macrophages promote tumour progression and metastasis. *Nat Rev Cancer* **4**, 71-8 (2004).
69. Gouon-Evans, V., Rothenberg, M.E. & Pollard, J.W. Postnatal mammary gland development requires macrophages and eosinophils. *Development* **127**, 2269-82 (2000).
70. Bingle, L., Brown, N.J. & Lewis, C.E. The role of tumour-associated macrophages in tumour progression: implications for new anticancer therapies. *J Pathol* **196**, 254-65 (2002).
71. Nakayama, Y., Nagashima, N., Minagawa, N., Inoue, Y., Katsuki, T., Onitsuka, K., Sako, T., Hirata, K., Nagata, N. and Itoh, H. Relationships between tumor-associated macrophages and clinicopathological factors in patients with colorectal cancer. *Anticancer research* **22**, 4291-4296 (2002).
72. Menetrier-Caux, C. et al. Inhibition of the differentiation of dendritic cells from CD34(+) progenitors by tumor cells: role of interleukin-6 and macrophage colony-stimulating factor. *Blood* **92**, 4778-91 (1998).
73. Dranoff, G. Cytokines in cancer pathogenesis and cancer therapy. *Nat Rev Cancer* **4**, 11-22 (2004).
74. Lin, E.Y., Nguyen, A.V., Russell, R.G. & Pollard, J.W. Colony-stimulating factor 1 promotes progression of mammary tumors to malignancy. *J Exp Med* **193**, 727-40 (2001).
75. Boudreau, N., Sympson, C.J., Werb, Z. & Bissell, M.J. Suppression of ICE and apoptosis in mammary epithelial cells by extracellular matrix. *Science* **267**, 891-3 (1995).
76. Hanahan, D. & Folkman, J. Patterns and emerging mechanisms of the angiogenic switch during tumorigenesis. *Cell* **86**, 353-64 (1996).
77. Bando, H. & Toi, M. Tumor angiogenesis, macrophages, and cytokines. *Adv Exp Med Biol* **476**, 267-84 (2000).
78. Lewis, J.S., Landers, R.J., Underwood, J.C., Harris, A.L. & Lewis, C.E. Expression of vascular endothelial growth factor by macrophages is up-regulated in poorly vascularized areas of breast carcinomas. *J Pathol* **192**, 150-8 (2000).
79. Leek, R.D. Macrophage infiltration is associated with VEGF and EGFR expression in breast cancer. *J. Pathol* **190**, 430-436 (2000).
80. Miles, D.W. et al. Expression of tumour necrosis factor (TNF alpha) and its receptors in benign and malignant breast tissue. *Int J Cancer* **56**, 777-82 (1994).
81. Luo, Y. et al. Targeting tumor-associated macrophages as a novel strategy against breast cancer. *J Clin Invest* **116**, 2132-2141 (2006).
82. Kweon, M.N. Shigellosis: the current status of vaccine development. *Curr Opin Infect Dis* **21**, 313-8 (2008).
83. Schafer, R. & Eisenstein, T.K. Natural killer cells mediate protection induced by a Salmonella aroA mutant. *Infect Immun* **60**, 791-7 (1992).

84. Stocker, B.A. Aromatic-dependent salmonella as anti-bacterial vaccines and as presenters of heterologous antigens or of DNA encoding them. *J Biotechnol* **83**, 45-50 (2000).
85. Brown, R.F. & Stocker, B.A. Salmonella typhi 205aTy, a strain with two attenuating auxotrophic characters, for use in laboratory teaching. *Infect Immun* **55**, 892-8 (1987).
86. Noriega, F.R. et al. Construction and characterization of attenuated delta aroA delta virG Shigella flexneri 2a strain CVD 1203, a prototype live oral vaccine. *Infect Immun* **62**, 5168-72 (1994).
87. Simonet, W.S. et al. Pulmonary malformation in transgenic mice expressing human keratinocyte growth factor in the lung. *Proc Natl Acad Sci U S A* **92**, 12461-5 (1995).
88. Muller, W.J., Sinn, E., Pattengale, P.K., Wallace, R. & Leder, P. Single-step induction of mammary adenocarcinoma in transgenic mice bearing the activated c-neu oncogene. *Cell* **54**, 105-15 (1988).
89. Donehower, L.A., Andre, J., Berard, D.S., Wolford, R.G. & Hager, G.L. Construction and characterization of molecular clones containing integrated mouse mammary tumor virus sequences. *Cold Spring Harb Symp Quant Biol* **44 Pt 2**, 1153-9 (1980).
90. Stewart, T.A., Pattengale, P.K. & Leder, P. Spontaneous mammary adenocarcinomas in transgenic mice that carry and express MTV/myc fusion genes. *Cell* **38**, 627-37 (1984).
91. Zebisch, A. & Troppmair, J. Back to the roots: the remarkable RAF oncogene story. *Cell Mol Life Sci* **63**, 1314-30 (2006).
92. Kolch, W. Meaningful relationships: the regulation of the Ras/Raf/MEK/ERK pathway by protein interactions. *Biochem J* **351 Pt 2**, 289-305 (2000).
93. Fensterle, J. [A trip through the signaling pathways of melanoma]. *J Dtsch Dermatol Ges* **4**, 205-17 (2006).
94. McCornick, F. How receptors turn Ras on. *Nature* **363**, 15-16. (1993).
95. Schaeffer, H.J. & Weber, M.J. Mitogen-activated protein kinases: specific messages from ubiquitous messengers. *Mol Cell Biol* **19**, 2435-44 (1999).
96. Fabian, J.R., Daar, I.O. & Morrison, D.K. Critical tyrosine residues regulate the enzymatic and biological activity of Raf-1 kinase. *Mol Cell Biol* **13**, 7170-9 (1993).
97. Chatterji, B. & Borlak, J. Serum proteomics of lung adenocarcinomas induced by targeted overexpression of c-raf in alveolar epithelium identifies candidate biomarkers. *Proteomics* **7**, 3980-91 (2007).
98. Wartmann, M. & Davis, R.J. The native structure of the activated Raf protein kinase is a membrane-bound multi-subunit complex. *J Biol Chem* **269**, 6695-701 (1994).
99. Brtva, T.R. et al. Two distinct Raf domains mediate interaction with Ras. *J Biol Chem* **270**, 9809-12 (1995).
100. Los, M. et al. Requirement of an ICE/CED-3 protease for Fas/APO-1-mediated apoptosis. *Nature* **375**, 81-3 (1995).
101. Stanton, V.P., Jr., Nichols, D.W., Laudano, A.P. & Cooper, G.M. Definition of the human raf amino-terminal regulatory region by deletion mutagenesis. *Mol Cell Biol* **9**, 639-47 (1989).
102. Heidecker, G. et al. Mutational activation of c-raf-1 and definition of the minimal transforming sequence. *Mol Cell Biol* **10**, 2503-12 (1990).
103. Avruch, J., Zhang, X.F. & Kyriakis, J.M. Raf meets Ras: completing the framework of a signal transduction pathway. *Trends Biochem Sci* **19**, 279-83 (1994).
104. Whitehurst, C.E., Owaki, H., Bruder, J.T., Rapp, U.R. & Geppert, T.D. The MEK kinase activity of the catalytic domain of RAF-1 is regulated independently of Ras binding in T cells. *J Biol Chem* **270**, 5594-9 (1995).

105. Korfhagen, T.R. et al. Cis-acting sequences from a human surfactant protein gene confer pulmonary-specific gene expression in transgenic mice. *Proc Natl Acad Sci U S A* **87**, 6122-6 (1990).
106. Glasser, S.W. et al. Genetic element from human surfactant protein SP-C gene confers bronchiolar-alveolar cell specificity in transgenic mice. *Am J Physiol* **261**, L349-56 (1991).
107. Wikenheiser, K.A., Clark, J.C., Linnoila, R.I., Stahlman, M.T. & Whitsett, J.A. Simian virus 40 large T antigen directed by transcriptional elements of the human surfactant protein C gene produces pulmonary adenocarcinomas in transgenic mice. *Cancer Res* **52**, 5342-52 (1992).
108. Kerkhoff, E. et al. Lung-targeted expression of the c-Raf-1 kinase in transgenic mice exposes a novel oncogenic character of the wild-type protein. *Cell Growth Differ* **11**, 185-90 (2000).
109. Allaoui, A., Mounier, J., Prevost, M.C., Sansonetti, P.J. & Parsot, C. icsB: a Shigella flexneri virulence gene necessary for the lysis of protrusions during intercellular spread. *Mol Microbiol* **6**, 1605-16 (1992).
110. Maurelli, A.T., Blackmon, B. & Curtiss, R., 3rd. Temperature-dependent expression of virulence genes in Shigella species. *Infect Immun* **43**, 195-201 (1984).
111. Sansonetti, P.J., Kopecko, D.J. & Formal, S.B. Involvement of a plasmid in the invasive ability of Shigella flexneri. *Infect Immun* **35**, 852-60 (1982).
112. Rymsa, B., Becker, H.D., Lauchart, W. & de Groot, H. Hypoxia/reoxygenation injury in liver: Kupffer cells are much more vulnerable to reoxygenation than to hypoxia. *Res Commun Chem Pathol Pharmacol* **68**, 263-6 (1990).
113. Lode, H.N. et al. Melanoma immunotherapy by targeted IL-2 depends on CD4(+) T-cell help mediated by CD40/CD40L interaction. *J Clin Invest* **105**, 1623-30 (2000).
114. J Fensterle, J., Bergmann, B, Yone, CLRP, Hotz, C, Meyer, SR, Spreng, S, Goebel, W, Rapp, UR and I Gentschev. Cancer immunotherapy based on recombinant Salmonella enterica serovar Typhimurium aroA strains secreting prostatespecific antigen and cholera toxin subunit B. *Cancer Gene Therapy* **0**(2007).
115. Datsenko, K.A. & Wanner, B.L. One-step inactivation of chromosomal genes in Escherichia coli K-12 using PCR products. *Proc Natl Acad Sci U S A* **97**, 6640-5 (2000).
116. Cherepanov, P.P. & Wackernagel, W. Gene disruption in Escherichia coli: TcR and KmR cassettes with the option of Flp-catalyzed excision of the antibiotic-resistance determinant. *Gene* **158**, 9-14 (1995).
117. Sambrook, J. & Gething, M.J. Protein structure. Chaperones, paperones. *Nature* **342**, 224-5 (1989).
118. Laemmli, U.K. Cleavage of structural proteins during the assembly of the head of bacteriophage T4. *Nature* **227**, 680-5 (1970).
119. Towbin, R., Dunbar, J.S. & Bove, K. Antrochoanal polyps. *AJR Am J Roentgenol* **132**, 27-31 (1979).
120. Elsinghorst, E.A. Measurement of invasion by gentamicin resistance. *Methods Enzymol* **236**, 405-20 (1994).
121. He, J., Whitacre, C.M., Xue, L.Y., Berger, N.A. & Oleinick, N.L. Protease activation and cleavage of poly(ADP-ribose) polymerase: an integral part of apoptosis in response to photodynamic treatment. *Cancer Res* **58**, 940-6 (1998).
122. Hardt, W.D., Chen, L.M., Schuebel, K.E., Bustelo, X.R. & Galan, J.E. S. typhimurium encodes an activator of Rho GTPases that induces membrane ruffling and nuclear responses in host cells. *Cell* **93**, 815-26 (1998).

123. Vaudaux, P. & Waldvogel, F.A. Gentamicin antibacterial activity in the presence of human polymorphonuclear leukocytes. *Antimicrob Agents Chemother* **16**, 743-9 (1979).
124. Fensterle, J., Bergmann, B, Yone, CLRP, Hotz, C, Meyer, SR, Spreng, S, Goebel, W, Rapp, UR and I Gentschev. Cancer immunotherapy based on recombinant Salmonella enterica serovar Typhimurium aroA strains secreting prostatespecific antigen and cholera toxin subunit B. *Cancer Gene Therapy* **15**, 85-93 (2008).
125. van den Berg, T.K. & Kraal, G. A function for the macrophage F4/80 molecule in tolerance induction. *Trends Immunol* **26**, 506-9 (2005).
126. Lewis, B.C. et al. Tumor induction by the c-Myc target genes rcl and lactate dehydrogenase A. *Cancer Res* **60**, 6178-83 (2000).
127. Leek, R.D. et al. Association of macrophage infiltration with angiogenesis and prognosis in invasive breast carcinoma. *Cancer Res* **56**, 4625-9 (1996).
128. Leek, R.D., Landers, R.J., Harris, A.L. & Lewis, C.E. Necrosis correlates with high vascular density and focal macrophage infiltration in invasive carcinoma of the breast. *Br J Cancer* **79**, 991-5 (1999).
129. Negus, R.P., Stamp, G.W., Hadley, J. & Balkwill, F.R. Quantitative assessment of the leukocyte infiltrate in ovarian cancer and its relationship to the expression of C-C chemokines. *Am J Pathol* **150**, 1723-34 (1997).
130. Kelly, P.M., Davison, R.S., Bliss, E. & McGee, J.O. Macrophages in human breast disease: a quantitative immunohistochemical study. *Br J Cancer* **57**, 174-7 (1988).
131. Volodko, N., Reiner, A., Rudas, M. & Jakesz, R. Tumour-associated macrophages in breast cancer and their prognostic correlations. *The Breast* **7**, 99-105 (1998).
132. Arnold, H. et al. Enhanced immunogenicity in the murine airway mucosa with an attenuated Salmonella live vaccine expressing OprF-OprI from Pseudomonas aeruginosa. *Infect Immun* **72**, 6546-53 (2004).
133. Mittrucker, H.W., Raupach, B., Kohler, A. & Kaufmann, S.H. Cutting edge: role of B lymphocytes in protective immunity against Salmonella typhimurium infection. *J Immunol* **164**, 1648-52 (2000).
134. Lewis, C.E. & Pollard, J.W. Distinct Role of Macrophages in Different Tumor Microenvironments. *Cancer Res* **66**, 605-612 (2006).
135. Mantovani, A., Schioppa, T., Porta, C., Allavena, P. & Sica, A. Role of tumor-associated macrophages in tumor progression and invasion. *Cancer Metastasis Rev* **25**, 315-22 (2006).
136. Minton, N.P. Clostridia in cancer therapy. *Nat Rev Microbiol* **1**, 237-42 (2003).
137. Dietrich, G. et al. Delivery of antigen-encoding plasmid DNA into the cytosol of macrophages by attenuated suicide Listeria monocytogenes. *Nat Biotechnol* **16**, 181-5 (1998).
138. Hoiseth, S.K. & Stocker, B.A. Aromatic-dependent Salmonella typhimurium are non-virulent and effective as live vaccines. *Nature* **291**, 238-9 (1981).
139. Hegele, A. et al. Immunostimulatory CpG oligonucleotides reduce tumor burden after intravesical administration in an orthotopic murine bladder cancer model. *Tumour Biol* **26**, 274-80 (2005).
140. Won, E.K., Zahner, M.C., Grant, E.A., Gore, P. & Chicoine, M.R. Analysis of the antitumoral mechanisms of lipopolysaccharide against glioblastoma multiforme. *Anticancer Drugs* **14**, 457-66 (2003).
141. Gregory, S.H., Sagnimeni, A.J. & Wing, E.J. Bacteria in the bloodstream are trapped in the liver and killed by immigrating neutrophils. *J Immunol* **157**, 2514-20 (1996).
142. Gregory, S.H. & Wing, E.J. Neutrophil-Kupffer cell interaction: a critical component of host defenses to systemic bacterial infections. *J Leukoc Biol* **72**, 239-48 (2002).

143. Zeisberger, S.M. et al. Clodronate-liposome-mediated depletion of tumour-associated macrophages: a new and highly effective antiangiogenic therapy approach. *Br J Cancer* **95**, 272-81 (2006).
144. Lewis, C. & Murdoch, C. Macrophage responses to hypoxia: implications for tumor progression and anti-cancer therapies. *Am J Pathol* **167**, 627-35 (2005).
145. Hamada, I. et al. Clinical effects of tumor-associated macrophages and dendritic cells on renal cell carcinoma. *Anticancer Res* **22**, 4281-4 (2002).
146. Hanada, T. et al. Prognostic value of tumor-associated macrophage count in human bladder cancer. *Int J Urol* **7**, 263-9 (2000).
147. Lissbrant, I.F. et al. Tumor associated macrophages in human prostate cancer: relation to clinicopathological variables and survival. *Int J Oncol* **17**, 445-51 (2000).
148. Farinha, P. et al. Analysis of multiple biomarkers shows that lymphoma-associated macrophage (LAM) content is an independent predictor of survival in follicular lymphoma (FL). *Blood* **106**, 2169-74 (2005).
149. Sica, A. et al. Macrophage polarization in tumour progression. *Semin Cancer Biol* (2008).
150. Nowicki, A. et al. Impaired tumor growth in colony-stimulating factor 1 (CSF-1)-deficient, macrophage-deficient op/op mouse: evidence for a role of CSF-1-dependent macrophages in formation of tumor stroma. *Int J Cancer* **65**, 112-9 (1996).
151. Bilyk, N. & Holt, P.G. The surface phenotypic characterization of lung macrophages in C3H/HeJ mice. *Immunology* **74**, 645-51 (1991).
152. Hume, D.A., Perry, V.H. and Gordon, S. . The mononuclear phagocyte system of the mouse defined by immunohistological localisations of antigen F4/80: Macrophages associated with epithelia. Anat. Rec. 210:503-12 (1984).

.

.

153. Nibbering, P.H., Leijh, P.C.J. and Van Furth, R. . Quantitative immunocytochemical characterization of mononuclear phagocytes. I. Monoblasts, promonocytes, monocytes and peritoneal and alveolar macrophages. .

Cell. Immunol. **105**, 374-85. (1987).
154. van de Verg, L.L. et al. Antibody and cytokine responses in a mouse pulmonary model of Shigella flexneri serotype 2a infection. *Infect Immun* **63**, 1947-54 (1995).
155. Brewer, N.R. *Respiratory physiology*, (Academic Press, Inc., New York, 1983).
156. Stein-Streilein, J. Immunobiology of lymphocytes in the lung. *Reg Immunol* **1**, 128-36 (1988).
157. Singh, R. & Paterson, Y. Listeria monocytogenes as a vector for tumor-associated antigens for cancer immunotherapy. *Expert Rev Vaccines* **5**, 541-52 (2006).

VIII. Attachment

VIII.1. List of abbreviations

°C	degree Celsius
%	per cent
*	in Gaussian distribution 5 cases out of 100 would exhibit this result
**	in Gaussian distribution 1 cases out of 100 would exhibit this result
***	in Gaussian distribution 1 cases out of 1000 would exhibit this result
+	positive control
-	negative control (not infected control)
A	Angstroms
aa	amino acid(s)
Amp	Ampicillin
Amp^R	Ampicillin resistance
BHI	brain heart infusion
BS176	*Shigella flexneri M90T*
bp, kb	base pairs, kilo base pairs
Caspase-1*	activated caspase-1 (p20)
CD	cluster of differentiation
CFU	colony forming units
CK	Cytokeratin
Cm	Chloramphenicol
Cm^R	Chloramphenicol resistance
d	day
DAB	diaminobenzidin
dH_2O	de-ionized water
EDTA	ethylene diamine tetraacetic acid
Ery	Erythromicin
Ery^R	Erythromicin resistance
FACS	fluorescence activated cell sorting
fcs	foetal calf serum
FITC	fluorescein isothiocyanate
Flp	flipase recombinase
FRT	flipase recombinase target
g	gram
GAPDH	glycerinaldehyd-3-phosphat-dehydrogenase
Gy	Gray
h	hour(s)
HRP	horseradish peroxidase
IFN	interferon
IL	interleukin
i.v.	intravenous
Kan	Kanamycin
Kan^R	Kanamycin resistance
kDa	kilo Dalton
l	liter
LB	Luria Bertani

LD_{50}	lethal dose, 50%
M	molar [mol l^{-1}]
m	meter
min	minute(s)
MOI	multiplicity of infection
MSZ	Institute for Medical Radiation and Cell Research
M90T	*Shigella flexneri M90T*
PAGE	polyacrylamid-gel-electrophoresis
PARP	poly-ADP-Ribose-Polymerase 1
cPARP	cleaved poly-ADP-Ribose-Polymerase 1
PBS	phosphate buffered saline
PCR	polymerase chain reaction
PE	phycoerythrin
PTP	protein tyrosine phosphatase
rpm	revolutions per minute
RT	room temperature
s	second(s)
s.c.	subcutan
SDS	sodium dodecyl sulphate
SPI-1	*Salmonella* pathogenicity island 1
SPI-2	*Salmonella* pathogenicity island 2
Stm	*Salmonella enterica* serovar Typhimurium *aroA* SL7207
TBE	tris borat-EDTA buffer
TAM	Tumor-associated macrophage
Tris	Tris (hydroxy methyl) aminomethane
V	Volt
wt	wildtype
x	times
x g	factor of gravity

VIII.2. Prefixes

f	femto	10^{-15}
p	pico	10^{-12}
n	nano	10^{-9}
µ	micro	10^{-6}
m	milli	10^{-3}
c	centi	10^{-2}
d	deci	10^{-1}
h	hecto	10^{2}
k	kilo	10^{3}
M	mega	10^{6}
G	giga	10^{9}

VIII.3. Units

%	per cent
Å	Angstroms
bp, kb	base pairs, kilo base pairs
°C	degree Celsius
F	farad
g	gram
h	hour(s)
kDa	kilo Dalton
l	liter
M	molar [mol l^{-1}]
m	meter
min	minute(s)
rpm	revolutions per minute
s	second(s)
V	Volt
× *g*	factor of gravity

IX. Curriculum vitae

Name:	Katharina Monika Galmbacher
Date of birth:	11 December 1979
Place of birth:	Erlenbach /Main
Nationality:	German
Family status:	Unmarried

STUDY AND GRADUATION

02/2005 - 05/2008	Julius-Maximilians-University Würzburg, Germany	PhD at the Institute of Medical Radiation and Cell Research, Prof. Dr. U. R. Rapp, Dr. Joachim Fensterle Thesis: "Caspase-1 as a target of bacterial tumor therapy."
11/1999 - 12/2004	Julius-Maximilians-University Würzburg, Germany	Biology-Diploma grades: major subject: Microbiology (1,3) minor subjecs: Biochemistry (1,0), Department of Behavioral Physiology and Sociobiology (1,7) Diploma-thesis (Microbiology): "Construction and phenotypical characterization of *Listeria monocytogenes* mutants in nitrogen metabolism" (1,0) Supervisor: Prof. Dr. W. Goebel, Dr. U. Rdest

EDUCATION

09/1990 - 06/1999	Julius-Echter-Gymnasium Elsenfeld	School Leaving Examination grade: 2,4. specialized courses: mathematics, biology
09/1986 - 07/1989	Elementary school in Klingenberg	

Datum Unterschrift

Curriculum vitae

Name:	Katharina Monika Galmbacher
Geboren:	11 Dezember 1979
Geburtsort:	Erlenbach /Main
Nationalität:	Deutsch
Familienstand:	Ledig

STUDIUM

02/2005 - 05/2008	Julius-Maximilians-Universität Würzburg, Deutschland	Doktorarbeit am Institut für Medizinische Strahlenkunde und Zellforschung (MSZ), Prof. Dr. U. R. Rapp, Dr. Joachim Fensterle Thema: "Caspase-1 as a target of bacterial tumor therapy."
11/1999 - 12/2004	Julius-Maximilians-Universität Würzburg, Deutschland	Biologie-Diplom: Hauptfach: Mikrobiologie (1,3) Nebenfächer: Biochemie (1,0), Lehrstuhl für Verhaltensphysiologie und Soziobiologie (1,7) Diplomarbeit (Mikrobiologie): "Construction and phenotypical characterization of *Listeria monocytogenes* mutants in nitrogen metabolism" (1,0) Betreuer: Prof. Dr. W. Goebel, Dr. U. Rdest

AUSBILDUNG

09/1990 - 06/1999	Julius-Echter-Gymnasium Elsenfeld	Hochschulreife: 2,4 Leistungskurse: Mathematik, Biologie
09/1986 - 07/1989	Grundschule in Klingenberg	

Datum Unterschrift

X. Publications

Patent 08-01Z:

Non-pathogenic and/or Attenuated Bacteria Capable of Inducing Apoptosis in Macrophages, Process of Manufacturing and Uses thereof. (Galmbacher, K, inventor share 20 %)

Poster:

Inhibition of tumor growth by elimination of TAMs with *Shigella flexneri*. Katharina Galmbacher, Christian Hotz, Martin Heisig, Jörg Wischhusen, Antoine Galmiche, Birgit Bergmann, Ivaylo Gentschev, Werner Goebel, Ulf R. Rapp, and Joachim Fensterle. Presentation at CIMT (Cancer immune therapy) symposium in Mainz 2008.

Paper:Block of tumor growth in an experimental breast cancer model by elimination of macrophages with a novel attenuated variant of *Shigella flexneri*. Submitted; 2008. Katharina Galmbacher, Christian Hotz, Martin Heisig, Jörg Wischhusen, Antoine Galmiche, Birgit Bergmann, Ivaylo Gentschev, Werner Goebel, Ulf R. Rapp and Joachim Fensterle.

XI. Acknowledgements

I especially want to thank the following persons:

I would like to thank my thesis advisors, Prof. Dr. U. R. Rapp and Prof. Dr. W. Goebel. I enjoyed very much their supervision. I wish to express my gratitude to Prof. Dr. U. R. Rapp for providing funding and a working place and his scientific suggestions opening myself for insights into cell signalling and tumor biology and his trust in my potential. Thank you a lot to Prof. Dr. W. Goebel for the several interesting discussions along the various stage of the work.

Dr. J. Fensterle. My supervisor. I came 4 years ago as an undergraduate student with the vision of working with cancer. Thank you for welcoming me into the fascinating world of scince and giving me the opportunity to stay. In addition I am grateful for encouraging me during this work and for standing by my side all these years. You have taught me independecy, critical thinking and believing in myself and for that I am forever grateful.

Dr. Gregoire Lauvau for his agreement to review the present thesis and for being part of my colloquium committee.

Dr. Jörk Wischhusen from the Clinics for Gynecology and Obstetrics in Wuerzburg for providing the human cancer ascites cells and for the interesting discussions along the manuscript.

I would like to express my gratitude to several additional individuals who helped with advice and discussion:

Martin Heisig, Christian Hotz and Birgit Bergmann who made valuable comments and suggestions regarding this work.

Dr. Matthias Becker with whom I had several interesting discussions along the various stage of the work.

Ivaylo Gentschev, Antoine Galmiche, Emanuele Zanucco, Katharina Lütkenhaus, Sandra Trüpschuh, Taner Dogan, and Hannes Drexler with whom I had further illuminating discussions regarding their domain of expertise.

The members of the DFG research training group 1141/1 (GCWN) for funding, organisation of events and support, especially Stefan Schroeder-Koehne and Ralf Schreck.

The whole institute (MSZ) and people from the "Tumour Therapy" group for the nice working ambience.
Especially to Gunther Tietsch and Ewald Lipp, the troubleshooters of the MSZ. Thank you for the illuminating discussions in the carport.

Finally, I would like to thank and to express my love to the most significant individuals in my life: my parents and my brothers Tobi and Andi and Susi. Thank you so much for the financial support during all these years and for being my source of inspiration, innovation and recreation. Last but not least I want to express my gratitude to Raphael, thank you for your support during hard times, building me up and bringing back motivation.